

*SIMULTANEOUS TRAJECTORY TRACKING AND
STIFFNESS CONTROL OF CABLE DRIVEN PARALLEL
MANIPULATOR*

by

KUN YU

FEBRUARY 2008

A thesis submitted to the Faculty of the Graduate School of the State University of New York at Buffalo in partial fulfillment of the requirements for the degree of

MASTER OF SCIENCE

Department of Mechanical and Aerospace Engineering
State University of New York at Buffalo
Buffalo, New York 14260

UMI Number: 1449908



UMI Microform 1449908

Copyright 2008 by ProQuest Information and Learning Company.
All rights reserved. This microform edition is protected against
unauthorized copying under Title 17, United States Code.

ProQuest Information and Learning Company
300 North Zeeb Road
P.O. Box 1346
Ann Arbor, MI 48106-1346

*To my family and friends
Without whom, I am nothing*

Abstract

Cable actuated parallel manipulators, also called cable robots, share many features in common with traditional parallel manipulators. However, such systems additionally feature considerably large workspace, large payload handling capacity and good disturbance rejection potentials over traditional parallel manipulator by virtue of the cable-band actuation. However, realizing their benefits poses numerous challenges to researchers. One critical issue is the unidirectional nature of forces exerted by cables, which only allows them to endure tensile force when performing tasks. Another critical issue in such systems is the actuation redundancy. In this thesis, we will examine these two aspects in the context of motion and active stiffness control scenarios.

First, we study the implication of actuation redundancy in the context of controller design and workspace (task space) stiffness property of cable robot system. Then suitable trajectory tracking control schemes are developed to achieve two different secondary goals under positive control input constraint: (a) minimal energy consumption among actuations; (b) active stiffness control to improve disturbance-rejection. Finally, these control schemes are evaluated within a virtual prototyping (VP) implementation framework.

Acknowledgements

First and foremost, I would first like to express my gratitude and sincerest thanks to my graduate advisor Dr. Venkat Krovi, without whom this work would not have been possible. His guidance and extensive knowledge in terms of academics, teaching, and research has propelled me during the past 2 years, constantly encouraging and enabling me to perform at my full potential. I feel fortunate to have such a great mentor and guide in my academic life.

I would also like to express my gratitude to Dr. Tarunraj Singh and Dr. Roger W. Mayne for serving as my thesis committee members.

Most importantly, I would like to express my deepest thanks to my parents; without their love and support I would not have been where I am today. I also give sincerest thanks to my wonderful girlfriend Huanhuan for her constant support and understanding. Over the past 5+ years her encouragement and caring has helped me encounter all difficulties in the way to my / our goal. This work is dedicated to them.

It is really hard to mention the names of all the friends beside me, who led me along the path towards the accomplishment of this work. Here I give my special thanks to Yijia, Tao, Zhengdan, Chen, Ming, Weiqi and CP for their concern, help, and support. I will never forget these friendships with them in my life.

Lastly I would also like to thank all my lab mates of ARM lab; they are CP, Rajan, Leng-Feng, Anand, Pat, Yao, Quishi, Hao, Madu, Srikanth and Shajan. It is my pleasure and honor to work with them during the past two years. Among them, especially thank CP for his countless help, inspiration, and guide throughout my graduate studies and the research work.

Contents

Abstract.....	iii
Acknowledgements.....	iv
List of Figures and Tables.....	ix
1 Introduction.....	1
1.1 Overview.....	1
1.2 Advantages.....	3
1.3 Challenges.....	6
1.4 Actuation Redundancy.....	7
1.5 Active Stiffness Control.....	9
1.6 Research Issues and Goals.....	12
1.6.1 Research Issues.....	12
1.6.2 Research Goals.....	13
1.7 Thesis Organization.....	14
2 Literature Survey.....	15
2.1 Similarity of Cable Robot, Parallel Robot and Robotic Hands.....	15
2.2 Workspace Quantification, Design and Optimization.....	15
2.2.1 Wrench Closure Workspace.....	16
2.2.2 Statically Reachable Workspace.....	17
2.2.3 Wrench Feasible Workspace.....	18
2.2.4 Dynamic Workspace.....	19
2.3 Singularity.....	19

2.4	Stability	20
2.5	Control	21
3	Cable Robot Kinematics and Dynamics	22
3.1	Preliminaries	22
3.2	Jacobian Analysis of Cable Robot	25
3.2.1	Screw Theory Based Jacobian Analysis	25
3.2.1.1	Screw Theory Based Jacobian of Example Gough-Stewart Platform ..	25
3.2.1.2	Screw Theory based Jacobian of Cable Robot	29
3.2.2	Conventional Jacobian Analysis of Cable Robot.....	31
3.3	Cable Robot Statics.....	32
3.4	Cable Robot Dynamics	33
4	Feedback Linearization Controller under Input Constraints.....	35
4.1	Feedback Linearization.....	35
4.2	Tension Actuation Redundancy Resolution Scheme.....	37
4.3	Pseudoinverse Based Approach.....	37
4.3.1	Determination of Minimal Parameterization of Null Space	38
4.3.2	Tension Optimization Formulation.....	39
5	Active Stiffness Control.....	41
5.1	Introduction.....	41
5.2	Active Stiffness Control of Cable Robot System	43
5.2.1	Cartesian Stiffness of Cable Robot System	43
5.2.2	Cartesian Stiffness Matrix Properties	45

5.2.3	Active Stiffness Control Schemes	46
5.2.3.1	Minimal Force Distribution with Desired Stiffness.....	47
5.2.3.2	Weighted Stiffness Matrix Approach	48
5.2.3.3	Lower Bound Stiffness Control (LBSC).....	49
6	Simulation.....	51
6.1	Virtual Model Simulation and Analysis Framework.....	51
6.2	MSC.visualNastran 4D Implementation Framework	52
6.2.1	Overall Simulation Routine	54
6.3	Our Systems.....	55
6.3.1	Planar Point Mass Cable Robot	56
6.3.2	Planar Rigid Body Cable Robot.....	57
6.3.3	Spatial Point Mass Cable Robot	57
6.3.4	Spatial Rigid Body Cable Robot.....	57
7	Results.....	59
7.1	Trajectory Tracking with Minimal Cable Force Distribution.....	60
7.1.1	Point Stabilization with Case B	60
7.1.2	Point Stabilization with Case D	62
7.1.3	Straight Line Tracking with Case B.....	63
7.1.4	Straight Line Tracking with Case D	64
7.1.5	Circle Tracking with Case A.....	65
7.1.6	Circle Tracking with Case C.....	66
7.1.7	Circle Tracking with Case D.....	68
7.2	Trajectory Tracking Augmented with Active Stiffness Control.....	69

7.2.1	Straight Line Tracking Augmented Stiffness Control with Case B.....	70
7.2.1.1	Weighted Stiffness Matrix	71
7.2.1.1.1	Control of Stiffness in X and Y Directions.....	71
7.2.1.1.2	Control of Stiffness in Rotational Direction.....	74
7.2.1.2	Lower Bound Stiffness Control	77
7.2.2	Circle Tracking with Augmented Stiffness Control with Case A.....	80
7.2.2.1	Weighted Stiffness Matrix	80
7.2.2.1.1	Control of Stiffness in X Direction.....	81
7.2.2.1.2	Control of Stiffness in X and Y Directions.....	83
7.2.2.2	Lower Bound Stiffness Control	85
7.3	Disturbance Rejection -- Straight Line Tracking.....	88
7.3.1	Straight Line Tracking under Disturbance Case 1	88
7.3.1.1	Case 1 without LBSC.....	88
7.3.1.2	Case 1 with LBSC $K_{\min}^{des} = 50 N / m$	90
7.3.2	Straight Line Tracking under Disturbance Case 2.....	91
7.3.2.1	Case 2 without LBSC.....	91
7.3.2.2	Case 2 with LBSC $K_{\min}^{des} = 50 N / m$	93
7.4	Discussion.....	94
8	Conclusions and Future Work	96
8.1	Summary.....	96
8.2	Future Work.....	96
	Bibliography	98

List of Figures and Tables

Figure 1-1 (a) Cable actuated parallel manipulator vs. (b) Typical Gough-Stewart parallel manipulator	1
Figure 1-2 Examples of Cable Robot System.....	5
Figure 1-3 Simple depiction of human upper limb [19] modeled as an articulated linkage system	8
Figure 1-4 Remote Center Compliance device from ATI Industrial Automation, Inc.	10
Figure 3-1: Serial robot/manipulator (a) KUKA KR 360 series industrial robot vs Parallel robot/manipulator (b) Moog 6 DOF Electric Motion Platform	23
Figure 3-2 Schematic of a <i>SPS</i> Gough-Stewart platform	26
Figure 3-3 Schematic of a 6-DOF Cable Robot.....	29
Figure 5-1 Schematic of stiffness control	41
Figure 5-2 Block diagram of Lower Bound Stiffness Control [75] for cable robot	50
Figure 6-1 An overhead crane model within MSC.visualNastran4D	52
Figure 6-2 MATLAB/Simulink, MSC. visualNastran integrated analysis framework	53
Figure 6-3 Block diagram of overall simulation routine	54
Figure 6-4 Virtual prototypes of cable robot systems.....	56
Figure 7-1 Point stabilization with Case B	61
Figure 7-2 Point stabilization with Case D.....	63
Figure 7-3 Straight line tracking with Case B	64
Figure 7-4 Straight line tracking with Case D	65
Figure 7-5 Circle tracking with Case A	66
Figure 7-6 Circle tracking with Case C	67

Figure 7-7 Circle tracking with Case D	69
Figure 7-8 Straight line trajectory with Case B	71
Figure 7-9 Controlling the stiffness in X and Y directions with Case B, $K_d = 50N / m$.	72
Figure 7-10 Controlling the stiffness in X and Y directions with Case B, $K_d = 100N / m$	73
Figure 7-11 Controlling the stiffness in rotational directions with Case B, $K_d = 50Nm / rad$	75
Figure 7-12 Controlling the stiffness in rotational directions with Case B, $K_d = 100Nm / rad$	76
Figure 7-13 Lower bound stiffness control with Case B, $K_{min}^{des} = 50 N / m$	78
Figure 7-14 Lower bound stiffness control with Case B, $K_{min}^{des} = 100 N / m$	79
Figure 7-15 Circle trajectory tracking with Case A.....	80
Figure 7-16 Controlling the stiffness in X directions with Case A, $K_d = 100N / m$	82
Figure 7-17 Controlling the stiffness in X directions with Case A, $K_d = 500N / m$	83
Figure 7-18 Controlling the stiffness in X and Y directions with Case A, $[K_{dx} K_{dy}] = [100 50] N / m$	84
Figure 7-19 Lower bound stiffness control with Case A, $K_{min}^{des} = 50 N / m$	86
Figure 7-20 Lower bound stiffness control with Case A, $K_{min}^{des} = 100 N / m$	87
Figure 7-21 Straight Line Tracking under disturbance 1 without LBSC with Case B.....	89
Figure 7-22 Straight Line Tracking under disturbance 1 with LBSC with Case B	91
Figure 7-23 Straight Line Tracking under disturbance 2 without LBSC with Case B.....	92
Figure 7-24 Straight Line Tracking under disturbance 2 with LBSC with Case B	94

Table 7-1 Select simulation scenarios for different cases..... 60

1 Introduction

1.1 Overview

Cable driven parallel manipulators, also called cable-driven robots or cable robots, poses the basic structure as a typical Gough-Stewart parallel manipulator (as shown in Figure 1-1 (b)) [1] but with cable-driven mechanism (as shown in Figure 1-1 (a)). Typical cable robots are formed simply by multiple cables connected to an end-effector/platform instead of articulated legs. And the motion of the end-effector is manipulated by different motors, which can either be fixed at remote positions or mounted on mobile bases, to extend or retract corresponding cables under positive cable tensions.

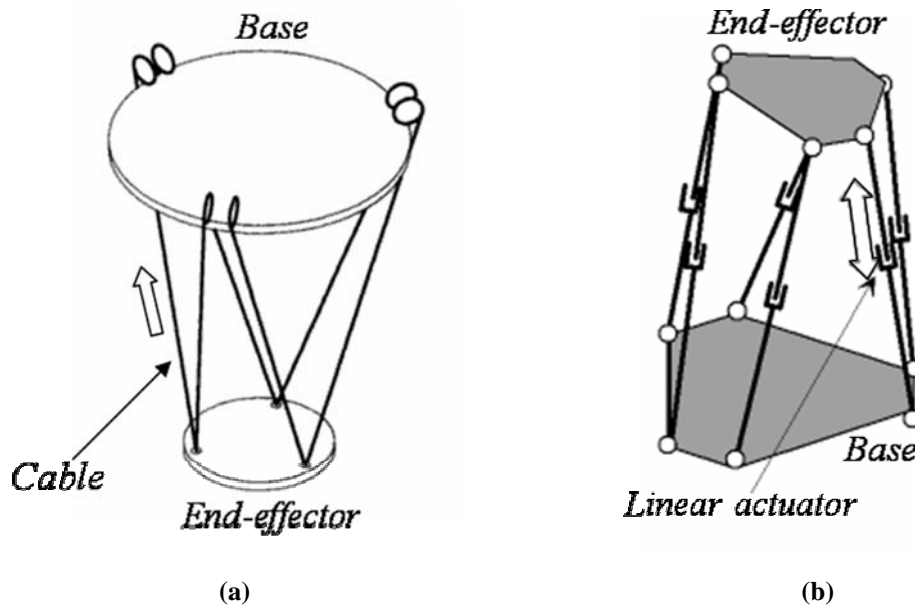


Figure 1-1 (a) Cable actuated parallel manipulator vs. (b) The Gough-Stewart parallel manipulator

A structural classification of cable robot system may be performed based on a) work environment, b) geometry of end-effector and c) degree-of-constraint.

a. Work environment: Planar vs Spatial

Planar space is 2 dimensional space (2 degree of freedom) while spatial space is 3 dimensional space (3 degree of freedom).

b. Geometry of End-effector: Point-mass vs. Rigid body

In point-mass cable robot, all cables are attached to the EE which can be considered a single point mass neglecting its geometric attributes, so all the cables intersect at this point, while in rigid body cable robot, all cables are attached to the EE which is common object with geometric attributes.

c. Degree-of-constraint: Fully/Overconstrained vs. Underconstrained

Fully/over constrained or underconstrained definition is based on the Degree of Freedom (DOF) of the end-effector and number of cables that drive the end-effector; it has been proven that a cable robot require $(n + 1)$ cables to fully constrain the end-effector, where n is the number DOF of the end-effector [2]. Here, DOF represent the number of independent parameters or inputs needed to specify the configuration of the mechanism completely [9].

In the fully constrained cable robot system, the posture (position/orientation) of the end-effector can be completely determined by the given lengths of the cables and achieve force closure [3], which means these cable robots can counteract arbitrary external force/moment through proper cable tensions with all feasible postures. On the other hand, the pose of the end-effector in underconstrained cable robot system can not be completely determined by the lengths of the cables, as fewer cables are used. Instead,

this type of system needs to take advantage of the gravity of the end-effector, which works as a virtual cable always pulling down with constant tension, to determine the resulting postures of the end-effector. In practical application, fully constrained cable robot design is not preferable though some of its properties as mentioned above are attractive, as it imposes more complex design and analysis; moreover, it also results in higher possibility of interference between cables and end-effectors or its environments, which will greatly degrade its workspace.

In general, we can always determine the number of cable needed to form a fully constrained cable robot based on the second and third factors above combined together to classify different Cable Robot systems. For example, for a spatial cable robot with finite size EE, we can say it needs 7 cables to be fully constrained, since its EE has 6 DOF.

1.2 Advantages

Due to its unique configuration, cable robot bears several attractive features, which can be summarized as follows:

1) It has a comparatively large workspace with desirable stiffness; in other words, cable robot provides us better balance between workspace and stiffness requirement than typical serial or parallel manipulators.

2) It has high payload-to-weight ratios and low inertial properties due to its light moving parts (cables) and fixed heavy parts (motors and controllers), so energy consumption is greatly reduced while cable robot is in operation.

3) It is easy to assemble/disassemble and reconfigure due to its flexible structure, so we can build cable robots to meet different requirements/tasks with same components and much shorter time.

4) It is cost-saving because of its relatively simple and cheap components and ease of transportation.

5) It is reliable due to its simple mechanism and comparable remote location of motors and controllers from the end-effectors. This feature is very useful when robots are needed to operate in extreme environment, like manipulating collusive and explosive objects.

With above desirable characteristics, cable robots are very useful in many real world applications, such as heavy payload handling, manufacturing operations, haptics, remote/hazardous areas operation, and high-speed manipulation/positioning. Some example systems have been developed during last decade. Figure 1-2 (a) [4] shows the RoboCrane, a typical six degrees of freedom parallel manipulator controlled by six cables, developed by NIST. Figure 1-2 (b) [5] shows Cable robot performing de-painting work. Figure 1-2 (c) shows the Cablecam [6] developed for the use as high speed video capture tracker in large field, etc. Figure 1-2 (d) [7] shows "Tetrahedral Robotic Apparatus" (TETRA) which integrate multi-cable suspended platform technology used with helicopters in payload transportations. Figure 1-2 (e) shows the WireMan, a portable haptic device driven by cables [8]. Figure 1-2 (f) shows Falcon-7, a high-speed cable robot with 6-DOF cable-driven robot that uses seven cables which can achieve acceleration up to 43g [9]. Figure 1-2 (g) [10] shows an automated cargo/container transfer robot used in ports developed based on the cable Array Robot [11] developed at Pennsylvania State University. Figure 1-2 (h) shows search and rescue cable robots [12] proposed for tasks such as de-mining, rescuing work, etc. Figure 1-2 (i) shows the

Charlotte Robot [13], which is developed to perform tasks such as space operation, transportation in space capsule, training of astronauts, etc.



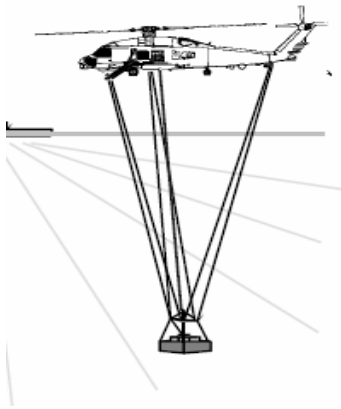
(a)



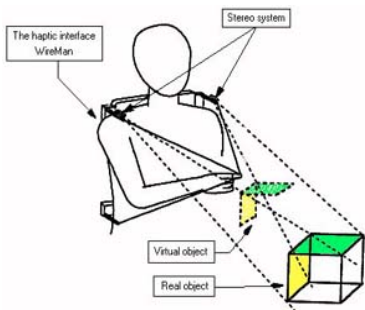
(b)



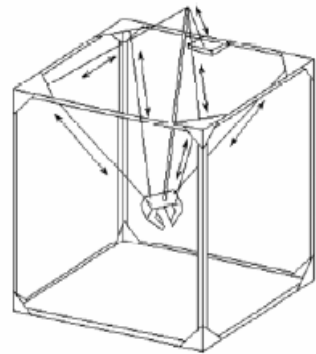
(c)



(d)



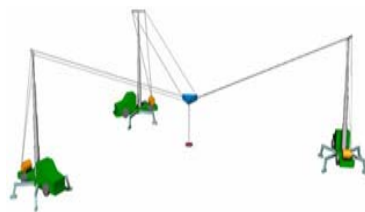
(e)



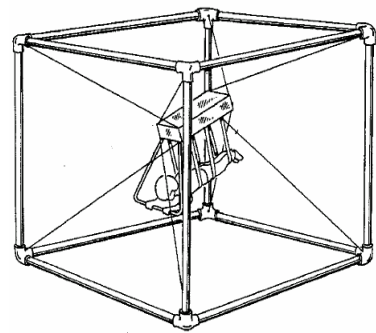
(f)



(g)



(h)



(i)

Figure 1-2 Examples of Cable Robot System

1.3 Challenges

In spite of many attractive properties and promising potentials, there are many challenges and obstacles regarding to design and development of cable robot. In literature, many of these issues have been addressed by researchers, and details are presented in Chapter 2. Main challenges for cable robot application can be summarize as following:

Design

- **Cable Interference Avoidance.** Variations in the geometrical configuration of system and tasks may impose the potential of cables interfering with each other, which may greatly limit the potentially usable workspace and add obstacles in controller design.
- **Cable Properties.** Variations in physical properties of different cable may cause different level of stretching, sagging and vibration, etc., which may greatly degrade the accuracy of the end-effector during operation.
- **Geometrical configuration.** During the process of design, factors such as number of cables, shape of platform, location of connectors, etc., may greatly limit important performance features such as singularity, stability, and wrench generation capability of the system.
- **Workspace quantification and optimization.** Workspace analysis can give analytical insights of a design to designers in the implementation stage. However, factors like the uni-directional constraint and potential

of interference imposed by cables make this kind of analysis more difficult than that of traditional robotic manipulators.

Control

- **Controller Design.** In order to achieve desired functionalities as traditional robotics systems, new controllers are necessary to incorporate possible limitations imposed by cables, such as uni-directional constraint (maintain cables in tension), cable interferences, vibrations, etc.
- **Hardware realization.** In many applications, real time operation of the control system is desired. However, the requirements of advanced sensors and efficient algorithms may cause the realization hard to deploy.
- **Calibration.** The pulley-spool mechanism and initial configuration of cable robot system can result in long and inaccurate calibration.

1.4 Actuation Redundancy

Redundancy can always adds more advantages and capabilities to a robotic system though make the system more complicated. Generally, there are two types of redundancy in robotic system - kinematic redundancy and actuation redundancy.

Kinematic redundancy arises when the degrees of freedom of a manipulator is greater than the dimensions of the task space/environment. The extra degrees of freedom enable the realization of dexterity, obstacle avoidance, optimal motion planning etc.

On the other hand, actuation redundancy arises if the number of the actuators that control the manipulator is larger than that of the degrees of freedom of the manipulator

configuration after years of evolution. Musculoskeletal system of human body, for example, upper limb (as shown in Figure 1-3), which has three joints with a total degree of 7 to position and orientation, uses 29 muscle groups for control [20] is characterized by both kinematic and actuation redundancy. Thus, the human body admits gross and dexterity motion and such system can be controlled by regulating muscle activation and neural feedback gain. Researchers have shown that when under external mechanical disturbances, purposeful motion can be executed in human and in animal natural limb in the absence of any feedback [21]. This motion is made possible under a given level of closed internal forces balance from antagonistic actuations by redundant muscles within the musculoskeletal system, thus, defines an equilibrium condition of the joints. Under this condition, deviation (the limb) from this equilibrium state will result in the generation of a restoring force/torque which is only related to the mechanical properties of muscles. Such mechanical property is called stiffness, which is introduced to describe the relationship between position deviation and force/torque exerted, more specifically, the ratio of the generated force to corresponding displacement. In other words, stiffness is a reason for generation of restoring forces or interaction forces with environment in the presence of disturbance.

1.5 Active Stiffness Control

In wide variety of robotic applications such as assembly and machining, a robot is required to perform tasks what needs to contact with environment while in prescribed robot motion. However, the interaction contact force/moment or uncertain disturbance between end-effector and environment tend to cause the end-effector be deflected away from its prescribed motion (position). For example, in part mating process performed by

a manipulator, inevitable mechanical contacts with constrained objects usually happen. Under this situation, position controller such as trajectory control may fail to perform desired task. The reaction forces provided may cause the end-effector deviates from desired trajectory so that parts are not mated tightly as expected. One way to solve this problem is to use structure composed of passive compliance, like Remote Center Compliance (RCC) device as shown in Figure 1-4.

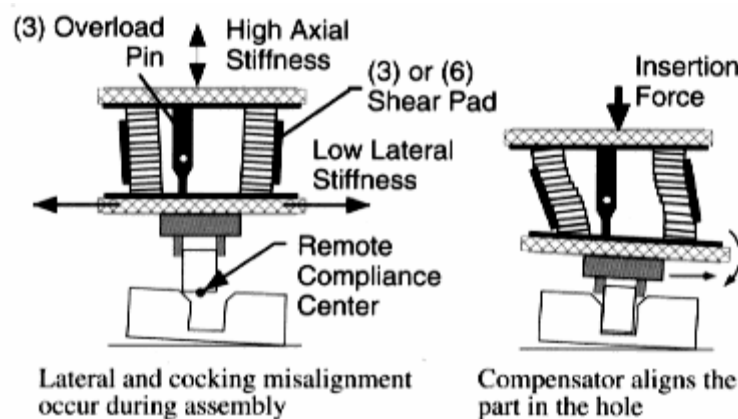


Figure 1-4 Remote Center Compliance device from ATI Industrial Automation, Inc.

However, since highly capable mechanism designs are costly and hard to obtain, such devices have very limited applicability and adaptability to different tasks. So to achieve comprehensive adaptability, software control method is necessary. A number of force control methods have been proposed to handle this issue -- a review of these approaches can be found in [22]. Stiffness control is one of the variation based on force control philosophy, this control scheme enable us to indirectly control interaction force between the manipulator and the environment through regulating the end-effector stiffness which denotes the relationship between the end-effector force and position as follows:

$F = K_d \delta X$, in which δX is a displacement from desired end-effector position, K_d is desired end-effector stiffness and F is desired responding end-effector resorting force. Just like in the prior example, through stiffness control, we can specify the stiffness in the desired direction of insertion to be high enough to minimize the impact of contact reaction force on this task.

The concept of stiffness in cable robots is the same as typical parallel robots. Stiffness property is directly related to the structure's rigidity and end-effector's accuracy. Albus et al. performed the first study of stiffness for cable robots in [23] and later they implemented the result during the design and development of the NIST RoboCrane. Verhoeven *et al.* [24] also presented a paper on the stiffness of cable actuated robots.

Control strategies, most generally known as stiffness control by redundant actuation [17], are developed to actively achieve desired end-effector stiffness. The significance of this control strategy is that the generation of active stiffness enables robot to dynamically counteract uncertain and unmodeled disturbance outside typical feedback control loop and thus strengthens the overall integrity and decrease computational load. The strategies are part of impedance control schemes where one can directly control the stiffness, instead of controlling forces and positions separately. Stiffness control schemes realized by employing redundant actuation are generally divided into: passive stiffness control, feedback stiffness control, and stiffness control realized by means of antagonistic actuation. Interested readers can refer to [25].

1.6 Research Issues and Goals

1.6.1 Research Issues

In this section, we highlight the research issue that we will address in this work in the form of two research questions and corresponding answers.

Research Question 1: How to incorporate uni-directional constraint into the control strategies to achieve good trajectory tracking performance in cable robot system?

As mentioned above, due to the nature of cables, cable robots system can function only when the cables are in tension. This imposes unidirectional constraint. Therefore, control schemes developed for typical parallel robots are no longer compatible with them, which is a major issue in the control of cable robot. To address this issue, we will introduce the actuation redundancy property of typical cable robot, which means the number of the actuators is larger than that of the degrees of freedom. With the fact that actuation redundancy allows us to re-distribute actuation forces among cables without generating any effective contributions in the workspace, actuation redundancy resolution schemes will be developed to effectively handle the unidirectional constraint problem in the realization of control strategy in dynamics level of cable robot system.

Research Question 2: How to achieve effective disturbance rejection through active stiffness control in cable robot system?

In the literature, the underlying relationship between stiffness of a system and its ability to achieve disturbance rejection has been pointed out. The specification of an appropriate stiffness can considerably simplify tasks in real world application. For example, in mating process in industrial assembly and machining, a robot is required to perform tasks what needs to contact with environment while in prescribed robot motion. However, the interaction contact force/moment between end-effector and environment tend to cause the end-effector be deflected away from its prescribed motion (position), moreover the reaction forces provided may cause trajectory controller fail to work effectively. Under such scenario, task can be effectively solved and simplified if it is possible to specify motion of the end effector in response to arbitrary disturbance forces through stiffness adjustment. Specifically, we can specify the stiffness in the desired direction of insertion to be high enough to minimize the impact of contact reaction force on this task. In this work, the significance of actuation redundancy on the active control over the stiffness of cable robot system is shown based on complete stiffness analysis. Therefore, by taking advantage of such redundancy within cable robot system, effective stiffness control schemes can be developed to reject external disturbances.

1.6.2 Research Goals

The first goal is that of modeling the nonlinear, complicated system dynamics of a cable robot so as to permit implementation of nonlinear control scheme which is capable to perform trajectory tracking task under consideration.

The second goal is of achieving disturbance compensation by transforming into a problem of stiffness design and subsequently stiffness control using available actuation redundancy. The goal then is to achieve a force distribution within the cables that can

achieve desired environmental interaction stiffness while being optimal in terms of energy consumption to achieve the desired tasks.

1.7 Thesis Organization

The remainder of the thesis is organized as follows

In Chapter 2, a comprehensive literature survey of the studies about major issues in cable robot research is presented.

In Chapter 3, screw theory based Jacobian analysis is performed in the context of cable robot system, kinematics and dynamics model of cable robot system are developed.

In Chapter 4, a trajectory tracking controller based on feedback linearization technique in dynamics level of cable robot is develop. Moreover, actuation redundancy resolution scheme is proposed to achieve optimal force distribution/minimal energy consumption by cables.

In Chapter 5, relationship between joint space stiffness, configuration, cable actuation and work space stiffness is studied and formulated based CCT stiffness approach. Then two active stiffness control schemes based on redundancy resolution is proposed: 1) weighted stiffness matrix; 2) lower bound stiffness control (LBSC).

In Chapter 6, our simulation environment - MATLAB/Simulink and MSC. visualNastran integrated simulation analysis frame work along with the our virtual prototype systems is presented.

In Chapter 7, the results of different simulation scenarios used to evaluate the performance of the control schemes developed in Chapter 4 and Chapter 5 are provided and discussed.

In Chapter 8, conclusions and future work are presented.

2 Literature Survey

In this chapter, we present a literature survey of studies regarding to main challenges of cable robot system, which are in two main categories: design and control. Interested reader can also refer to an early stage general study presented by Ming and Higuchi regarding to the properties, design, control and purpose of cable robots ([26] and [27]).

2.1 Similarity of Cable Robot, Parallel Robot and Robotic Hands

Although cable robots share similar configuration/structure as typical parallel robot manipulators, the uni-directional constrained imposed by cables make it impossible to apply many well-studied results from parallel manipulators to cable robots. Some researchers have realized the close relationship between cable robots and multi-fingered robot hands ([3] and [9]), mainly based on the similar constrain between cable robots and robot hands, as while cables can only pull it end-effector, fingers of robot hand can only push to manipulate an object. Voglewede and Ebert-Uphoff proposed antipodal cable theorem which deals with force closure issue in cable robots, based on antipodal grasp theorem from multi-fingered robot hands research in [28]. And more studies origin from research results in robot hands to cable robot are coming out.

2.2 Workspace Quantification, Design and Optimization

In robotic system study, workspace is always one of the most important issues, and the same to cable robot research. In general, a workspace is defined as the set of all

postures that the end-effector of the robot can reach and operate in. In literature, several different types of workspace have been addressed based on different definitions. Some researchers pointed out the reachable workspace definition from typical parallel robots is the same for cable robots, which refer to the geometry space that the end-effector reference point can reach depending on the geometric configuration (length of cables and mounting position of motors, cable connection locations, etc) of the cable robot. However, some researcher pointed out that not all postures in reachable workspace are necessarily useful due to the unique property of cables, and then several new definition criteria for functional workspace classification are proposed and studied, including: (a) wrench closure, (b) reachability, (c) controllability, and (d) dynamic workspace.

2.2.1 Wrench Closure Workspace

One of most general work definition is refer to the workspace in which any wrench can be generated at the end-effector (platform) by cables in tension. It is usually termed as wrench closure workspace. From a general design point of view, parallel cable-driven mechanism is said to be manipulable while operating in such workspace. Gosselin terms such workspace as Wrench-Closure Workspace (WCW) [29], and Williams, II names it statics workspace [30], [31]. Researchers also pointed out the necessary condition for the existence of such workspace is the cable robot system must be fully constrained or overconstrained, which means the number of cables must be greater than the number of DOFs of the platform as mentioned in previous section. Hence, from a general design point of view, the WCW is of great interest. However, what should be pointed out is, this kind of workspace is too ideal in some extent, since the system is required to be able to generate arbitrary unbounded wrench set in such workspace.

2.2.2 Statically Reachable Workspace

A number of researchers addressed the set of postures that the end-effector can attain statically (only taking gravity into account) [32], [33], [34], [35], etc. Since not all postures in reachable workspace are statically attainable, it is a subset of reachable workspace for cable robots. Various names are used to term this workspace, Agrawal *et al.* termed it as Statically Reachable Workspace [33], while Ebert-Uphoff *et al.* called it Static Equilibrium Workspace in [3]. And a similar concept termed the cable force region is also explored by Koshikawa *et al.* in [36].

In most studies of this kind of workspace, numerical approaches are used to find out the corresponding workspace for specific system, such as "brute force" method mentioned in [37], where the entire task space is discretized and exhaustively searched to find the matching workspace. Verhoeven extended a little further, he incorporated tension constrain into similar numerical approach in his thesis [38]. But in those studies, the closed form expressions for the boundary of the workspaces are not available. Few researcher proposed analytical approaches to this issue, Agrawal *et al.* analytically derive the boundaries of the workspace for an underconstrained and fully-constrained planar cable robot in [34], In addition, Albus *et al.* analytically formulate such workspace for the RoboCrane [37]. However, they did not generalize their specific case to other cable robot systems. Later, Oh and Agrawal proposed a novel analytical approach to derive the reachable workspace applicable to all class of cable robot with cable tension limits and disturbance by choosing a proper set-point controller correspondingly [39].

2.2.3 Wrench Feasible Workspace

Moreover, some researchers addressed a set of postures when cable robots are needed to exert particularly required force/moment combinations to interact with environment besides maintain its own static equilibrium. Ebert-Uphoff *et al.* termed this force/moment combination as wrench and name this type of workspace as Wrench-Feasible Workspace in [3]. Verhoeven *et al.* addressed almost the same concept named Controllable Workspace (defined as the set of postures where a force and torque equilibrium can be obtained with positive tensions) in [24] and [40] for tendon-based Stewart Platform. Additionally, he also proposed “workspace with tension conditions” defined as the Controllable Workspace with the constraint that all cable tensions must remain within range of cable tension value (usually between its minimum and maximum tension value), and “workspace with stiffness conditions” defined as the Controllable Workspace with the constraint that the stiffness of the end-effector must be above a threshold value in [24]. Gosselin *et al.* introduced Force-Closure Workspace [41], which only considered effect of forces.

For many applications, this kind of workspace constitutes the most “usable” workspace of cable robot, since they are built to interact with the physical real world somehow. In literature, the study of this kind of workspace has also generally been formed numerically using an exhaustive search approach [42], [24], [40]. However, few analytical approaches exist. Gosselin *et al.* determined the boundaries of the such workspace for planar 4-cable fully-constrained cable robots analytically in [41], but assumed them with infinite upper tension limits. Ebert-Uphoff *et al.* proposed a analytical method to formulate such workspace that is applicable to all class of cable robot with

cable tension limits in [43], [44], [45], but this method become very inefficient when the system becomes complicated. Stump and Kumar also proposed approach to find the closed-form expression for the boundaries of such workspace, which is applicable on both constrained and unconstrained planar or parallel cable robot. However, when constrains that the cable tension limits, the effectiveness is greatly degenerated, and cable interferences problem is not considered [46], [47]. In terms of studying the effect of cable interferences to such workspace, some researchers did some work, but either experimentally [42] or numerically [31].

2.2.4 Dynamic Workspace

Another workspace that has been addressed is the dynamic workspace along with a set of wrench called pseudo-pyramid, defined by Gosselin *et al.* as the set of all postures of the end-effector of the cable robot with specific acceleration requirement, and boundaries of this type of workspace are analytically formed for planar cable robots in [48].

2.3 Singularity

A singularity configuration of a traditional parallel manipulator refers to a particular manipulator configuration in which the manipulator loses or gains one more degrees of freedom, instantaneously [49], which will greatly degrade performance such as kinematics and force transmission of the system. Obviously, it is undesirable and should be excluded from the workspace. Hence, singularity analysis is an important issue in the design and application of any types of parallel manipulators. For typical cable robot system, there exist only Type II singularity [24] in the strict sense, which means

there are variation of Cartesian variables δX that do not affect joint variables q . In other words, (the end-effector of) the system gains additional, unwanted, uncontrollable DOF. Since it is always true that $m > n$, where m is the number of joint variable, and n is the number of degree of freedom of end-effector. From the analytical condition for singularities, singularities will result only when $rank(J) < n$, where J refers to the Jacobian of the system. Based on analysis of rank of Jacobian condition, Ma and Angeles [50] pointed out a very meaningful notion called “architecture singularity” in the design point of view, a singular architecture refers to highly symmetric design of the manipulator, (i.e. when the base and end-effector are both squares or similar polygons), in such design, singularity will appear in the most or whole of its workspace, which is consider to be the worst case. Therefore, in the process of achieving optimal singularity-free design, we should refer it as a guideline.

2.4 Stability

Stability issue has been pointed out for underconstrained cable robots. While the posture of fully constrained cable robot can be fully determined only by its own configuration, underconstrained cable robot needs to rely on gravity to determine the posture of the end-effector, so external disturbance may cause the change of the posture, which can be considered as unstable. In literature, study about the condition for stability of a spatial 3-cable crane was proposed based on the curvature of the path of the center of mass in [51]. Bosscher and Ebert-Uphoff developed a Disturbance Robustness Measure ([52], [37], and [53]) to explore the ability of underconstrained cable robots to resist external disturbance with the goal to provide guideline in the design of cable robot with maximal disturbance robustness.

2.5 Control

Since cable robots impose unidirectional constrain as mentioned above, control schemes developed for typical parallel robots are no longer compatible with them, which is a major issue in the control of cable robot. Agrawal *et al.* proposed some effective approaches to deal with this in [33], [54], [55] and [56]. Some control schemes such as feedback linearization control and sliding mode control have been applied to cable robots [33], [54], [57], [11], [26] and [58], the anti-sway control proposed in [58] and [59] by Yamamoto *et al.* is to maintain accuracy of the end-effector by reducing the sway or vibration introduced by the flexibility of the cable.

3 Cable Robot Kinematics and Dynamics

In robotics, kinematics of a robot describes the relationship between motion of the joints driving the robot and resulting motion of the end-effector of the robot without the inclusion of masses and force information. In this level, geometrical property such as position and its corresponding time derivatives such as velocity, acceleration are our concern. On the other hand, dynamics of a robot describes the relationship between actuation forces or torques from joints and the motion of the end-effector of the robot. The dynamics of a robot manipulator is much more complex than kinematics. However, it is necessary for the realization of real-world robot application, as most information in dynamics level of a robot such as forces and torques output from joints actuators, external forces, inertial properties are important in the system modeling to achieve high physical fidelity.

3.1 Preliminaries

In the study of robotics, a robotic system can be classified into two main categories according to their kinematic structure or structural topologies [60]. One is serial robot/manipulator as shown in Figure 3-1(a) formed by open-loop kinematic chain, the other is parallel robot/manipulator as shown in Figure 3-1(b) formed by closed-loop kinematic chains.

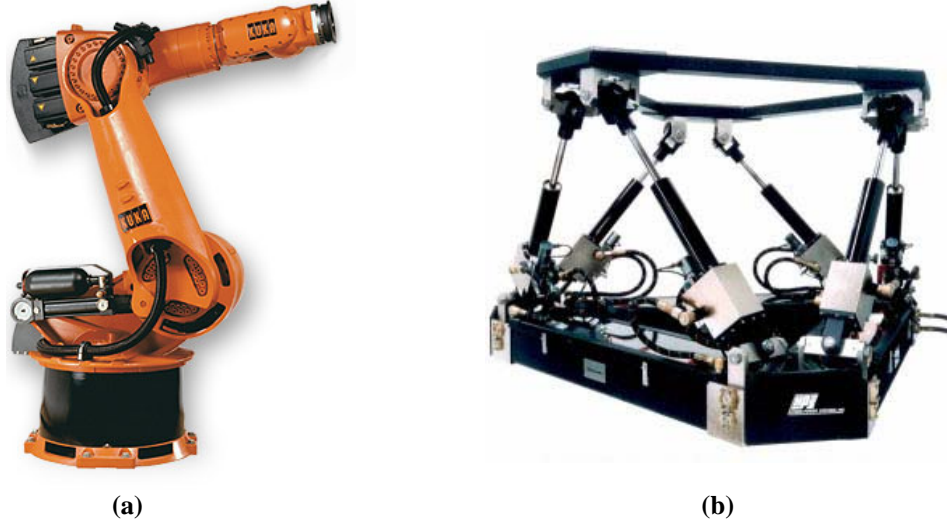


Figure 3-1: Serial robot/manipulator (a) KUKA KR 360 series industrial robot vs Parallel robot/manipulator (b) Moog 6 DOF Electric Motion Platform

A brief review of the kinematics and statics of serial and parallel manipulators is as follows. Here, let $X = [x \ y \ z \ \psi \ \theta \ \phi]^T$ denotes the position and orientation of the end-effector. Let $W = [f_x \ f_y \ f_z \ m_x \ m_y \ m_z]^T$ denotes the wrench (forces and torques) of the end-effector. For a serial manipulator with n degree of freedom among joints, the forward position kinematics can be written in the form $X = f(\bar{\theta})$, in which $\bar{\theta}_{(n \times 1)}$ denotes joint variable. The forward velocities kinematics can be derived as follows

$$\dot{X} = J_s \dot{\theta} \quad (1)$$

where $J_{s(6 \times n)}$ denotes the serial manipulator Jacobian matrix. The Jacobian matrix, in robotics, is used to describes the relationship between joint and end-effector velocities. At the statics level, by the principle of virtual work the Jacobian also relates joint torques to end- effector wrench as follow:

$$\tau = J_s^T W \quad (2)$$

in which τ denotes joint torques exerted by actuators.

Based on screw system theory, as the result of the well known duality of motion screw axes and wrenches [61] between serial and parallel manipulators, for a parallel manipulator with n degree of freedom, the inverse position kinematics can be written in the form $\bar{\theta} = f(X)$, then the inverse velocities kinematics can be derived as follows

$$\dot{\theta} = J_p \dot{X} \quad (3)$$

where $J_{p(n \times 6)}$ denotes the parallel manipulator Jacobian matrix relates joint velocities to end-effector velocities. At statics level, by the principle of virtual work the Jacobian also relates joint torques to end-effector wrench as follow:

$$W = J_p^T \tau \quad (4)$$

where τ denotes joint torques exerted by actuators.

From above, we can see for a serial manipulator, close-form solution always exists in the forward kinematics, while it may not exist in the inverse kinematics. Conversely, due to the duality for a parallel manipulator, closed-form solution always exists in the inverse kinematics, it may not exist in the forward kinematics. In this work, we will concentrate on analysis of parallel manipulator of our interest. Because of their closed loops structure formed by different links, analysis of parallel chain manipulators is much more difficult than the analysis of serial ones. In the literature, there are many ways of deriving the Jacobian [60]. In the following section, we will focus on screw theory based Jacobian analysis of parallel manipulator and extend it to cable robot of our interest.

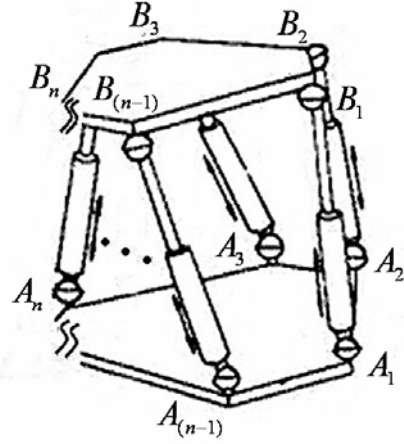
3.2 Jacobian Analysis of Cable Robot

3.2.1 Screw Theory Based Jacobian Analysis

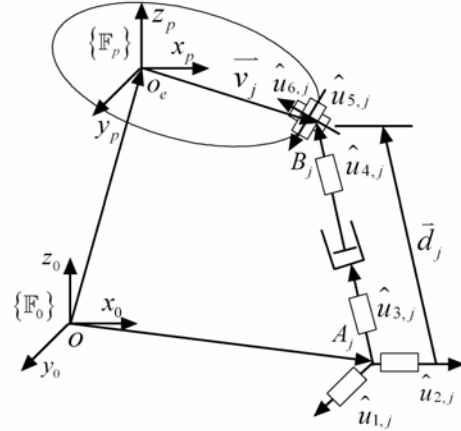
The kinematics of a mechanical system can be expressed in terms of screw coordinates. Interested readers can refer to several of the excellent materials ([62], [60], [63]) for details. Unlike conventional but straightforward method which usually involves derivatives during derivation in modeling, one of the major advantages of screw-theoretic method is it provide us a low-resolution computational model based on the geometric insight of the system.

3.2.1.1 Screw Theory Based Jacobian of Example Gough-Stewart Platform

The configuration of Cable robot and Gough-Stewart Platform is very similar by nature. A typical spatial cable robot can be considered as being evolved from letting a Gough-Stewart Platform with \underline{SPS} (underling here means actuation) limbs upside down and substituting the rigid prismatic joints with cables. And the connections where tendons are attached to base and end-effector can be considered as ideal spherical joints of infinite stiffness. In this section, we use screw theory based Jacobian analysis for a \underline{SPS} Gough-Stewart Platform to derive cable robot kinematics. Then by taking advantage of the similarity of configuration, we can analyze the kinematics of cable robot based on the techniques used in analysis of Gough-Stewart Platform. In what follows we will summarize this work briefly to highlight the critical features.



(a) a \underline{SPS} Gough- Stewart platform



(b) Kinematic structure of an \underline{SPS} limb

Figure 3-2 Schematic of a \underline{SPS} Gough-Stewart platform

Figure 3-2 (a) shows a spatial 6-dof parallel manipulator (Gough-Stewart platform) with n identical \underline{SPS} limbs, for a typical Gough-Stewart Platform $n = 6$. The upper plate, which is considered as the moving end-effector is connected by six identical limbs to the lower fixed base by spherical joints B_j and A_j , $j = 1, 2, \dots, n$. Several close loop kinematic chains are formed by the six limbs. Without loss of generality, each of the planes is assumed to have n connection-points distributed at the vertices of an arbitrary polygon.

Let's define an instantaneous reference frame: $\mathbb{F}_p(x_p, y_p, z_p)$ attached to the moving platform with the origin located at point o_e and the axes x_p, y_p, z_p parallel to the axes of frame $\{\mathbb{F}_0\}$. Then we express all the joint screws with respect to this instantaneous reference frame $\{\mathbb{F}_p\}$. Then, the Jacobian matrix of the Gough-Stewart Platform can be derived by applying the concept of reciprocal screws (for detail about concept of screw coordinates and reciprocal screw, refer to [60]), Figure 3-2 (b) shows the equivalent kinematic chain of an \underline{SPS} limb, we can consider this limb as the lower

spherical joint be replaced by two intersecting unit screws, $\hat{\$}_1$ and $\hat{\$}_2$, the middle prismatic joint as unit screws, $\hat{\$}_3$, the upper spherical joint as three intersecting unit screws, $\hat{\$}_4$, $\hat{\$}_5$ and $\hat{\$}_6$. Among these six joints with each limb, only the third joint (prismatic joint) is actuated; the remaining five joints are passive. Let $\hat{u}_{i,j}$ be unit vector along the i th joint axis of the j th limb in frame $\{\mathbb{F}_p\}$, $j=1, 2, \dots, n$. Then the six unit joint screws can be written as

$$\begin{aligned}\hat{\$}_{i,j} &= \begin{bmatrix} \hat{u}_{i,j} \\ (\bar{v}_j - \bar{d}_j) \times \hat{u}_{i,j} \end{bmatrix}; i=1, 2. \\ \hat{\$}_{3,j} &= \begin{bmatrix} 0 \\ \hat{u}_{3,j} \end{bmatrix} \\ \hat{\$}_{i,j} &= \begin{bmatrix} \hat{u}_{i,j} \\ \bar{v}_j \times \hat{u}_{i,j} \end{bmatrix}; i=4, 5, 6.\end{aligned}\tag{5}$$

where \bar{l}_j is the vector corresponding to j th limb in frame $\{\mathbb{F}_p\}$. \bar{v}_j is the position of the j th connection point relative to the robot's coordinate frame $\{\mathbb{F}_p\}$.

Now, we can get end-effector twist with respect to this instantaneous reference frame $\{\mathbb{F}_p\}$ as:

$$\$_t = \begin{bmatrix} V \\ \omega \end{bmatrix} = \begin{bmatrix} \hat{\$}_{1,j} & \hat{\$}_{2,j} & \hat{\$}_{3,j} & \hat{\$}_{4,j} & \hat{\$}_{5,j} & \hat{\$}_{6,j} \end{bmatrix} \begin{bmatrix} \dot{\theta}_{1,j} \\ \dot{\theta}_{2,j} \\ \dot{d}_j \\ \dot{\theta}_{4,j} \\ \dot{\theta}_{5,j} \\ \dot{\theta}_{6,j} \end{bmatrix}; j=1, 2, \dots, n.\tag{6}$$

Since the axes of all the unactuated joints in each limb intersect the line passing through points A_j and B_j , which define the vector \bar{d}_j , we can define a unique screw that is reciprocal to all the unactuated joint as :

$$\hat{\$}_{r3,j} = \begin{bmatrix} \hat{u}_{3,j} \\ \bar{v}_j \times \hat{u}_{3,j} \end{bmatrix} \quad (7)$$

Here, $\hat{\$}_{r3,j}$ can be considered as the zero-pitch unit screw coincident with each limb.

Then, by taking orthogonal product of both sides of Eq. (6) by $\hat{\$}_{r3,j}$, we can get

$$\hat{\$}_{r3,j}^T \$_t = \dot{d}_j \quad (8)$$

Last, by writing n times for each of n limbs, we can get

$$\dot{q} = J\dot{X} \quad (9)$$

where

$$J = \begin{bmatrix} \hat{u}_{3,1}^T & (\bar{v}_1 \times \hat{u}_{3,1})^T \\ \hat{u}_{3,2}^T & (\bar{v}_2 \times \hat{u}_{3,2})^T \\ \hat{u}_{3,3}^T & (\bar{v}_3 \times \hat{u}_{3,3})^T \\ \vdots & \vdots \\ \hat{u}_{3,n}^T & (\bar{v}_n \times \hat{u}_{3,n})^T \end{bmatrix} \quad (10)$$

and

$$\dot{X} = [\dot{x} \ \dot{y} \ \dot{z} \ \omega_x \ \omega_y \ \omega_z]^T, \quad \dot{q} = [\dot{d}_1 \ \dot{d}_2 \ \dot{d}_3 \ \dots \ \dot{d}_n]^T \quad (11)$$

3.2.1.2 Screw Theory based Jacobian of Cable Robot

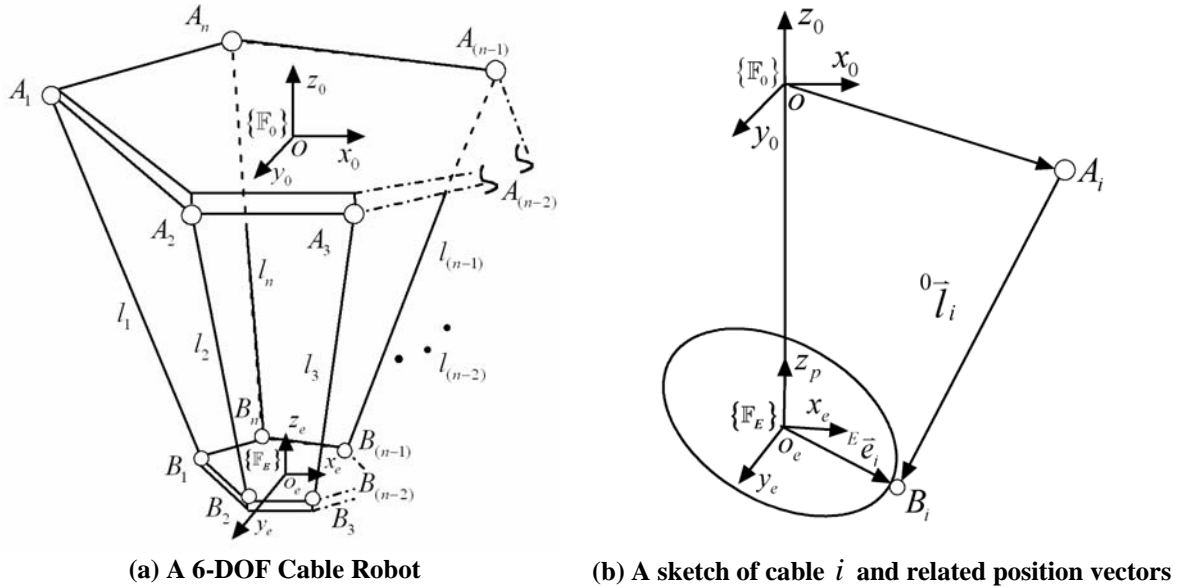


Figure 3-3 Schematic of a 6-DOF Cable Robot

Figure 3-3 (a) shows a spatial 6-dof cable robot actuated by n identical cables. The lower plate, which is considered as the moving end-effector is connected by n identical cables to the upper fixed base at connection-points A_i and B_i , $i = 1, 2, \dots, n$, which are considered distributed at the vertices of an arbitrary polygon without loss of generality. In this system, several close loop kinematic chains are formed by the cables.

Let's define two Cartesian coordinate system: $\mathbb{F}_0(O, x_0, y_0, z_0)$ attached to the base with the origin located at the center, and $\mathbb{F}_E(O_e, x_e, y_e, z_e)$ attached to the moving platform (end-effector) with the origin O_e located at the center, the origin the two frames are located at the center of the corresponding planes. Moreover, it is assumed that all vectors and matrices are represented in the base frame $\{\mathbb{F}_0\}$ unless otherwise indicated. Let the location of the i th external cable connection be denoted by 0B_i and the i th on

board cable connection be denoted by 0A_i . Through the same derivation process as shown in Section 3.2.1.1, we can get the Jacobian of cable robot in similar form

$$\dot{l} = J\dot{X} \quad (12)$$

where

$$J = \begin{bmatrix} \hat{l}_1^T & ({}^0\bar{e}_1 \times \hat{l}_1)^T \\ \hat{l}_2^T & ({}^0\bar{e}_2 \times \hat{l}_2)^T \\ \hat{l}_3^T & ({}^0\bar{e}_3 \times \hat{l}_3)^T \\ \vdots & \vdots \\ \hat{l}_n^T & ({}^0\bar{e}_n \times \hat{l}_n)^T \end{bmatrix} = \begin{bmatrix} \hat{l}_1^T & -(\hat{l}_1 \times {}^0R_E {}^E\bar{e}_1)^T \\ \hat{l}_2^T & -(\hat{l}_2 \times {}^0R_E {}^E\bar{e}_2)^T \\ \hat{l}_3^T & -(\hat{l}_3 \times {}^0R_E {}^E\bar{e}_3)^T \\ \vdots & \vdots \\ \hat{l}_n^T & -(\hat{l}_n \times {}^0R_E {}^E\bar{e}_n)^T \end{bmatrix} \quad (13)$$

and

$$\dot{X} = [\dot{x} \ \dot{y} \ \dot{z} \ \omega_x \ \omega_y \ \omega_z]^T, \quad \dot{l} = [\dot{l}_1 \ \dot{l}_2 \ \dot{l}_3 \ \cdots \ \dot{l}_n]^T \quad (14)$$

As shown in Figure 3-3 (b), in Eq. (13) and Eq. (14), ${}^0\bar{l}_i$ is the position vector of i th cable ($i = 1, 2, \dots, n$) with respect to frame $\{\mathbb{F}_0\}$, $\hat{l}_i = \frac{{}^0\bar{l}_i}{\|{}^0\bar{l}_i\|}$ is the unit length vector of i th cable. Ee_i is the position of the i -th onboard cable connector relative to the end-effector coordinate frame $\{\mathbb{F}_E\}$. \dot{l}_i represents the velocity of i th cable, and $\dot{X} = [\dot{x} \ \dot{y} \ \dot{z} \ \omega_x \ \omega_y \ \omega_z]^T$ is the velocity vector for the reference point in moving platform with respect to base frame $\{\mathbb{F}_0\}$. Moreover, 0R_E is the rotation matrix that relates the orientation of end-effector coordinate frame $\{\mathbb{F}_E\}$ to base frame $\{\mathbb{F}_0\}$, using a fixed axis rotation sequence of ψ , ϕ , and θ about x , y , and z axes of $\{\mathbb{F}_0\}$, respectively.

$${}^0R_E = R_z(\theta)R_y(\phi)R_x(\psi) = \begin{bmatrix} c\theta c\phi & c\theta s\phi s\psi - s\theta c\psi & c\theta s\phi c\psi + s\theta s\psi \\ s\theta c\phi & s\theta s\phi s\psi + c\theta c\psi & s\theta s\phi c\psi - c\theta s\psi \\ -s\phi & c\phi s\psi & c\phi c\psi \end{bmatrix} \quad (15)$$

In the cases of cable robot with pure transitional or point mass moving platform, we can get simplified general representation of $\dot{l} = J\dot{X}$, where

$$J = \begin{bmatrix} \hat{l}_1^T & \hat{l}_2^T & \hat{l}_3^T & \cdots & \hat{l}_n^T \end{bmatrix}^T \quad (16)$$

$$\dot{X} = [\dot{x} \ \dot{y} \ \dot{z}]^T, \quad \dot{l} = [\dot{l}_1 \ \dot{l}_2 \ \dot{l}_3 \ \cdots \ \dot{l}_n]^T \quad (17)$$

Furthermore, when dealing with the planar case, l_i , 0p_i , 0b_i , 0X_E and Ee_i , ${}^0X_E = [x \ y \ \theta]^T$ are vectors in the plane and the orientation is given by

$${}^0R_E = R(\theta) = \begin{bmatrix} c\theta & -s\theta & 0 \\ s\theta & c\theta & 0 \\ 0 & 0 & 1 \end{bmatrix} \quad (18)$$

3.2.2 Conventional Jacobian Analysis of Cable Robot

In this section, we will show a straightforward analytical method to derive Jacobian of cable robot to verify the result from Section 3.2.1.2.

As show in Figure 3-3 (b), in the base frame $\{\mathbb{F}_0\}$, the vector representing the i th cable can be written as

$$l_i = {}^0B_i - {}^0A_i = {}^0B_i - {}^0X_E - {}^0R^E \bar{e}_i \quad (19)$$

Let $L_i = \|l_i\|$ denotes the length of i -th cable, by differentiating $L_i = \|l_i\|$, one can derive the inverse kinematics relation between the end-effector twist and joints velocity as

$$\dot{l} = J\dot{X} \quad (20)$$

where J is the same as one derive from the screw-based method in Section 3.2.1.2, and ${}^0X_E = [x \ y \ z \ \psi \ \theta \ \phi]^T$ denotes the position of the center of the end-effector O_e . In frame $\{\mathbb{F}_0\}$, Ee_i denotes the position of the i -th onboard cable connector relative to the robot's coordinate frame $\{\mathbb{F}_E\}$, and the rotation matrix has the same form as Eq. (15) and Eq. (18).

3.3 Cable Robot Statics

The statics of cable robot is closely related to the inverse kinematics. Let $W = [f \ m]^T$ represent the vector of output wrenches (forces and moments) on the end-effector, $F = [F_1 \ F_2 \ \dots \ F_n]^T$ ($F \geq 0$) represents the vector of tensions applied by cables. δX represents the vector of virtual displacements on the inertia frame caused by W , δl represents the vector of virtual cable displacement caused by F .

According to the D'Alembert's principle (also known as the principle of virtual work) [60], we can have

$$-F^T \delta l - W^T \delta X = 0 \quad (21)$$

The minus sign in front of the $F^T \delta l$ term is because that the tensions and displacements are collinear but in reverse direction. Moreover, as the virtual displacement δl and δX are related by Jacobian matrix, which has the form

$$\delta l = J \delta X \quad (22)$$

Thus,

$$(F^T J + W^T) \delta X = 0 \quad (23)$$

Eq. (23) holds for any virtual displacement, δX . Then by eliminating δX , we can get

$F^T J + W^T = 0$, by taking transpose of it, yields

$$W = -J^T F \quad (F \geq 0) \quad (24)$$

3.4 Cable Robot Dynamics

In this section, a general form of equation of motion of cable robot is derived based on spatial rigid body case (6 DOF). Here, we assume the cables are massless and stiff so that the inertias and spring stiffness of cables will have no effect. Furthermore, we ignore the inertia/dynamics of motors that drive cables and friction losses between cables and pulleys. According to Newton-Euler's law, output wrenches (forces and moments) on the end-effector W can be written as

$$W = \begin{bmatrix} f_x & f_y & f_z & m_x & m_y & m_z \end{bmatrix}^T = \begin{bmatrix} m\ddot{x} \\ m\ddot{y} \\ m(\ddot{z} - g) \\ I \begin{pmatrix} \alpha_x \\ \alpha_y \\ \alpha_z \end{pmatrix} + \begin{pmatrix} \omega_x \\ \omega_y \\ \omega_z \end{pmatrix} \times I \begin{pmatrix} \omega_x \\ \omega_y \\ \omega_z \end{pmatrix} \end{bmatrix} \quad (25)$$

where m is the mass, g is the acceleration due to gravity and I is the moment of inertia of the end-effector about its center of mass.

By substituting $W = -J^T F$ ($F \geq 0$) in Eq. (24) into Eq. (25), we can get the equation of motion of cable robot system as

$$\begin{bmatrix} m\ddot{x} \\ m\ddot{y} \\ m(\ddot{z} - g) \\ I \begin{pmatrix} \alpha_x \\ \alpha_y \\ \alpha_z \end{pmatrix} + \begin{pmatrix} \omega_x \\ \omega_y \\ \omega_z \end{pmatrix} \times I \begin{pmatrix} \omega_x \\ \omega_y \\ \omega_z \end{pmatrix} \end{bmatrix} = -J^T \begin{bmatrix} F_1 \\ F_2 \\ F_3 \\ \vdots \\ F_{(n-1)} \\ F_n \end{bmatrix}, \quad (F \geq 0) \quad (26)$$

which can be rewritten to a general form as

$$M(X)\ddot{X} + h(X, \dot{X}) + g(X) = -J^T F \quad (F \geq 0) \quad (27)$$

where $M(X)$ is the inertial matrix, $h(X, \dot{X})$ term represents the Coriolis and centrifugal forces, $g(X)$ represents the gravitational force.

$$M(X) = \begin{bmatrix} mI_{3 \times 3} & 0_{3 \times 3} \\ 0_{3 \times 3} & I \end{bmatrix}$$

$$h(X, \dot{X}) = \begin{bmatrix} 0_{3 \times 1} \\ \begin{pmatrix} \omega_x \\ \omega_y \\ \omega_z \end{pmatrix} \times I \begin{pmatrix} \omega_x \\ \omega_y \\ \omega_z \end{pmatrix} \end{bmatrix}$$

$$g(X) = \begin{bmatrix} 0 \\ 0 \\ -mg \\ 0_{3 \times 1} \end{bmatrix} \quad (28)$$

What should point out here is the equation of motion of cable robot system is valid only if system input force $F \geq 0$, which means the cables must be in tension to maintain the configuration and workability of the system.

4 Feedback Linearization Controller under Input Constraints

In this Chapter, we consider the position control problem for cable robot system - given a desired trajectory, how to modulate exerting forces of cables so that the end-effector will converge to that trajectory.

4.1 Feedback Linearization

The basic idea of feedback linearization is to construct a control law to cancel all nonlinearities of a nonlinear dynamical system via full-state nonlinear feedback, allowing traditional linear control techniques such as PID control to be easily implemented on the nonlinear system. Due to its very good performance characteristics proven in literature, it is popular and widely used control method in field of Robotics. However, it is necessary to note that its computational efficiency and need an accurate system (both model structure and parametric values) dynamics model limits the applicability. There are formal methods derived from nonlinear control theory using lie bracket analysis of vector fields to help choose expressions of control law to achieve feedback linearization, interested readers can refer to [64].

In this section, we briefly summarize the application of such feedback linearization it to our cable robot system. From Eq. (27), we can see our system shares the same general form of equation of motion as simple mechanical system [65], thus, we can derive the feedback linearization control law in same way. For reader's convenience, we repeat the equation of motion of cable robot in Eq. (27) as follows

$$-J^T F = M(X)\ddot{X} + h(X, \dot{X}) + g(X) \quad (F \geq 0) \quad (29)$$

To meet the trajectory tracking requirement in our work, we consider a PD controller based feedback linearization technique. Let $X_d(t)$, $\dot{X}_d(t)$ and $\ddot{X}_d(t)$ represents the desired trajectory information. Define error between actual and desired trajectory as

$$e = X_d(t) - X(t) \quad (30)$$

Let $\ddot{X} = \ddot{X}_d + K_p e + K_d \dot{e}$ and substitute it in Eq.(29), we have the control input,

$$F = (-J^T)^{-1}[M(X)(\ddot{X}_d + K_p e + K_d \dot{e}) + h(X, \dot{X}) + g(X)] \quad (31)$$

Then, by substituting Eq. (31) into Eq. (29), we have the error dynamics of the system as follows

$$M(X)(\ddot{e} + K_p e + K_d \dot{e}) = 0 \quad (32)$$

Since $M(X)$ is inertia matrix of the system, $M(X) \neq 0$. We have the linear differential equation that governs the error between the actual and desired trajectories, as follows

$$\ddot{e} + K_p e + K_d \dot{e} = 0 \quad (33)$$

By choosing K_p and K_d as positive definite, symmetric matrices, we can easily ensure that the controlled system is stable and $e \rightarrow 0$ exponentially when $t \rightarrow \infty$.

Proof: By taking the laplace transform of the error dynamics equation, we have

$$s^2 e(s) + sK_d e(s) + K_p e(s) = 0 \quad (34)$$

Then we have the characteristic equation for the linearized system as follows

$$s^2 + sK_d + K_p = 0 \quad (35)$$

The roots of the characteristic equation are

$$s = -\frac{1}{2}K_d \pm \frac{1}{2}\sqrt{K_d^2 - 4K_p} \quad (36)$$

From Eq. (36) we can see, by the system will be stable as long as K_p and K_d are positive definite, symmetric matrices.

4.2 Tension Actuation Redundancy Resolution Scheme

It has been mentioned in previous chapters, due to the unidirectional force constraint imposed by cables (cables must be in tension), cable robot system should possess “actuation redundancy” property in order to maintain its functionality and usability. Since the indeterminacy of internal actuation forces caused by actuation redundancy can be utilized as optimization formulation to satisfy the unidirectional force constraint. In this section, effective actuation redundancy resolution schemes are developed for cable robot, the schemes are formulated as solving optimization problem based on typical pseudo-inverse solution to the system. The redundancy resolution schemes are used to incorporate with the control law developed in Section 4.1 in order to meet the requirement of input unidirectional force constraint among cables.

4.3 Pseudoinverse Based Approach

As shown in Section 3.4, the equation of motion of cable robot system can be written as

$$W_{(m \times 1)} = S_{(m \times n)} F_{(n \times 1)}, (F \geq 0) \quad (37)$$

where

$$S = -J^T \quad (38)$$

To solve the inverse dynamics of the system, a general pseudo-inverse solution for Eq. (37) can be written as

$$F = S^\#W + (I - S^\#S)z = F_p + F_h \quad (39)$$

where I is $n \times n$ identity matrix, z is an arbitrary n -vector, and $S^\#$ is Moore-Penrose pseudoinverse of S , since the cable robot system under our consideration is almost always redundantly actuated (underconstrained), which means $m < n$, $S^\#$ can be computed as $S^\# = S^T(SS^T)^{-1}$, the first term of Eq. (39) corresponds to the particular solution. When the second term $F_h = 0$, we have $F = F_p$, which corresponds to least squares minimum-norm solution to the system of equations. However, the positiveness of this solution is indetermined, which implicates that unidirectional force constraint may be violated. And the second term corresponds to the homogeneous solution that maps z to the null space of S . Since F_h can take on any value, there will result in infinite set of possible solutions to the system. As shown in [66, 67], authors interpreted F_p as the equilibrating force and F_h as internal force respectively. The equilibrating force represents the least squares solution to the system, and the internal forces can always balance each other within the system therefore these forces do not contribute to the effective work to the environment, most importantly, due to redundancy, internal force distribution within the system is not unique. Thus, the positiveness of forces can be ensured by properly modulating internal actuation distribution.

4.3.1 Determination of Minimal Parameterization of Null Space

In Eq.(39), let $H = (I - S^\#S)$, Typically H matrix is found to be rank deficient: $\text{rank}(I - S^\#S) = (n - m) < n$, which means non-independent components exist within the null space of S . As the result of that, discontinuity may result in z [68] due to different

set of $(n-m)$ independent columns of H can be chosen for S in each iterative steps. Thus, in this section, we present an approach to find the minimal parameters to uniquely represent the null space solution.

To solve this problem, we can perform singular value decomposition (MATLAB routine SVD) to obtain the full rank nullspace component of the system

$$H = U\Delta V^T \quad (40)$$

where U and V are $n \times n$ orthogonal matrices, and Δ is the diagonal matrix contains the singular value of H in the form $\Delta = \text{diag}\{\sigma_1, \sigma_2, \dots, \sigma_{(n-m)}, 0, \dots, 0\}$ with $\sigma_i > 0, i = 1, 2, \dots, n-m$. By choosing $N(S)$ as the first $(n-m)$ columns of U matrix corresponding to first $(n-m)$ non-zero singular value: $N(S) = [U_1 \ U_2 \ \dots \ U_{(n-m)}]$, (obviously $\text{rank}(N(S)) = n-m$ since U is orthogonal matrix), then, an equivalent expression for Eq. (39) becomes

$$F = S^{\#}W + \sum_{j=1}^{n-m} \alpha_j N_j = F_p + N(S)\bar{\alpha} \quad (41)$$

where $N(S) = [n_1 \ n_2 \ \dots \ n_i]_{n \times (n-m)}$ denotes the full rank null space or kernel matrix of S , and $\bar{\alpha} = [\alpha_1 \ \alpha_2 \ \dots \ \alpha_i]^T$ is an arbitrary $(n-m)$ vector. Here, $i = (n-m)$ where n is the number of cables and m is the dimension of the Cartesian space or rank of matrix S .

4.3.2 Tension Optimization Formulation

In cases, least squares minimum-norm solution F_p results in some negative tensions, certain criteria is needed to choose a proper homogeneous solution F_h to guarantee the positiveness of F . According to the attribute of null space in our control

input solution as mentioned in Section 4.3.1, we can maintain positive input in the form of achieving certain secondary goals by properly specifying the tension among cables while controlling the cable robot system to perform primary tasks -- like trajectory tracking in our work. In this work, we will adopt optimization techniques to achieve our control purpose. Specifically, we can optimize the tension among cables by imposing proper objective function and considering components of $\bar{\alpha}$ vector in Eq. (41) as design variable in the optimization processes.

By setting our goal as minimum energy consumption, in the other words, optimal force distribution, optimization schemes using linear programming and quadratic programming can be carried out to in the form of minimizing the actuation forces exerted by cables. Following shows two optimization schemes formulated for this goal in the general form of linear programming as follows.

$$\begin{aligned}
 \min: & \quad W_f^T F \\
 \text{where: } & \quad F = S^{\#}W + \sum_{j=1}^{n-m} \alpha_j N_j = F_p + N(S)\bar{\alpha} \\
 \text{subject to: } & \quad -N(S)\bar{\alpha} \leq F_p
 \end{aligned} \tag{42}$$

W_f is a weighting matrix. For example, If all components of W_f are 1, the objective function becomes $(F_1 + F_1 + \dots + F_n)$

Alternatively, Eq. (42) can be reformulated as follows

$$\begin{aligned}
 \min: & \quad W_f^T \bar{\alpha} \\
 \text{subject to: } & \quad -N(S)\bar{\alpha} \leq F_p
 \end{aligned} \tag{43}$$

5 Active Stiffness Control

5.1 Introduction

The stiffness of robot system has a direct relation with the position accuracy. So, control strategies, generally known as stiffness control, which would provide accurate and stable motion in terms of desired motion trajectory and relationships between position error and external force exerted by the end-effector is proposed. The Stiffness control strategy can be thought as a special case of impedance control that considers only the steady state force/displacement relationship. The stiffness control, while describing the steady state response of stable systems, does not adequately describe nor control the transient response, that is, the transient forces resulting from the dynamic behavior of the system [69].

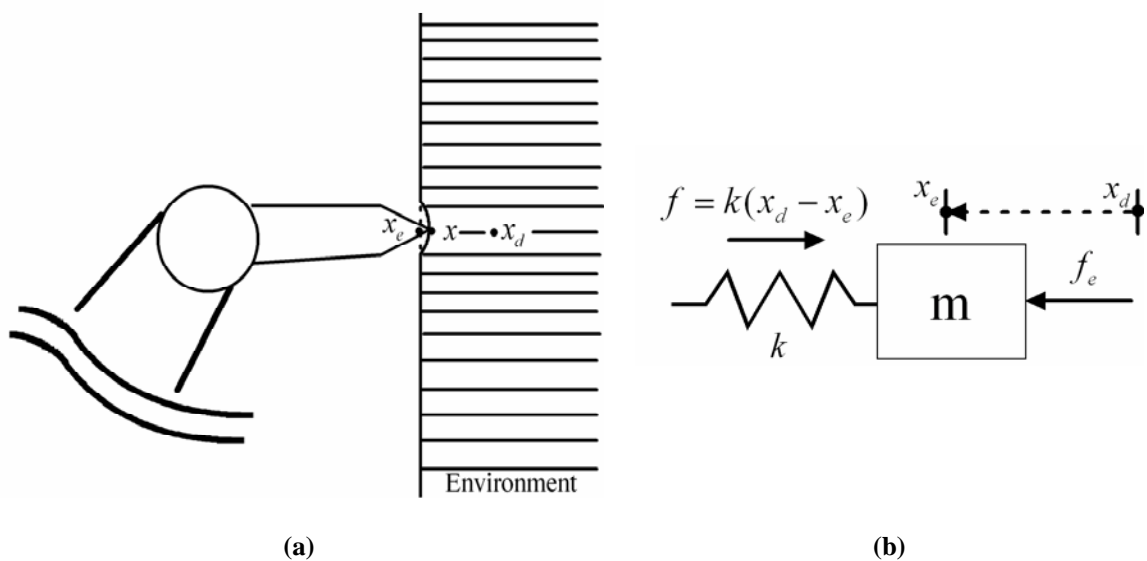


Figure 5-1 Schematic of stiffness control

A simple illustration active stiffness control is shown in Figure 5-1 (a). We assume the end-effector of the manipulator is in contact with the environment whose position is x_e . If the position of the manipulator is $x > x_e$ then the reaction force from the environment can be modeled as

$$f_e = k_e(x - x_e) \quad (44)$$

where k_e is stiffness of the environment,

Moreover, the equation of motion of the system can be given by

$$f = m\ddot{x} + k_e(x - x_e) \quad (45)$$

where f is the force exerted by end-effector to the environment.

In steady state, Eq. (45) can be simplified as

$$f = k_e(x - x_e) = f_e \quad (46)$$

Now, if we want the end-effector to reach the desired position x_d , we can implement a control law as follows

$$f_d = -k(x - x_d) \quad (47)$$

In the new steady state, we will have

$$f_d = f_e \quad (48)$$

By substituting Eq.(46) and Eq.(47) into Eq.(48), then,

$$f_e = \frac{kk_e}{k + k_e}(x_d - x_e) \quad (49)$$

If the environment stiffness k_e is large enough, Eq.(49) can be simplified as

$$f = f_e = k(x_d - x_e) = kdx \quad (50)$$

This control approach as shown in Eq. (50) can be illustrated in Figure 5-1 (b). Through the effect of k , the position error will try to eliminate itself by resulting in resorting force exerted on the environment f_e . Here, k is interpreted as the stiffness of the manipulator, thus we can achieve relationship between interaction force and position error by actively controlling desired stiffness k .

5.2 Active Stiffness Control of Cable Robot System

5.2.1 Cartesian Stiffness of Cable Robot System

Typical cable robot system has “actuation redundancy” property, which means the number of the actuators is larger than that of the degrees of freedom. The advantage of such system is obvious: in one hand, the internal actuation forces distribution is not unique while it executes same effective work to environment in such system; in the other hand, internal actuation forces can generate variation of system stiffness from stiffness analysis in the following section. Based on this property, effective stiffness control strategies can be carried out.

The forces and moments acting on the end-effector, or the reaction forces and moments exerted to the environment by the end-effector, $W = [f \ m]^T$ and deflection of the end-effector δX caused by W can be related by a stiffness matrix K_x as

$$dW = K_x dX \quad (51)$$

where K_x is called Cartesian or task space stiffness matrix. Similarly, tension forces exerted by cables $F = [F_1 \ F_2 \ \dots \ F_n]^T$ and displacement within cables

$\delta l = [\delta l_1 \ \delta l_2 \ \dots \ \delta l_n]$ caused by F can be related by a stiffness matrix (cables are assumed to have linear stiffness property) K_l as

$$dF = K_l dl \quad (52)$$

where K_l is called joint space stiffness matrix, and it is usually a diagonal matrix composed of cable stiffness constants.

Now we can get relationship between joint torques and the end-effector force according to cable system dynamic equation

$$W = SF \quad (53)$$

By taking differentiation of Eq. (53), we get

$$dW = (dS)F + S(dF) \quad (54)$$

and substitute Eq. (51) and Eq. (52) into Eq. (54), we have

$$K_x dX = (dS)F + SK_l(dl) \quad (55)$$

where, $dS = \sum_{i=1}^6 \frac{\partial S}{\partial x_i} dx_i$, which is derived by taking differentiation upon task space

variables $X = (x_1, x_2, \dots, x_6)$. Then, along with the Jacobian $J = \frac{dl}{dX}$, Eq. (55) can be re-

written as

$$K_x = K_g + K_c \quad (56)$$

where

$$K_g = \left[\frac{\partial S}{\partial x_1} F \quad \frac{\partial S}{\partial x_2} F \quad \dots \quad \frac{\partial S}{\partial x_6} F \right] \quad (57)$$

$$K_c = SK_l J = -J^T K_l J \quad (58)$$

Eq. (56) represents the relationship of mapping between Cartesian stiffness and joint stiffness. The term K_g includes the differential Jacobian (a Hessian–3D tensor) and internal actuation force. Since it depends on configuration and cable forces, it can be nonpositive definite and asymmetric.

From the relationship of mapping between Cartesian stiffness and joint stiffness derived above, we can see that Cartesian stiffness is not only related to changes in joint stiffness, but also to changes in system configuration as well as changes in actuation forces or torques in joints. Kao *et, al.* [70] termed this mapping between Cartesian stiffness and joint stiffness as conservative congruence transformation (CCT), and they pointed out the incompleteness of the conventional formulation purposed by Salisbury in [71] based on the fact that work done in joint space and Cartesian space within a robotic system should obey the law of conservation of energy. In conventional mapping between Cartesian stiffness and joint stiffness, the importance of changes in actuation forces or torques to the total stiffness matrix is omitted; however, its contribution to the total stiffness of a system can be very significant, especially in the case of the actuation redundant system.

5.2.2 Cartesian Stiffness Matrix Properties

In literature, studies about stiffness have shown when a system is in its static equilibrium, the resulting stiffness matrix is always symmetric. However, the stiffness matrix can be asymmetric while the system is away from its equilibrium [72], which indicates that some non-conservative forces or moments are applied to the system, such as disturbance forces or moments.

In this work, we only consider the static equilibrium situation, since we are mainly interested in steady state response of stable systems. Thus, stiffness matrix K in our study is always symmetric (as shown in the simulation results in Chapter 7).

Svinin *et al.* [73] studied the stiffness matrix for the stability analysis of fully parallel manipulators. Here, stiffness stability analysis was defined as a property showing if the system with actuation redundancy can be stabilized by actuation forces, which implies that the stiffness can be always improved by increasing the actuation forces. It was shown that for the stabilizability of a redundantly actuated system, the total resulting stiffness matrix should be positive definite. Specifically, a typical cable robot system, if the resulting stiffness of the system can be always improved by increasing the actuation forces in the cables; or mathematically, if the stiffness matrix is positive definite, we call the system is stable. It is also shown that the stiffness matrix which results from the joint compliance is positive definite and hence stable as long as all the joint stiffness coefficients are positive. However, the stiffness matrix which arises from the internal forces is asymmetric and may be unstable if there is an external torque applied to the end-effector [74].

5.2.3 Active Stiffness Control Schemes

By taking advantage of the indeterminacy of actuation forces resulting from actuation redundancy, effective stiffness schemes can be formulated as optimization problem. With different criteria, we can achieve different goals by formulating different objective functions in optimization. $\bar{\alpha}$ vector in Eq. (41) is design variable in optimization process, following shows general form of four schemes based on different scenario.

Before we formulate the optimization schemes, first we need to rewrite Eq. (56) into the following form

$$\overline{K}_X = \overline{K}_g + \overline{K}_c \quad (59)$$

where

$$\overline{K}_X = [K_X(:,1) \ : \ K_X(:,2) \ : \ \dots \ : \ K_X(:,m)]^T_{(m \times (m \times 1))} \quad (60)$$

$$\overline{K}_c = [K_c(:,1) \ : \ K_c(:,2) \ : \ \dots \ : \ K_c(:,m)]^T_{(m \times (m \times 1))} \quad (61)$$

$$\begin{aligned} \overline{K}_g &= HF = H(F_p + N(S)\bar{\alpha}) = HF_p + HN(S)\bar{\alpha} \\ H &= \left[\frac{\partial S}{\partial x_1} \ : \ \frac{\partial S}{\partial x_2} \ : \ \dots \ : \ \frac{\partial S}{\partial x_m} \right]^T_{m \times (m \times n)} \end{aligned} \quad (62)$$

By substituting Eq. (62) into Eq. (59), we will get a form of \overline{K}_X with implicit $\bar{\alpha}$ as

$$\overline{K}_X = \overline{K}_c + HF_p + HN(S)\bar{\alpha} \quad (63)$$

Now, from this we can define the general form of the optimization using Eq. (63) as following.

5.2.3.1 Minimal Force Distribution with Desired Stiffness

$$\begin{aligned} \text{Min:} & \quad W_f^T F \\ \text{Where:} & \quad \overline{K}_c + HF_p + HN(S)\bar{\alpha} = c \\ \text{Subject to:} & \quad -N(S)\bar{\alpha} \leq F_p \end{aligned} \quad (64)$$

c is constant that represents desired end-effector stiffness. W_f is a weighting matrix.

However, this scheme is greatly limited when the number of extra cables is less than $(\gamma - 1)$, γ is the number of independent components of desired stiffness matrix. As we can prove the number of extra cables denotes the dimension of design variable $\bar{\alpha}$, However, in most cases, too many extra cables is not desired, as it will impose the higher

possibility of cable interference and greatly limit the workspace. As the result of that, feasible solution does not always exist in Eq. (64), which means desired stiffness can not be achieved in most designs under this strict criteria. Due to its ineffectiveness and limitation, we will not consider this approach as candidate for active stiffness control schemes.

5.2.3.2 Weighted Stiffness Matrix Approach

Define the error between the desired stiffness and actual stiffness as

$$dK_x = \overline{K_x} - \overline{K_{xd}} \quad (65)$$

Our objective is to reduce dK_x by controlling the redundantly actuated forces exerted by cables. However, as mentioned in Section 5.2.3.1, it is not always possible to realize the desired stiffness in all directions of Cartesian space. Thus, it is necessary that an order of priority can be specified among stiffness of different directions. In this way, flexibility and usability of the control scheme are greatly enhanced. For this purpose, we can formulate the optimization problem as a Quadratic programming problem as follows

$$\begin{aligned} \text{Min:} \quad & \frac{1}{2} dK_x^T W_k dK_x \\ \text{Where:} \quad & \overline{K_x} = \overline{K_c} + HF_p + HN(S)\bar{\alpha} \\ \text{Subject to:} \quad & -N(S)\bar{\alpha} \leq F_p \end{aligned} \quad (66)$$

$$W_k = \begin{bmatrix} w_{11} & 0 & \cdots & 0 \\ 0 & w_{22} & \cdots & 0 \\ \vdots & \vdots & \ddots & \vdots \\ 0 & 0 & 0 & w_{mm} \end{bmatrix}_{\left(\frac{n(n+1)}{2} \times \frac{n(n+1)}{2}\right)} \quad \text{with} \quad \sum_{i=1}^{\frac{n(n+1)}{2}} w_{ii}^2 = 1 \quad (67)$$

where dK_x is a $(\frac{n(n+1)}{2} \times 1)$ vector formed by the unique elements of the stiffness matrix, since the stiffness matrix is symmetric, for a stiffness with n dimension the number of unique elements is $\frac{n(n+1)}{2}$, W_k is a diagonal weighting matrix with its elements corresponding to each unique elements in dK_x .

5.2.3.3 Lower Bound Stiffness Control (LBSC)

The joint space stiffness matrix K_l is usually treated as a constant diagonal matrix composed of the cable stiffness constants representing the stiffness of each of the cables (which are modeled as linear springs), moreover, we only consider controlling cable robot in steady state / equilibrium state, thus, task space (Cartesian) stiffness matrix K_x is a positive semidefinite symmetric matrix and its eigenvalues represent the coefficient of stiffness in the principal directions given by the eigenvectors. These directions are in fact represented by twist vectors, i.e., generalized velocity vectors. [18]. Therefore, we can guarantee the stiffness lower bound σ_{\min}^{des} through the control of the smallest eigenvalue $\sigma_{\min}(K_x)$ of task space stiffness matrix K_x , and the directions of maximum and minimum stiffness are determined by the eigen vectors σ_{\min} and σ_{\max} of K_x .

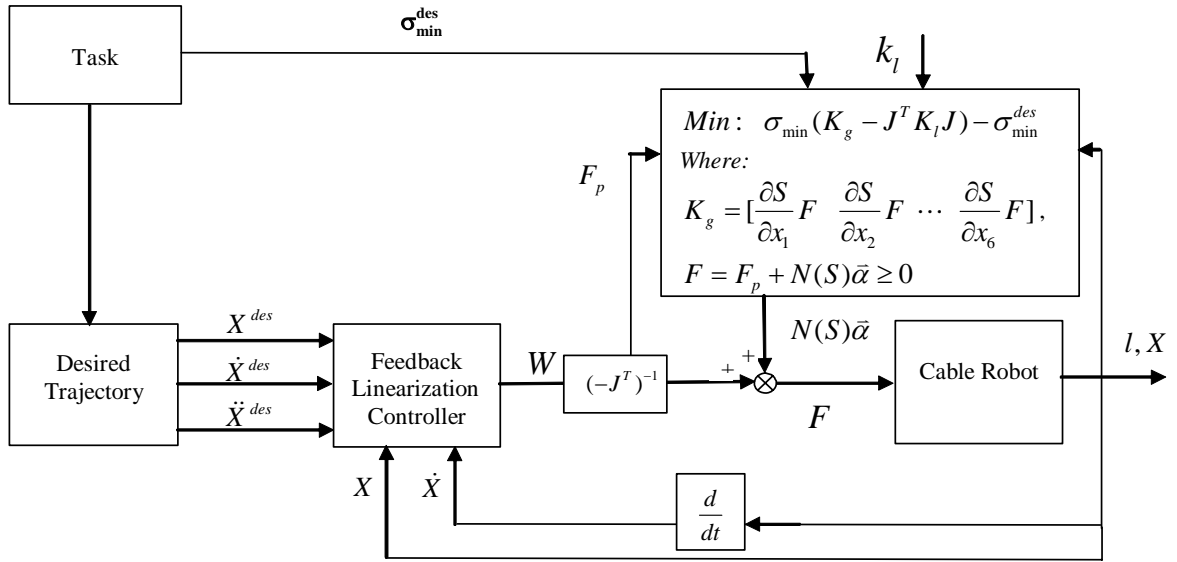


Figure 5-2 Block diagram of Lower Bound Stiffness Control [75] for cable robot

The principle of this control scheme is shown in Figure 5-2. k_l is prescribed stiffness constant of each cable. In each iteration, cable control input forces are solved as an optimization problem with explicit design variable $\bar{\alpha}$ to minimize the objective function $f = \sigma_{\min}(K_X) - \sigma_{\min}^{des} = \sigma_{\min}(K_g - J^T K_l J) - \sigma_{\min}^{des}$ under constraint of positive cable input forces F . Then the simultaneous position and velocity information of the cable robot are feedback to the feedback linearization controller, such that new task space control output is generated according to errors between desired and actual kinematics information of the cable robot. This output then is filtered through the inverse dynamics operator $(-J^T)^{-1}$ to calculate the particular solution and homogenous solution of new cable control input forces candidates in terms of design variable $\bar{\alpha}$ (for details refer to Section 4.3.1.) Last, the design variable $\bar{\alpha}$ is solved through the optimization solver and the optimized new cable control input forces F is obtained to complete a control loop.

6 Simulation

6.1 Virtual Model Simulation and Analysis Framework

In past decade, great advances in computational power and tools enable engineers and researcher to perform many computer based high fidelity simulations. People can use computer to simulate the visualized physical response of their virtual 3D CAD model in the area of their interest, such as kinematics, dynamics, heat transfer, vibration, stress models with related software package in controlled virtual environment. This methodology is termed as Virtual Prototyping (VP), also known as Simulation-Based Design (SBD). Although a virtual prototype can never fully replace a physical prototype mainly because of the lack of fully understandings of some complex physical effects, it enables people to learn about the actual operation and performance of their theoretical designs realistically, accurately and quantitatively before getting into costly, time-consuming and sometimes inaccurate physical prototype test too early. With these advantages, Virtual Prototyping has rapidly gained popularity and become a crucial part of most engineering design processes [76].

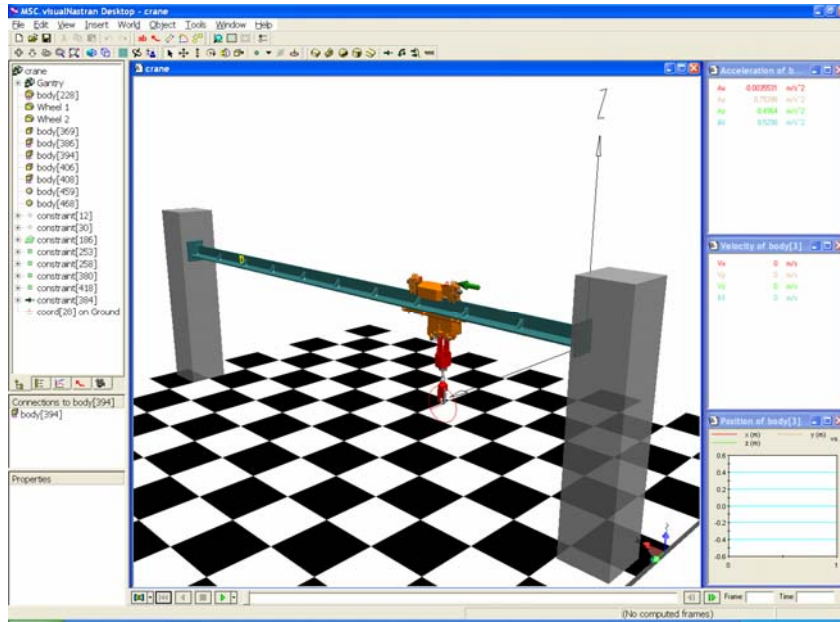


Figure 6-1 An overhead crane model within MSC.visualNastran4D

One of the well known simulation packages includes MSC.visualNastran4D, an example of the use of such a tool is illustrated in Figure 6-1. It shows an overhead crane model examined within MSC.visualNastran4D, the crane is supported by a horizontal beam 10m in length. Below it hangs a large hook for carrying loads. A horizontal force (e.g., via a cable) is applied to the crane to move it along the beam. With this model, users can do various simulations based on design intentions; for example, evaluate the torque output of driving motor needed to move the crane from one point along the beam to another in a timely fashion without exceeding performance limits.

6.2 MSC.visualNastran 4D Implementation Framework

The next step undertaken is the implementation in a virtual simulation, control, and analysis framework to simulate our control schemes for cable robot system. In this section, we will discuss the development of the development of a MATLAB Simulink MSC visualNastran integrated analysis framework for virtual simulation of our design,

MATLAB Simulink. Finally, different disturbance forces from environment were also imposed to validate the effectiveness of our stiffness control scheme.

6.2.1 Overall Simulation Routine

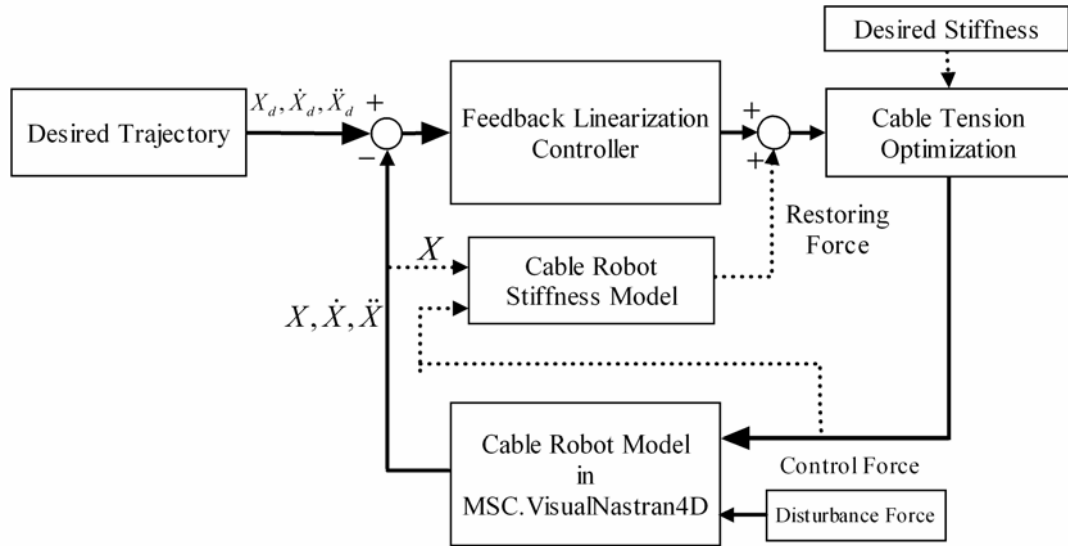


Figure 6-3 Block diagram of overall simulation routine

A block diagram of our simulation routine is shown in Figure 6-3. It is composed of seven blocks: desired trajectory, feedback linearization controller, cable tension optimization, cable robot model in MSC. visualNastran 4D, Desired stiffness, cable robot stiffness model and disturbance force. The *Cable Robot model in MSC. visualNastran 4D* block contains the virtual prototype of cable robot system built in MSC. visualNastran 4D, it serves as the plant being controlled by cable forces input that are generated in MATLAB/Simulink in the simulation routine. This block outputs simultaneous information of the robot system in position, velocity and acceleration levels, which serves as the feedback input to the *Feedback Linearization Controller* block, such that correcting control inputs to the cable robot will be generated according to desired

trajectory information specified in *desired trajectory* block. The *Cable Tension Optimization* block serves as the decision making and secondary tasks block to regulate control inputs from Feedback Linearization Controller block depending on different redundancy resolution schemes implemented. In our work, it is used to achieve minimal forces exertion among cables and active stiffness control in the premise of maintaining cables in tension. The *Desired Stiffness* block is used to specify desired end-effector stiffness of cable robot in active stiffness control. The *Cable Robot Stiffness* block contains the stiffness model of cable robot developed in Section 5.2.3 and serves a part of active stiffness control scheme. Inputs of this block include the position information, input control cable forces, cables stiffness constant and configuration information of current system. The Output of this block is the resorting force corresponding to controlled stiffness along with position error generated by disturbance force from *Disturbance Force* block. This resorting force serves as the compensation in disturbance rejection scenario.

6.3 Our Systems

In our work, a variety of cable robot systems based on different configurations are studied. Each configuration of virtual prototype in our simulation is discussed in greater detail as follows.

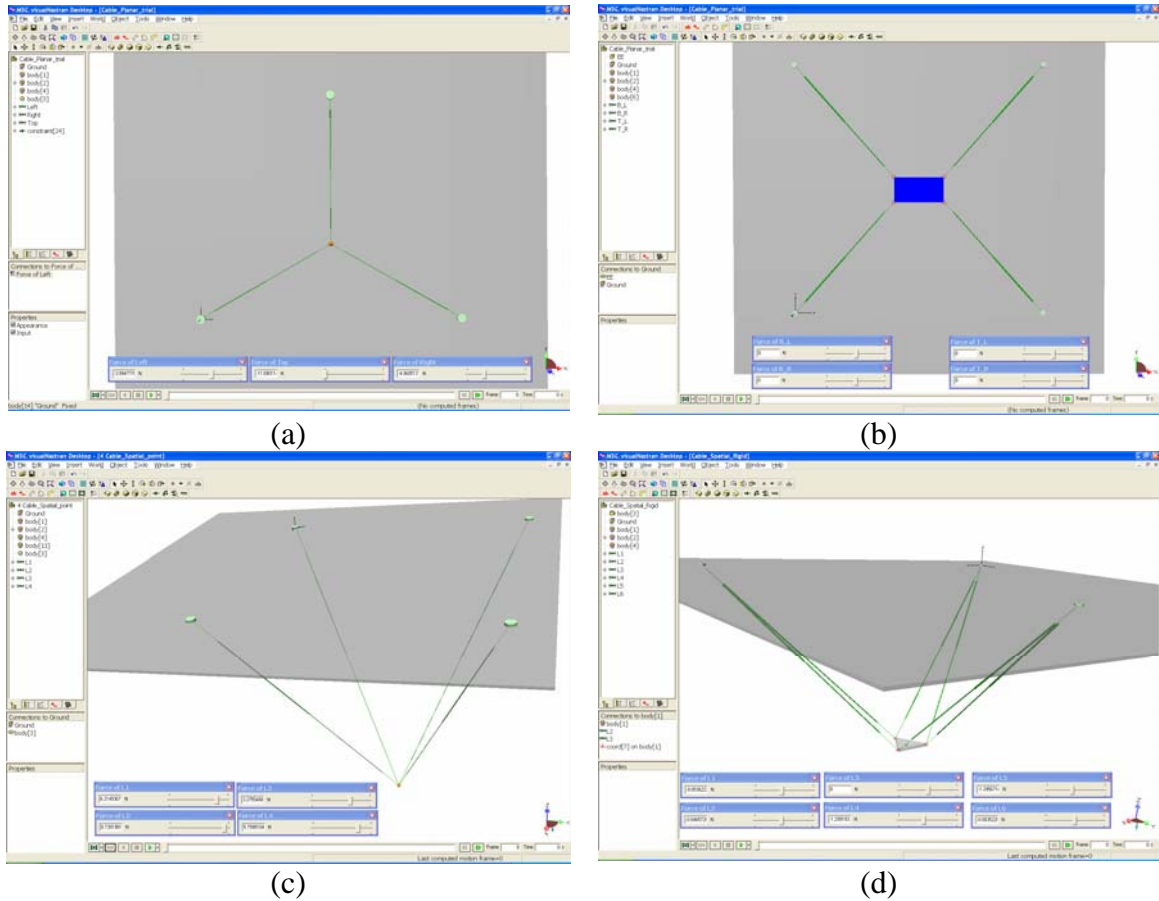


Figure 6-4 Virtual prototypes of cable robot systems

6.3.1 Planar Point Mass Cable Robot

In planar point mass cable robot system as shown in Figure 6-4 (a), the end-effector is modeled as a point mass and attached by three cables, which are actuated by one motor separately in a plane. The three motors forming the base are located at $(0, 0)$ m, $(0.6, 0)$ m, and $(0.3, 0.52)$ m. The initial position of the end-effector is located at $(0.35, 0.173)$ m, which is the center of the equilateral triangle formed by the boundary of the base. As we can see, this system is fully constrained as defined in Section 1.1. It has one redundant actuation since the end-effector has two DOF while it is driving by three cables.

6.3.2 Planar Rigid Body Cable Robot

In planar rigid body cable robot system as shown in Figure 6-4 (b), the end-effector is modeled as a rigid cuboid and attached by four cables, which are actuated by one motor separately in a plane. The four motors forming the base are located at (0, 0) m, (1, 0) m, (1, 1) m and (0, 1) m. The initial position of the end-effector is located at (0.5, 0.5) m, which is the center of the square formed by the boundary of the base. As we can see, As we can see, this system is fully constrained as defined in Section 1.1. It has one redundant actuation since the end-effecotr has three DOF while it is driving by four cables.

6.3.3 Spatial Point Mass Cable Robot

In spatial point mass cable robot system as shown in Figure 6-4 (c), the end-effector is modeled as a point mass and attached by four cables, which are actuated by one motor separately in a 3-D space. The four motors forming the base are located at (0, 0) m, (0.6, 0) m, (0.6, 0.6) m and (0, 0.6) m. The initial position of the end-effector is located at (0.3, 0.3, - 0.6) m, which is the center of the square formed by the boundary of the base in X-Y direction. As we can see, this system is fully constrained as defined in Section 1.1. It has one redundant actuation since the end-effecotr has three DOF while it is driving by four cables.

6.3.4 Spatial Rigid Body Cable Robot

In spatial rigid body cable robot system as shown in Figure 6-4 (d), the end-effector is modeled as a point mass and attached by six cables, which are actuated by one motor separately in a 3-D space. The six motors forming the base are located at (0, 0) m,

(1, 0) m, and (0.5, 0.866) m. The initial position of the end-effector is located at (0.5, 0.2887, - 0.5) m, which is the center of the equilateral triangle formed by the boundary of the base in X-Y direction. As we can see, the end-effecotr of this system has six DOF while it is driving by six cables. In our work, we can also consider such system has one redundant actuation, since the gravity of the end-effector can serve as an actuation with fixed magnitude and direction.

7 Results

In this section, we will discuss the results of application of the control schemes developed in Chapter 4 and Chapter 5 to a variety of cable robot configurations described in Section 6.3, which are summarized as follows:

Case A -- Planar Point Mass:

In planar point mass cable robot system, the end-effector is modeled as a point mass and attached by three cables and actuated by one motor separately in a plane as shown in Fig Figure 6-4 (a).

Case B -- Planar Rigid Body:

In planar rigid body cable robot system, the end-effector is modeled as a rigid cuboid and attached by four cables and actuated by one motor separately in a plane as shown in Fig Figure 6-4 (b).

Case C -- Spatial Point Mass:

In spatial point mass cable robot system, the end-effector is modeled as a point mass and attached by four cables and actuated by one motor separately in a 3-D space as shown in Figure 6-4 (c).

Case D -- Spatial Rigid Body:

In spatial rigid body cable robot system, the end-effector is modeled as a point mass and attached by six cables and actuated by one motor separately in a 3-D space as shown in Figure 6-4 (d).

According to the control schemes, difference simulation scenarios are introduced. First we will perform trajectory tracking tasks with minimal force distribution among

cables. Then we will perform trajectory tracking tasks augmented with active stiffness control schemes – (a) weighted stiffness matrix; (b) Lower bound stiffness control. Last, we will introduce disturbance to test the effectiveness of our active stiffness control scheme. The case studies to be shown in this section are listed in Table 7-1. In the subsequent results we only highlight the parameters that make each result unique.

	Trajectory Type	Case A	Case B	Case C	Case D
Minimal Force Distribution	<i>Point stabilization</i>		×		×
	<i>Straight line tracking</i>		×		×
	<i>Circle tracking</i>	×		×	×
Active Stiffness Control	<i>Straight line tracking</i>		×		
	<i>Circle tracking</i>	×			
Response to Disturbance	<i>Straight line tracking</i>		×		

Table 7-1 Select simulation scenarios for different cases

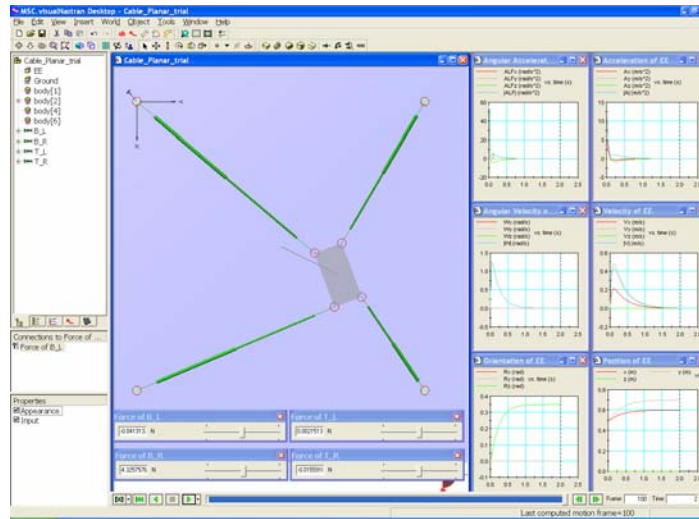
7.1 Trajectory Tracking with Minimal Cable Force Distribution

In this section, the simulation results show the performance of cable robots with various configurations mentioned in Section 6.3 implemented by trajectory tracking controller developed in Section 4.1 and the actuation redundancy resolution scheme with the goal of minimization of input control force among cables developed in Section 4.3.

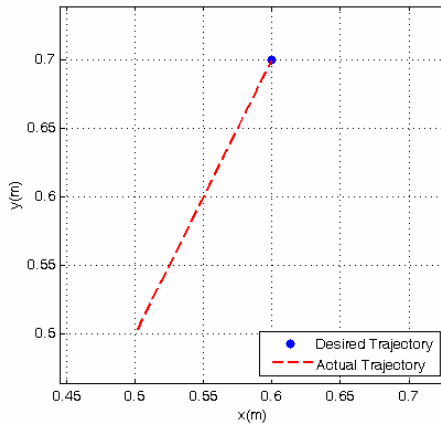
7.1.1 Point Stabilization with Case B

In this simulation scenario, the end-effector of case B is initially at $(0.5, 0.5)m$, $\phi = 0 \text{ rad}$, and the desired final position is $(0.6, 0.7)m$, $\phi = \pi/9 \text{ rad}$. Figure 7-1 (b) shows the path the end-effector move to the desired position. In Figure 7-1 (c) and Figure 7-1 (d), we can see the initial position converges to the desired position asymptotically in very short time span. Moreover, the tension profile among cables that

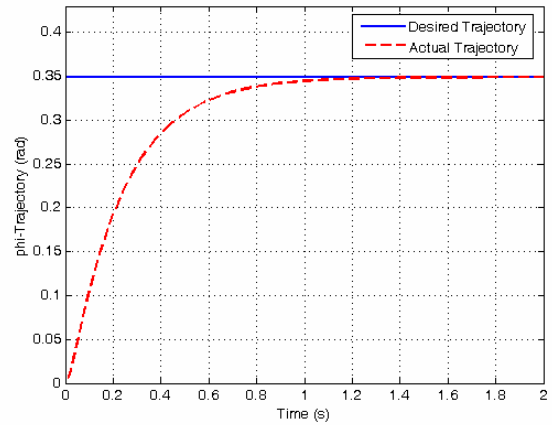
driving the end-effector shown in Figure 7-1 (e) are always positive, and they are being controlled to reduce to zero while the end-effector is converging to desired position.



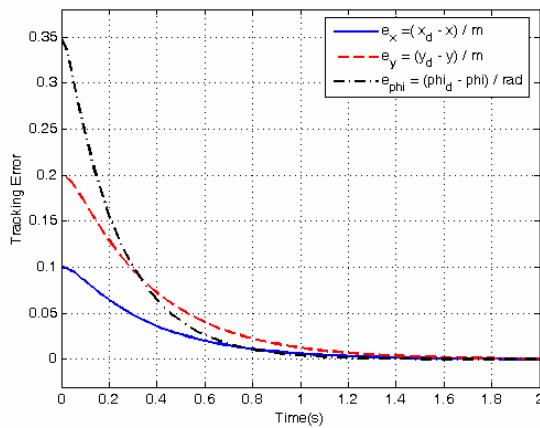
(a)



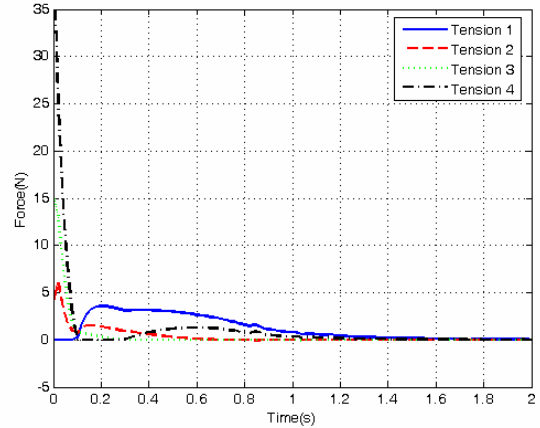
(b)



(c)



(d)

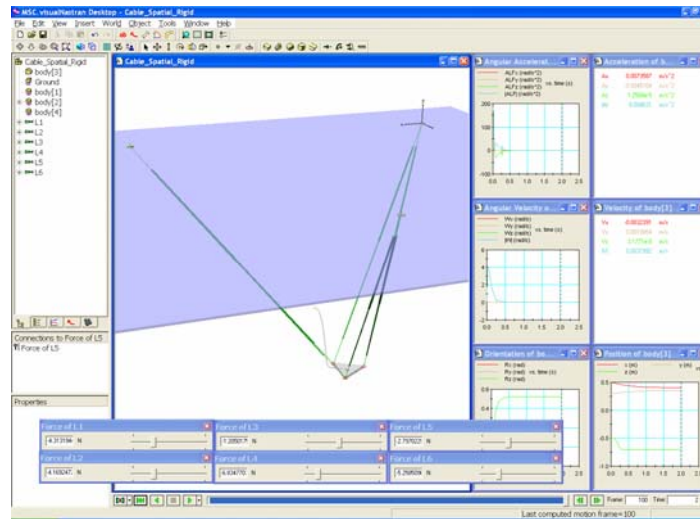


(e)

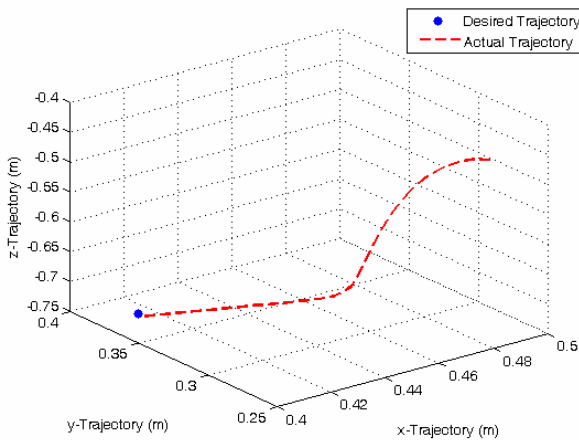
Figure 7-1 Point stabilization with Case B

7.1.2 Point Stabilization with Case D

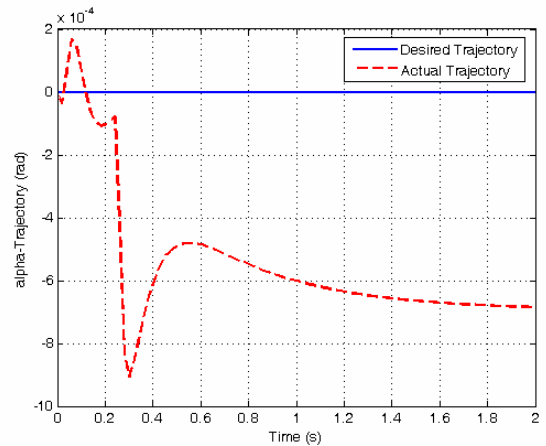
In this simulation scenario, the end-effector of case D is initially at $(0.5, 0.2887, -0.5)m$, $\alpha = 0 \text{ rad}$, $\beta = 0 \text{ rad}$, $\phi = 0 \text{ rad}$ and the desired final position is $(0.4m, 0.35, -0.7) m$, $\alpha = 0 \text{ rad}$, $\beta = 0 \text{ rad}$, $\phi = \pi/6 \text{ rad}$. Figure 7-2 (b) shows the path the end-effector move to the desired position. In Figure 7-2 (c-f), we can see the initial position converges to the desired position asymptotically in very short time span. Moreover, the tension profile among cables that driving the end-effector shown in Figure 7-2 (g) are always positive, and they are being controlled to reduce to constant values while the end-effector is converging to desired position.



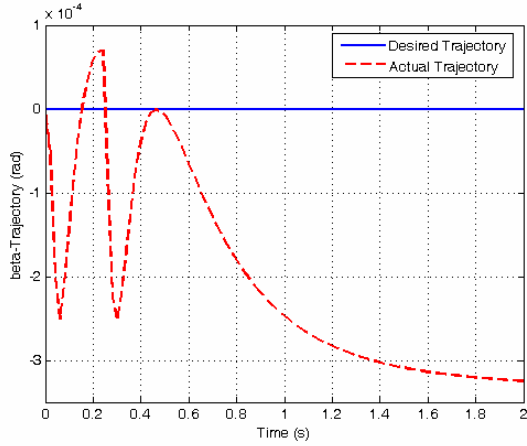
(a)



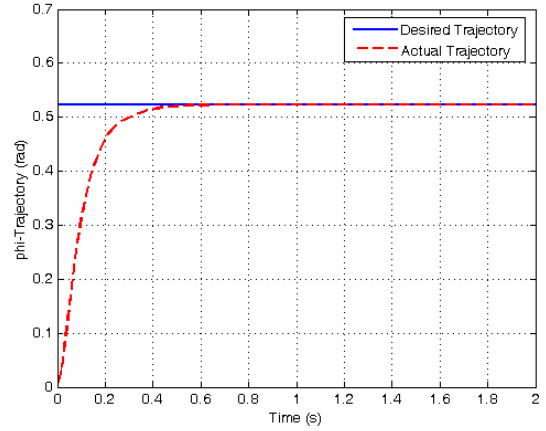
(b)



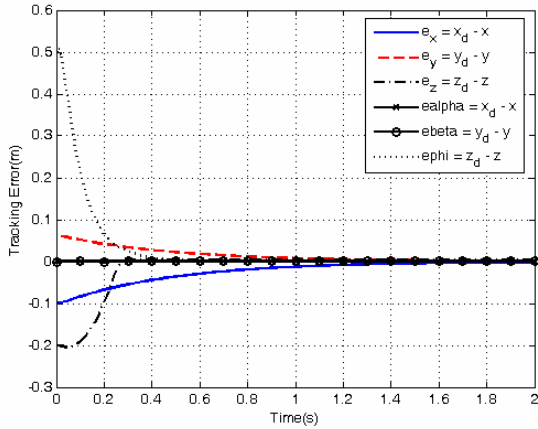
(c)



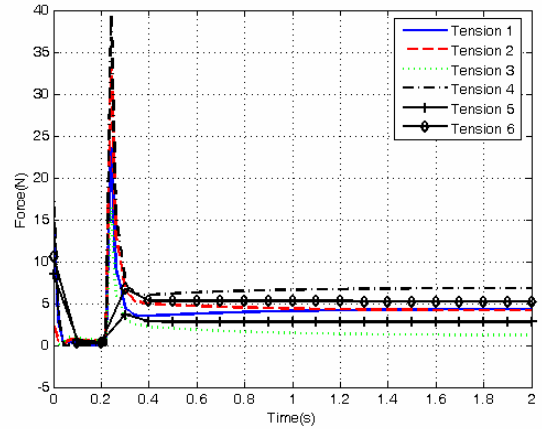
(d)



(e)



(f)

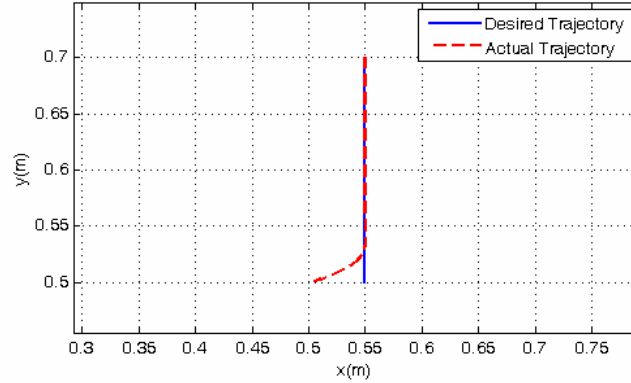


(g)

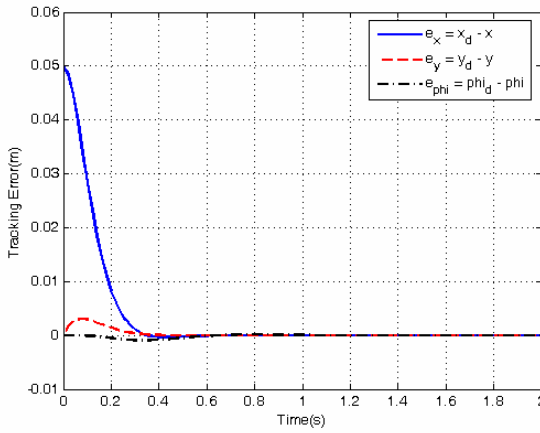
Figure 7-2 Point stabilization with Case D

7.1.3 Straight Line Tracking with Case B

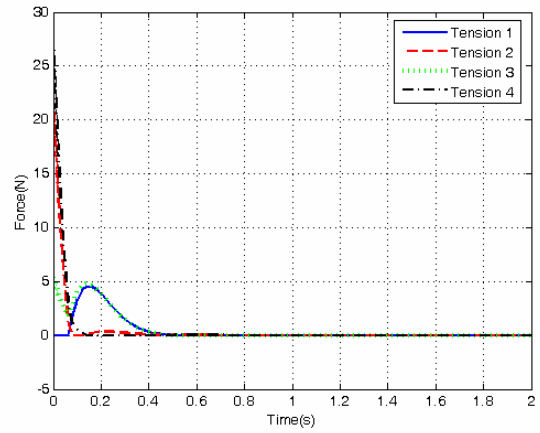
In this simulation scenario, the end-effector of case B is initially at $(0.5, 0.5) m$, $\phi = 0 rad$ and the desired end-effector trajectory is a straight line $x = 0.55 m$, $y = (0.5 + 0.1t) m$, $\phi = 0 rad$ such that the desired velocity is $0.1 m/s$. In Figure 7-3 (a) and Figure 7-3 (b), we can see the initial position converges to the desired trajectory asymptotically in very short time span. Moreover, the tension profile among cables that driving the end-effector shown in Figure 7-3 (c) are always positive, and they are being controlled to reduce to zero while the end-effector is converging to desired trajectory.



(a)



(b)



(c)

Figure 7-3 Straight line tracking with Case B

7.1.4 Straight Line Tracking with Case D

In this simulation scenario, the end-effector of case D is initially at $(0.5, 0.3, -0.5)m$, $\alpha = 0 \text{ rad}$, $\beta = 0 \text{ rad}$, $\phi = 0 \text{ rad}$ and the desired end-effector trajectory is a straight line $x = 0.53m$, $y = (0.3 + 0.1t)m$, $z = (-0.5 + 0.1t)m$ such that the desired velocity is 0.1414 m/s . In Figure 7-4 (a) and Figure 7-4 (b), we can see the initial position converges to the desired trajectory asymptotically in very short time span. Moreover, the tension profile among cables that driving the end-effector shown in

Figure 7-4 (c) are always positive while the end-effector is converging to desired trajectory.

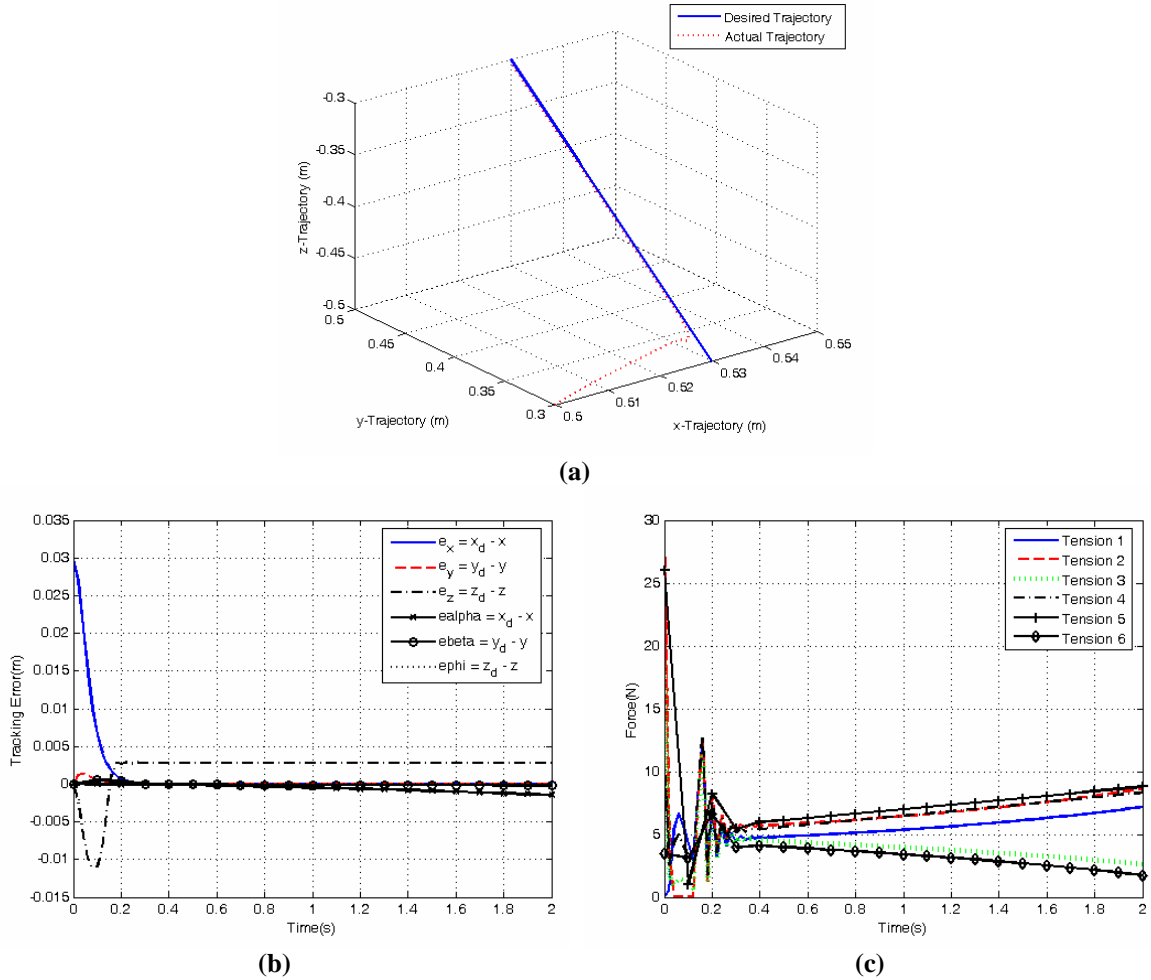


Figure 7-4 Straight line tracking with Case D

7.1.5 Circle Tracking with Case A

In this simulation scenario, the end-effector of case A is initially at $(0.3, 0.173) m$ and the desired end-effector trajectory is a straight line $x = (0.3 + 0.1\cos(t)) m$, $y = (0.173 + 0.1\sin(t)) m$ such that the desired velocity is $0.1 m/s$. In Figure 7-5 (a) and Figure 7-5 (b), we can see the initial position converges to the desired trajectory asymptotically in very short time span. Moreover, the tension profile

among cables that driving the end-effector shown in Figure 7-5 (c) are always positive, and they are being controlled to reduce to zero while the end-effector is converging to desired trajectory.

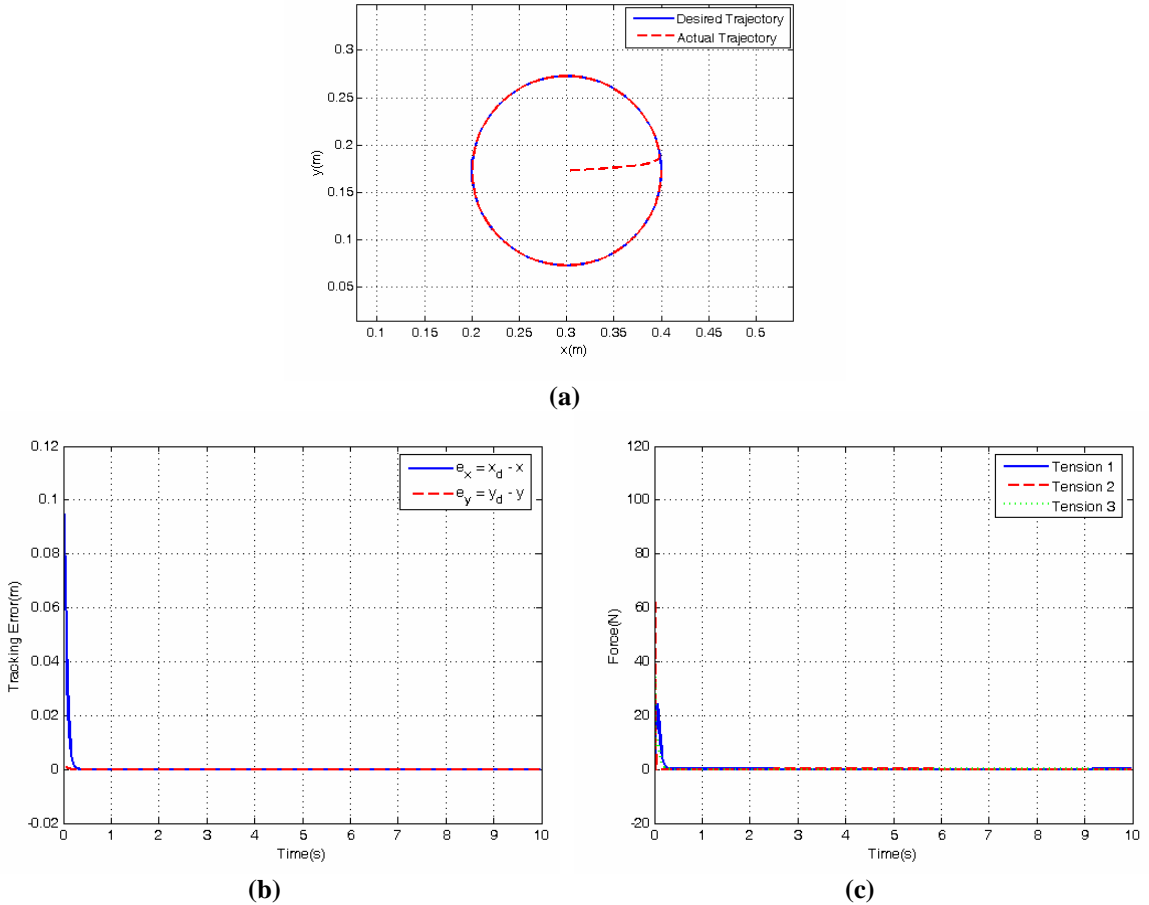
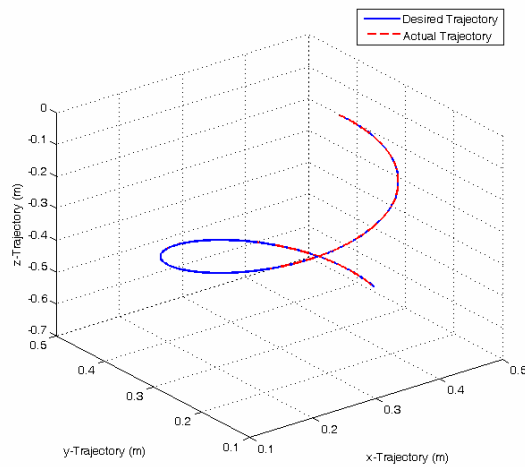
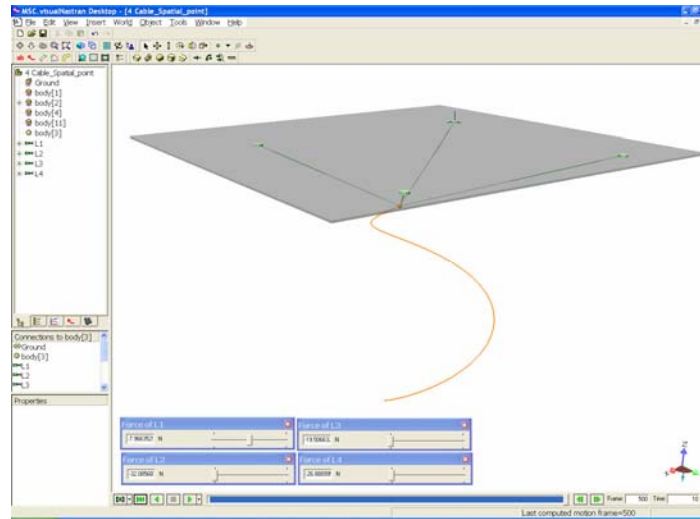


Figure 7-5 Circle tracking with Case A

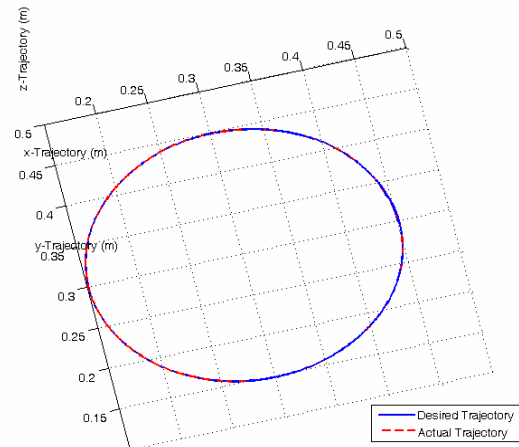
7.1.6 Circle Tracking with Case C

In this simulation scenario, the end-effector of case C is initially at $(0.45, 0.3, -0.6)m$ and the desired end-effector trajectory is a circle in X-Y plane: $x = (0.3 + 0.15 \cos(2t/3))m$, $y = (0.3 + 0.15 \sin(2t/3))m$, $z = (-0.6 + 0.05t)m$. In Figure 7-6 (a-c), we can see the end-effector tracks the desired trajectory very well.

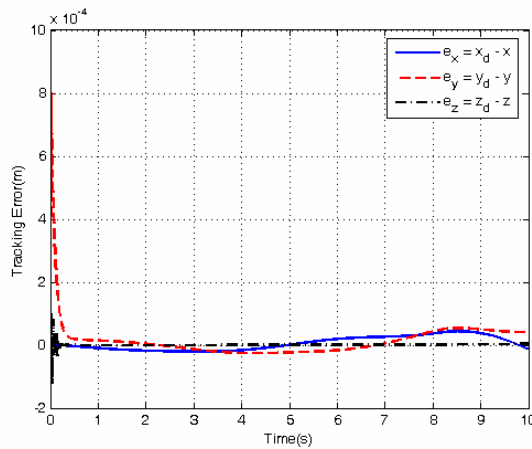
Moreover, the tension profile among cables that driving the end-effector shown in Figure 7-6 (d) are always positive while the end-effector is tracking desired trajectory.



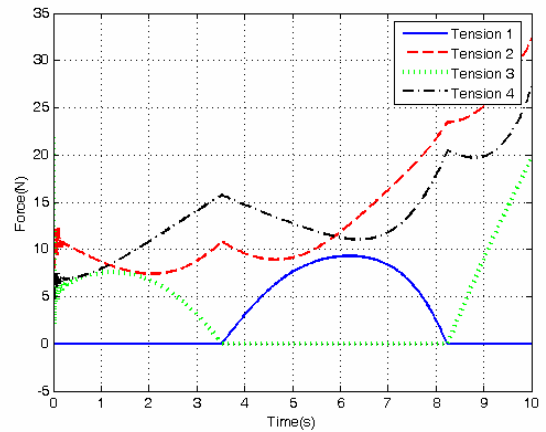
(a)



(b)



(c)

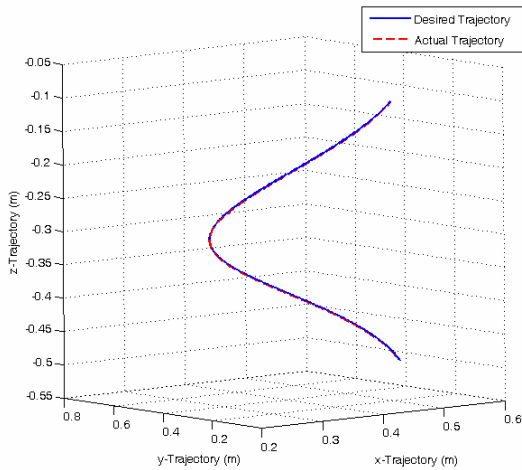
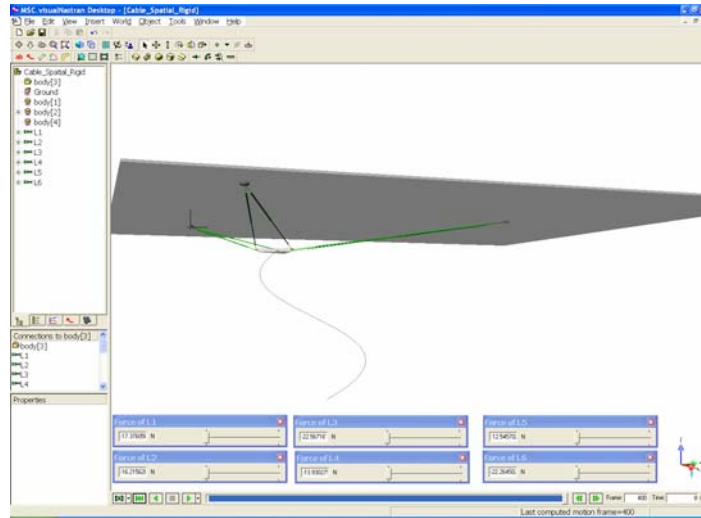


(d)

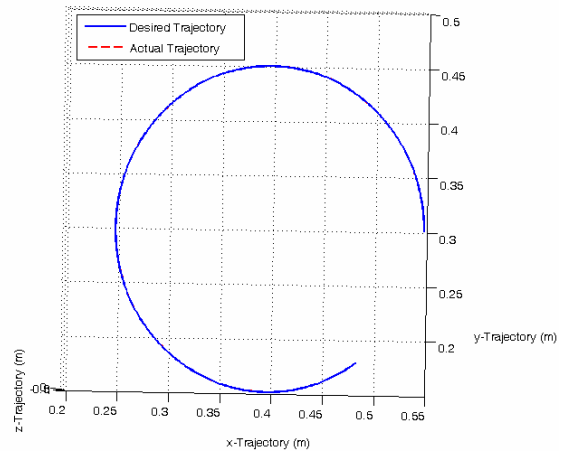
Figure 7-6 Circle tracking with Case C

7.1.7 Circle Tracking with Case D

In this simulation scenario, the end-effector of case D is initially at $(0.55, 0.3, -0.5)m$, $\alpha = \beta = \phi = 0 \text{ rad}$ and the desired end-effector trajectory is a circle in X-Y plane: $x = (0.4 + 0.15 \cos(2t/3))m$, $y = (0.3 + 0.15 \sin(2t/3))m$, $z = (-0.6 + 0.05t)m$, $\alpha = \beta = \phi = 0 \text{ rad}$. In Figure 7-7 (a-c), we can see the end-effector tracks the desired trajectory very well. Moreover, the tension profile among cables that driving the end-effector shown in Figure 7-7 (d) are always positive while the end-effector is tracking desired trajectory.



(a)



(b)

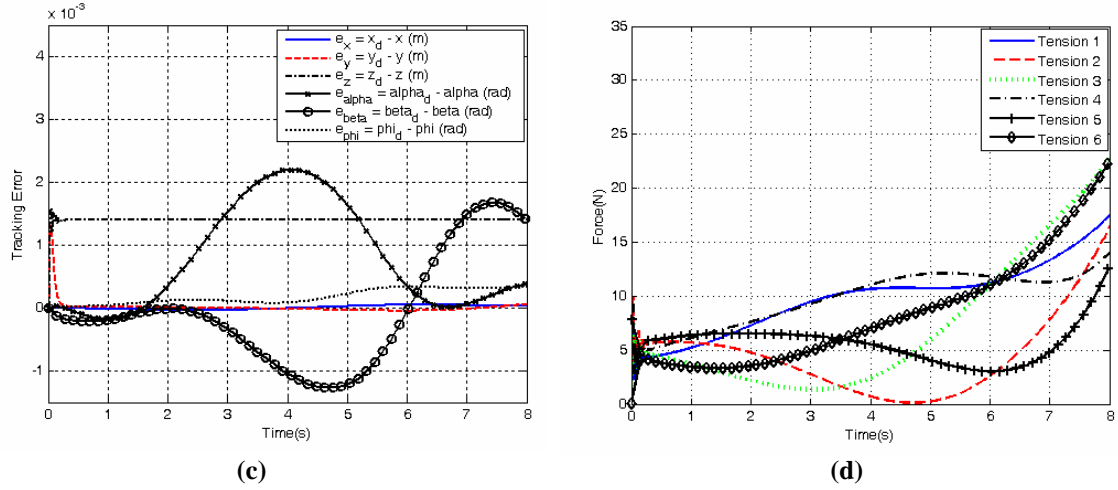


Figure 7-7 Circle tracking with Case D

7.2 Trajectory Tracking Augmented with Active Stiffness Control

In this section, the simulation results show the performance of cable robots with various configurations mentioned in Section 6.3 implemented by trajectory tracking controller developed in Section 4.1 and the two active stiffness control schemes in Section 5.2.3. Without loss of generality, the stiffness constant of cables in all cases is set to 1 N/m . The active stiffness schemes are briefly summarize as follows:

Weighted Stiffness Matrix:

As mentioned in Section (5.2.3), it is not always possible and necessary to realize the desired stiffness in all directions of end-effecotr (Cartesian space) of a cable robot system. Thus, We can achieve the control of stiffness in desired directions by assigning a weighting matrix to prioritize the elements in the stiffness matrix to be controlled. Specifically, in our work, we will only consider the diagonal elements in the stiffness matrix when formulating the weighting matrix, since the non-diagonal elements are highly coupled, and they have much less effect than the diagonal element to the overall stiffness of the workspace of cable robot system.

Lower Bound Stiffness Control (LBSC):

This scheme guarantees a lower bound of the end-effector stiffness, thus, it is very useful in the applications that need high enough stiffness in all directions of the end-effector during interaction with environment under uncertain disturbances.

In the subsequent sections, several simulation scenarios are performed to validate the effectiveness of these two schemes proposed in this work, they are summarized as follows:

7.2.1 Straight line tracking augmented with active stiffness control with case B

7.2.1.1 Weighted stiffness matrix

7.2.1.1.1 Controlling the stiffness in X and Y directions

7.2.1.1.2 Controlling the stiffness in rotational direction

7.2.1.2 Lower bound stiffness control

7.2.2 Circle Tracking augmented with active stiffness control with case A

7.2.2.1 Weighted stiffness matrix

7.2.2.1.1 Controlling the stiffness in X directions

7.2.2.1.2 Controlling the stiffness in X and Y direction

7.2.2.2 Lower bound stiffness control

7.2.1 Straight Line Tracking Augmented Stiffness Control with Case B

In this simulation scenario, the end-effector of case B is initially at $(0.5, 0.5)m$, $\phi = 0 \text{ rad}$ and end-effector trajectory, as shown in Figure 7-8, is a straight line $x = 0.55m$, $y = (0.5 + 0.1t)m$, $\phi = 0 \text{ rad}$ such that the desired velocity is 0.1 m/s .

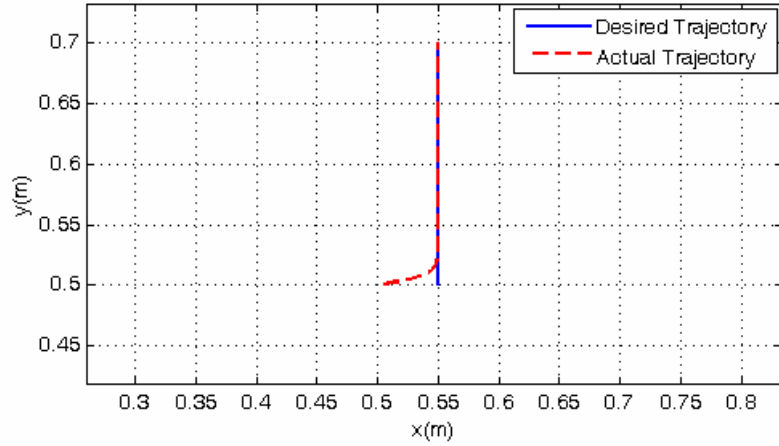


Figure 7-8 Straight line trajectory with Case B

7.2.1.1 Weighted Stiffness Matrix

According to Section 5.2.3.2 , the general form of weighted stiffness matrix for case B can be written as

$$dK_x = [dK_{xx} \quad dK_{xy} \quad dK_{x\phi} \quad dK_{yy} \quad dK_{y\phi} \quad dK_{\phi\phi}]^T \quad (68)$$

and the weighting matrix

$$W = \text{diag}[W_{K_x} \quad W_{K_{xy}} \quad W_{K_{x\phi}} \quad W_{K_y} \quad W_{K_{y\phi}} \quad W_{K_{\phi}}] \quad (69)$$

7.2.1.1.1 Control of Stiffness in X and Y Directions

Case Study 1: $[K_{dx} \quad K_{dy} \quad K_{d\phi}] = [50N/m \quad 50N/m \quad 50Nm/rad]$

In this case, the desired stiffness in all direction is $K_d = \text{diag}[K_{dx} \quad K_{dy} \quad K_{d\phi}] = [50N/m \quad 50N/m \quad 50Nm/rad]$. However, the stiffness in X and Y directions (K_x and K_y) are primarily important. Hence, our goal is to reduce $dK_x = (K_{dx} - K_x)$ and $dK_y = (K_{dy} - K_y)$ with equal priority. Accordingly, we set the weighting matrix in Eq.(7.2) as $W = \text{diag}[\sqrt{0.5} \quad 0 \quad 0 \quad \sqrt{0.5} \quad 0 \quad 0]$, which means

$W_{K_x} = \sqrt{0.5}$, $W_{K_y} = \sqrt{0.5}$, $W_{K_\phi} = 0$. In Figure 7-9 (b), we can see the end-effector tracks the desired trajectory very well, while the corresponding tension profile among cables that driving the end-effector shown in Figure 7-9 (a) are always positive. Moreover, in Figure 7-9 (c-d), we can see the stiffness in x and y -directions are very near the desired stiffness 50 N/m and with similar errors, however, the value of stiffness in ϕ directions is around 10 N/m, which is far less than the desired stiffness.

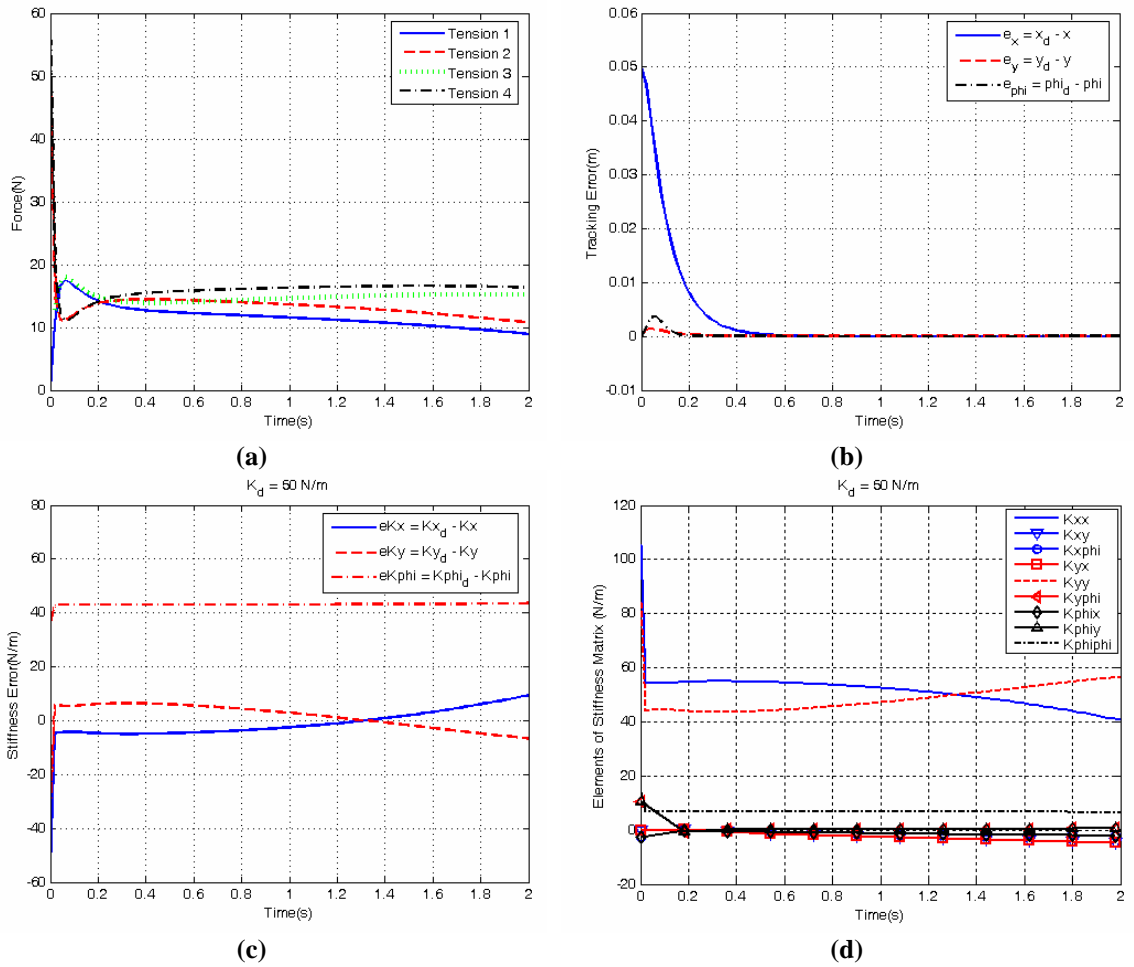


Figure 7-9 Controlling the stiffness in X and Y directions with Case B, $K_d = 50 \text{ N/m}$

Case Study 2: $[K_{dx} \ K_{dy} \ K_{d\phi}] = [100N/m \ 100N/m \ 100Nm/rad]$

In this case, the desired stiffness in all direction is $K_d = \text{diag}[K_{dx} \ K_{dy} \ K_{d\phi}] = [100N/m \ 100N/m \ 100Nm/rad]$. However, the stiffness in X and Y directions (K_x and K_y) are primarily important. Hence, our goal is to reduce $dK_x = (K_{dx} - K_x)$ and $dK_y = (K_{dy} - K_y)$ with equal priority. Accordingly, we set the weighting matrix in Eq.(7.2) as $W = \text{diag}[\sqrt{0.5} \ 0 \ 0 \ \sqrt{0.5} \ 0 \ 0]$, which means $W_{Kx} = \sqrt{0.5}$, $W_{Ky} = \sqrt{0.5}$, $W_{K\phi} = 0$.

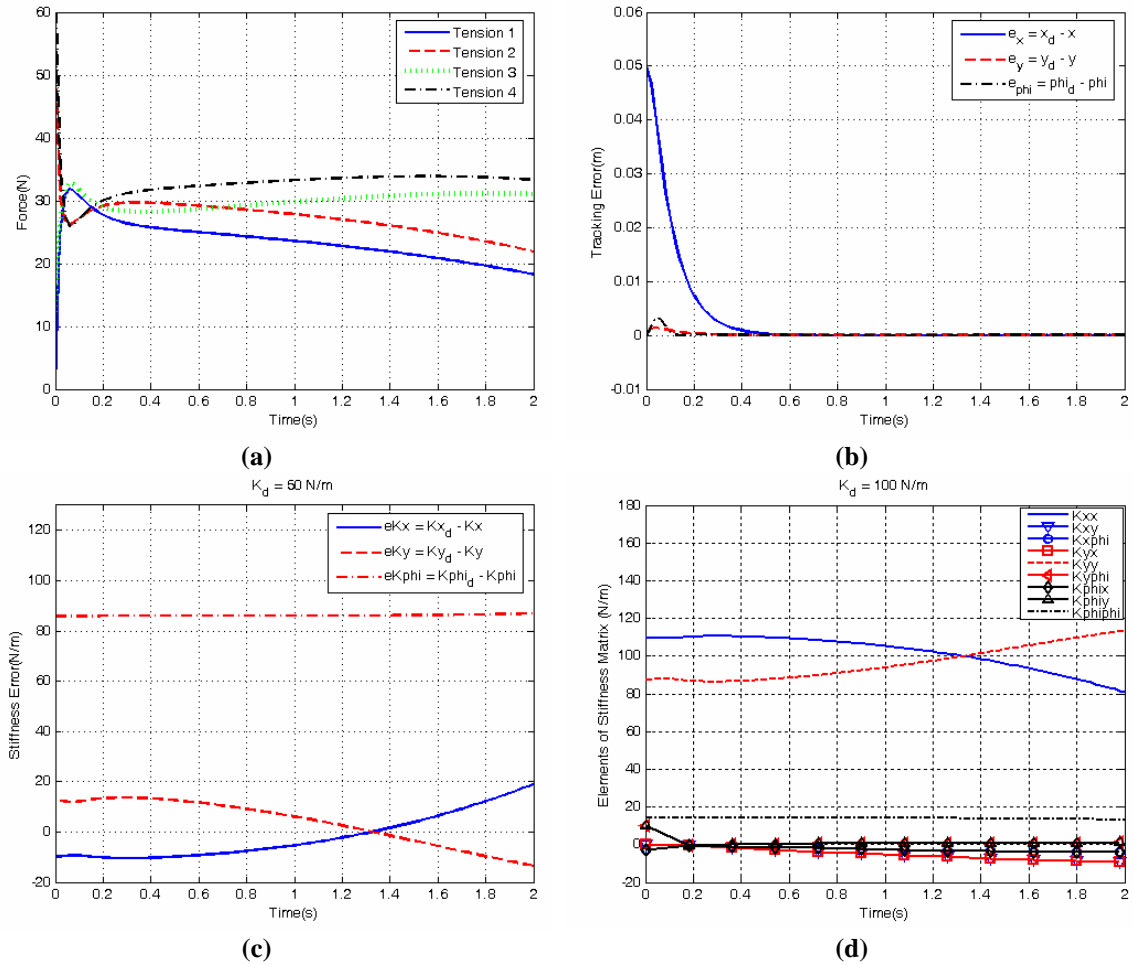


Figure 7-10 Controlling the stiffness in X and Y directions with Case B, $K_d = 100N/m$

In Figure 7-10 (b), we can see the end-effector tracks the desired trajectory very well, while the corresponding tension profile among cables that driving the end-effector shown in Figure 7-10 (a) are always positive. Moreover, in Figure 7-10 (c-d), we can see the stiffness in X and Y directions are very near the desired stiffness 100 N/m and with similar errors, however, the value of stiffness in ϕ directions is around 18 N/m, which is far less than the desired stiffness.

7.2.1.1.2 Control of Stiffness in Rotational Direction

Case Study 1: $[K_{dx} \ K_{dy} \ K_{d\phi}] = [50N/m \ 50N/m \ 50Nm/rad]$

In this case, the desired stiffness in all direction is $K_d = diag[K_{dx} \ K_{dy} \ K_{d\phi}] = [50N/m \ 50N/m \ 50Nm/rad]$. However, the stiffness in the rotational directions ϕ (K_ϕ) are primarily important. Hence, our goal is to reduce $dK_\phi = (K_{d\phi} - K_\phi)$ with priority. Accordingly, we set the weighting matrix in Eq.(7.2) as $W = diag[0 \ 0 \ 0 \ 0 \ 0 \ 1]$, which means $W_{K_x} = 0$, $W_{K_y} = 0$, $W_{K_\phi} = 1$. In Figure 7-11 (b), we can see the end-effector tracks the desired trajectory very well, while the corresponding tension profile among cables that driving the end-effector shown in Figure 7-11 (a) are always positive. Moreover, in Figure 7-11 (c-d), we can see the stiffness in ϕ directions are at the desired stiffness 50 N/m, however, the value of stiffness x and y -directions ranges from around 300 N/m to 400 N/m, which is far more than the desired stiffness.

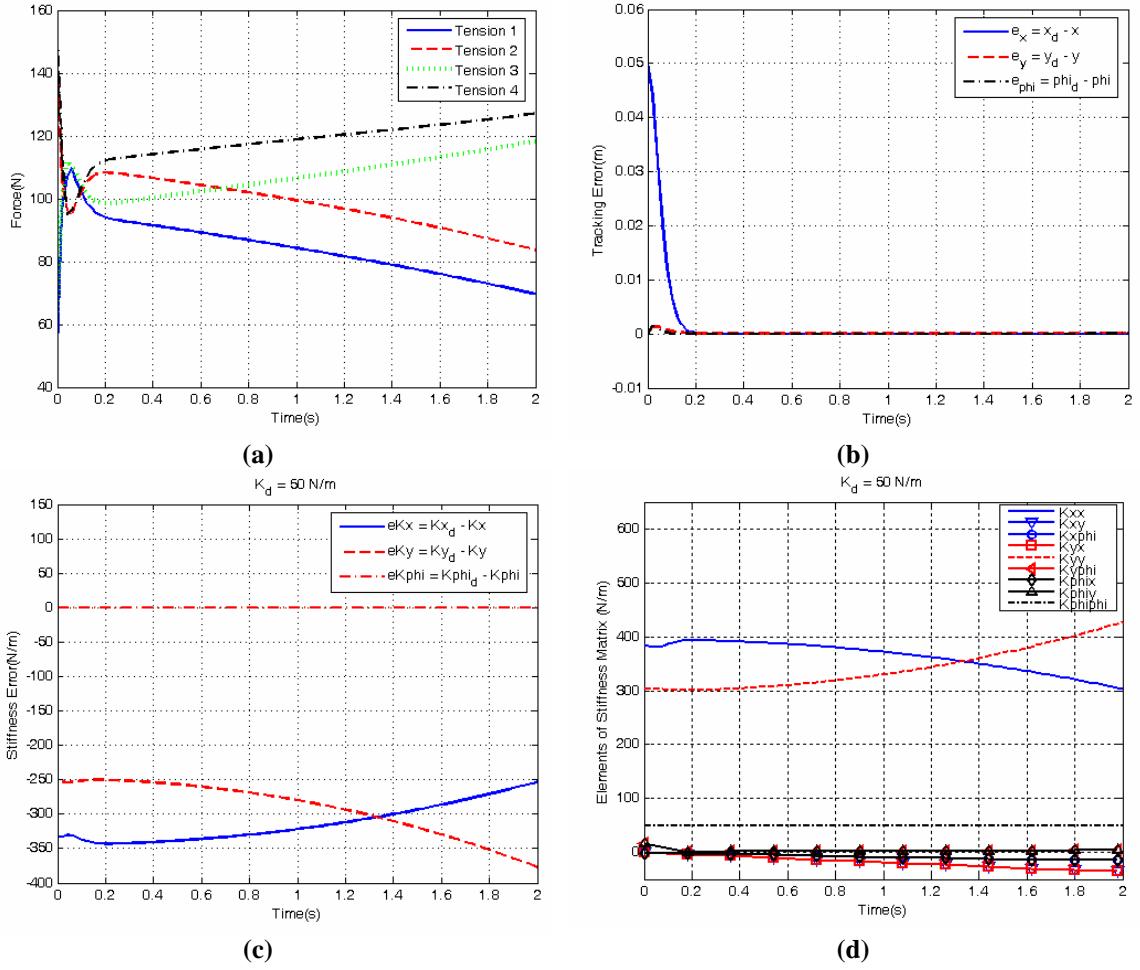


Figure 7-11 Controlling the stiffness in rotational directions with Case B, $K_d = 50 \text{ Nm/rad}$

Case Study 2: $[K_{dx} \ K_{dy} \ K_{d\phi}] = [100 \text{ N/m} \ 100 \text{ N/m} \ 100 \text{ Nm/rad}]$

In this case, the desired stiffness in all direction is $K_d = \text{diag}[K_{dx} \ K_{dy} \ K_{d\phi}] = [100 \text{ N/m} \ 100 \text{ N/m} \ 100 \text{ Nm/rad}]$. However, the stiffness in the rotational directions ϕ (K_{ϕ}) are primarily important. Hence, our goal is to reduce $dK_{\phi} = (K_{d\phi} - K_{\phi})$ with priority. Accordingly, we set the weighting matrix in Eq.(7.2) as $W = \text{diag}[0 \ 0 \ 0 \ 0 \ 0 \ 1]$, which means $W_{K_x} = 0$, $W_{K_y} = 0$, $W_{K_{\phi}} = 1$. In Figure 7-12 (b), we can see the end-effector tracks the desired trajectory very well, while the corresponding tension profile among cables that driving the end-effector shown in Figure

7-12 (a) are always positive. Moreover, in Figure 7-12 (c-d), we can see the stiffness in ϕ directions are at the desired stiffness 100 N/m, however, the value of stiffness x and y directions ranges from around 600 N/m to 800 N/m, which is far more than the desired stiffness.

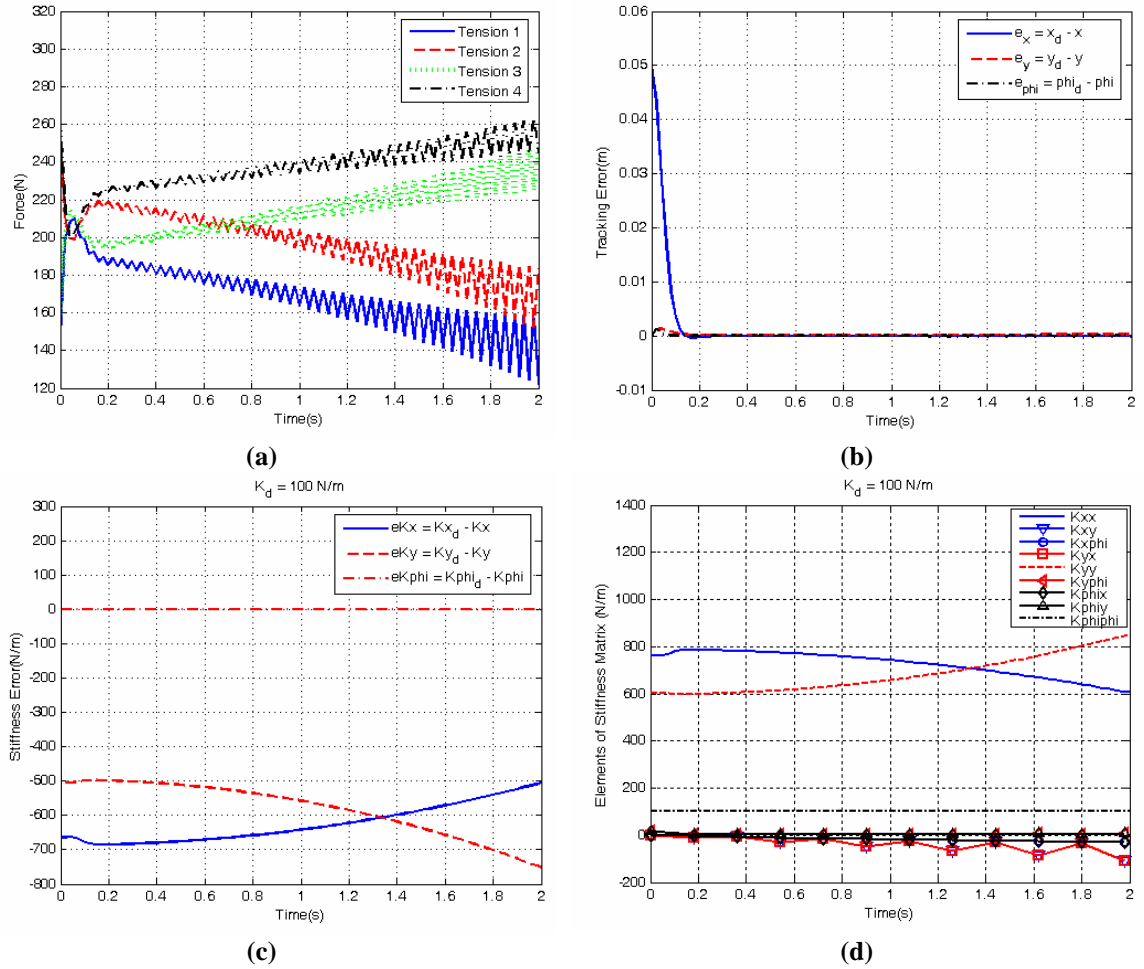


Figure 7-12 Controlling the stiffness in rotational directions with Case B, $K_d = 100 Nm/rad$

7.2.1.2 Lower Bound Stiffness Control

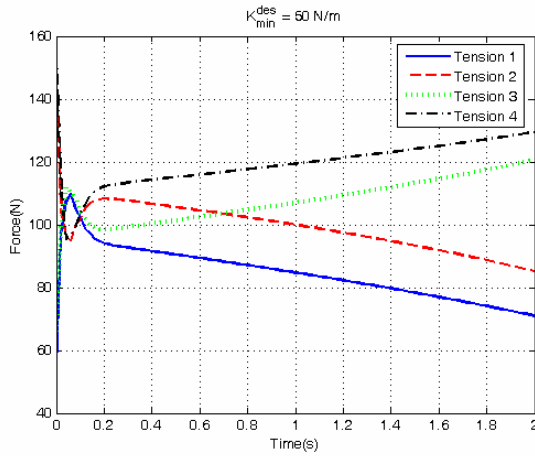
According to Section 5.2.3.3 , for Case B we have,

$$\sigma_{\min}(K_g - J^T K_l J) = \sigma_{\min}^{des} \quad (70)$$

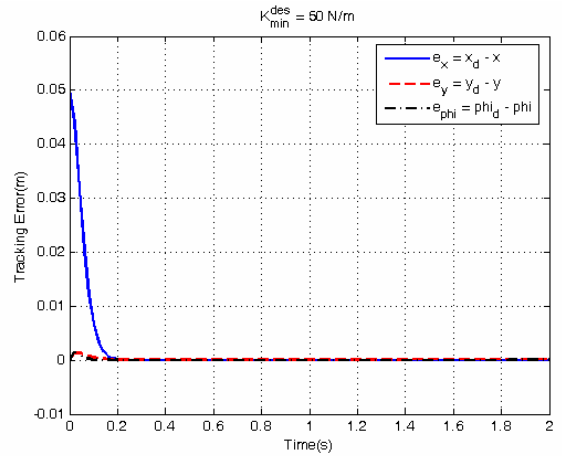
where

$$K_g = \left[\frac{\partial S}{\partial x} F \quad \frac{\partial S}{\partial y} F \quad \frac{\partial S}{\partial \phi} F \right], \quad F = [F_1 \quad F_2 \quad F_3 \quad F_4]^T \geq 0 \quad (71)$$

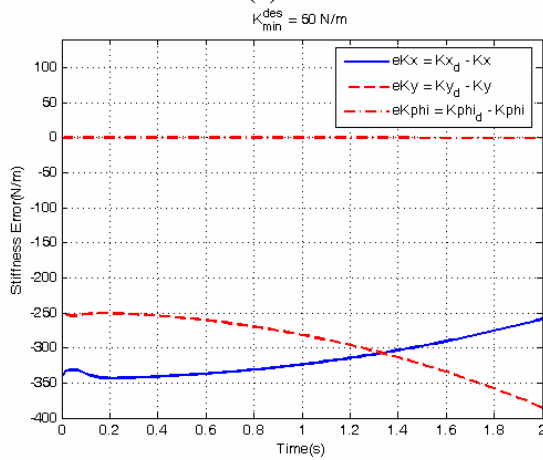
Case Study 1: $K_{\min}^{des} = 50 \text{ N/m}$



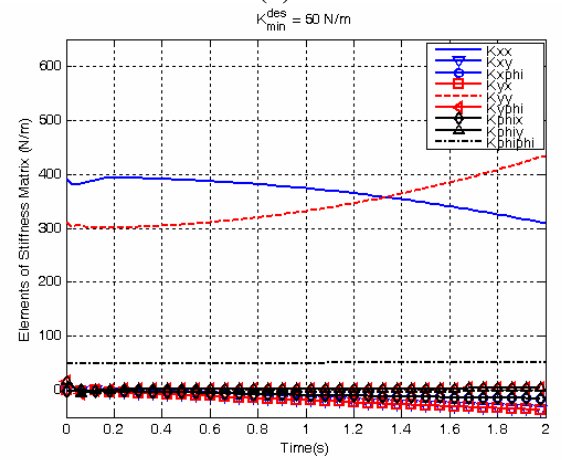
(a)



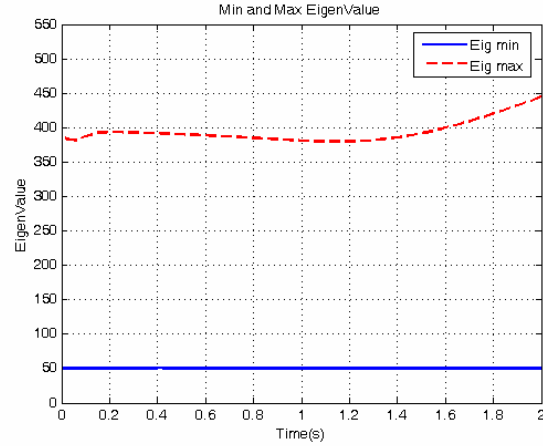
(b)



(c)



(d)



(e)

Figure 7-13 Lower bound stiffness control with Case B, $K_{\min}^{des} = 50 \text{ N/m}$

In this case, the desired lower bound for the main diagonal elements of the stiffness matrix is $\sigma_{\min}^{des} = 50 \text{ N/m}$. In Figure 7-13 (b), we can see the end-effector tracks the desired trajectory very well, while the corresponding tension profile among cables that driving the end-effector shown in Figure 7-13 (a) are always positive. Moreover, in Figure 7-13 (c-d), we can see the lower bound stiffness of all directions is at the desired value 50 N/m. Moreover, in Figure 7-13 (e) we can see the maximum and minimum eigenvalue (or stiffness) generated by LBSC along the trajectory, the minimum stiffness of the system is always at 50 N/m.

Case Study 2: $K_{\min}^{des} = 100 \text{ N/m}$

In this case, the desired lower bound for the main diagonal elements of the stiffness matrix is $\sigma_{\min}^{des} = 100 \text{ N/m}$. In Figure 7-14 (b), we can see the end-effector tracks the desired trajectory very well, while the corresponding tension profile among cables that driving the end-effector shown in Figure 7-14 (a) are always positive. Moreover, in Figure 7-14 (c-d), we can see the lower bound stiffness of all directions is at the desired value 50 N/m. Moreover, in Figure 7-14 (e) we can see the maximum and minimum

eigenvalue (or stiffness) generated by LBSC along the trajectory, the minimum stiffness of the system is always at 100 N/m.

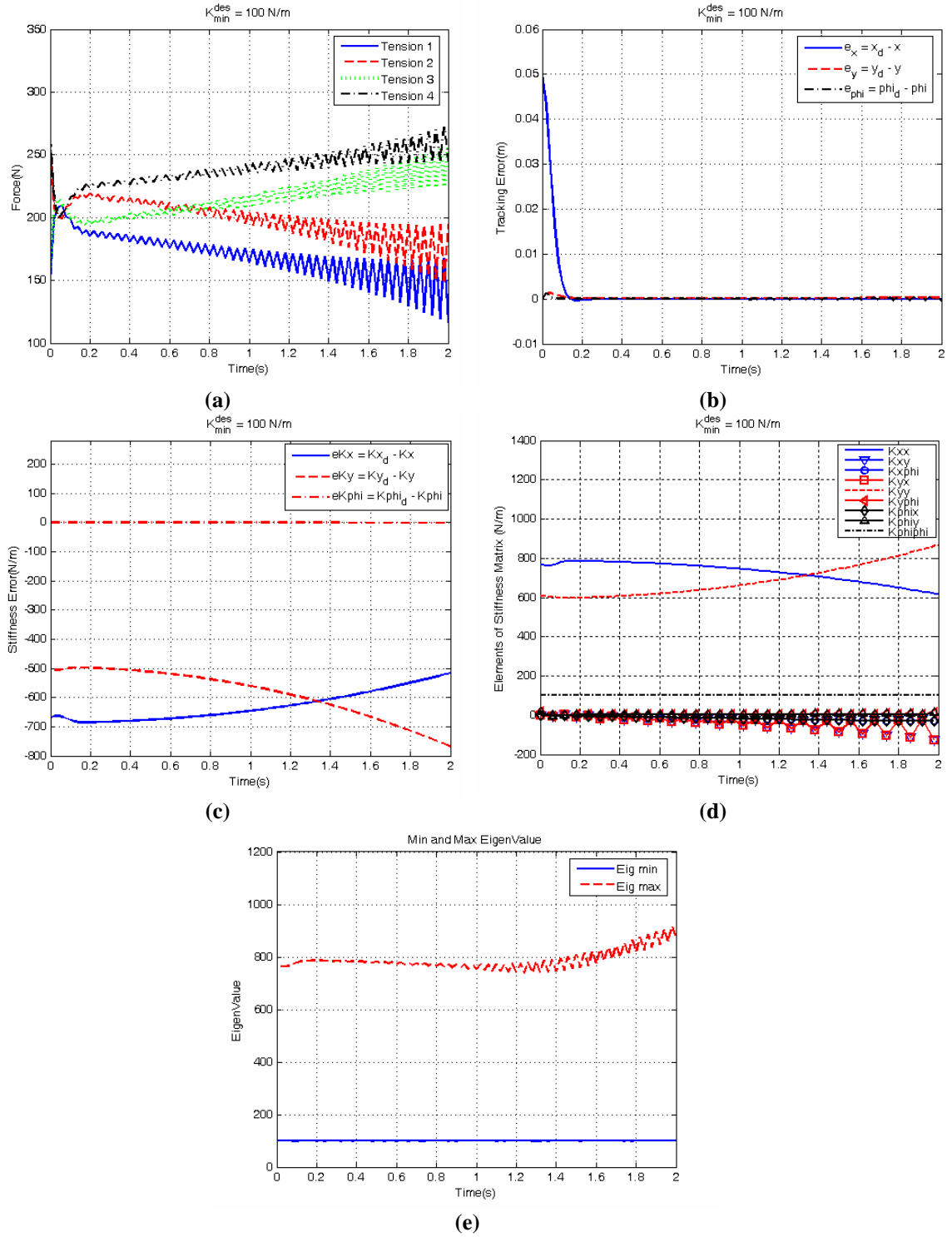


Figure 7-14 Lower bound stiffness control with Case B, $K_{min}^{des} = 100 \text{ N/m}$

7.2.2 Circle Tracking with Augmented Stiffness Control with Case A

In this simulation scenario, the end-effector of case B is initially at $(0.3, 0.173)m$ and the desired end-effector trajectory is a circle $x = (0.3 + 0.1\cos(t)) m$, $y = (0.173 + 0.1\sin(t)) m$, such that the desired velocity is $0.1 m/s$.

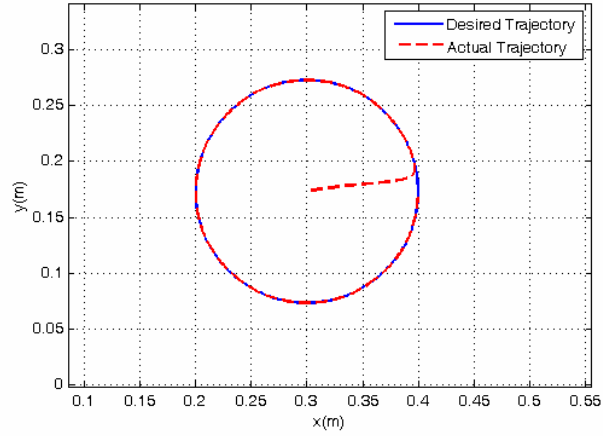


Figure 7-15 Circle trajectory tracking with Case A

7.2.2.1 Weighted Stiffness Matrix

According to Section 5.2.3.2, the general form of weighted stiffness matrix x for case A can be written as

$$dK_x = [dK_{xx} \quad dK_{xy} \quad dK_{yy}]^T \quad (72)$$

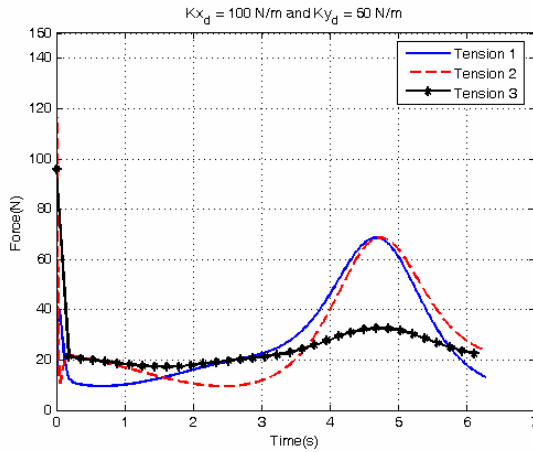
and the weighting matrix

$$W = \text{diag}[W_{Kx} \quad W_{Kxy} \quad W_{Ky}] \quad (73)$$

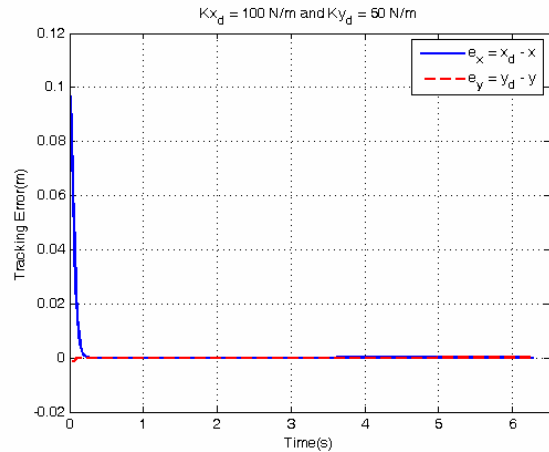
7.2.2.1.1 Control of Stiffness in X Direction

Case Study 1: $[K_{dx} \ K_{dy}] = [100 \ 50] \text{ N/m}$

In this case, the desired stiffness $K_d = \text{diag}[K_{dx} \ K_{dy}] = [100 \ 50] \text{ N/m}$, we assume that the stiffness in x directions (K_x) are primarily important. Hence, our goal is to reduce $dK_x = (K_{dx} - K_x)$ with first priority. Accordingly, we set the weighting matrix in Eq.(7.6) as $W = \text{diag}[1 \ 0 \ 0]$, which means $W_{K_x} = 1$, $W_{K_y} = 0$. In Figure 7-16 (b), we can see the end-effector tracks the desired trajectory very well, while the corresponding tension profile among cables that driving the end-effector shown in Figure 7-16 (a) are always positive. Moreover, in Figure 7-16 (c-d), we can see the stiffness in x -directions are at the desired stiffness 100 N/m while the value of stiffness in y -directions is changing in a wide range, which is around from 30 N/m to 420 N/m.



(a)



(b)

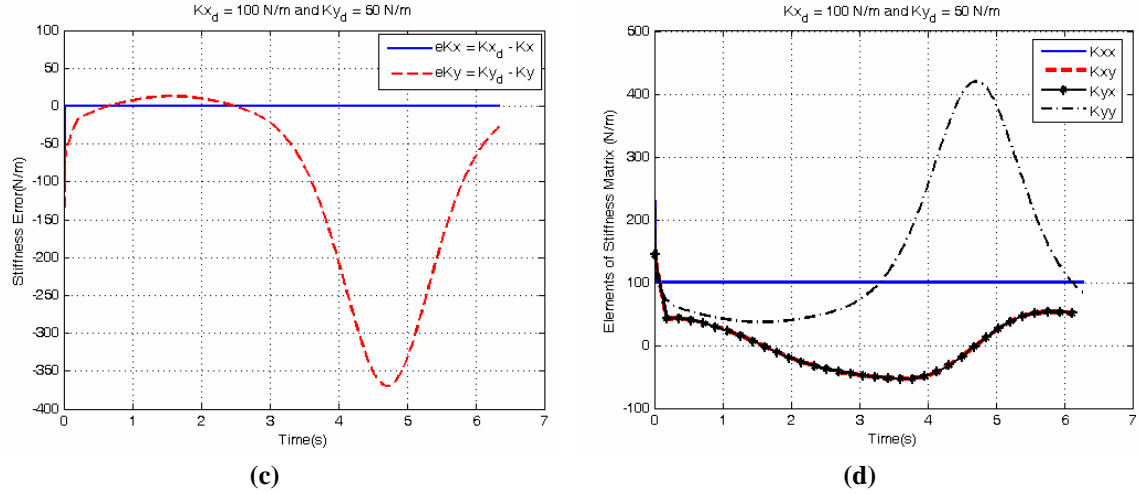


Figure 7-16 Controlling the stiffness in X directions with Case A, $K_d = 100 \text{ N/m}$

Case Study 2: $[K_{dx} \ K_{dy}] = [500 \ 50] \text{ N/m}$

In this case, the desired stiffness $K_d = \text{diag}[K_{dx} \ K_{dy}] = [500 \ 50] \text{ N/m}$, we assume that the stiffness in X directions (K_x) are primarily important. Hence, our goal is to reduce $dK_x = (K_{dx} - K_x)$ with first priority. Accordingly, we set the weighting matrix in Eq.(7.6) as $W = \text{diag}[1 \ 0 \ 0]$, which means $W_{K_x} = 1$, $W_{K_y} = 0$. In Figure 7-17 (b), we can see the end-effector tracks the desired trajectory very well, while the corresponding tension profile among cables that driving the end-effector shown in Figure 7-17 (a) are always positive. Moreover, in Figure 7-17 (c-d), we can see the stiffness in x -directions are at the desired stiffness 500 N/m while the value of stiffness in y -directions is changing in a wide range, which is around from 250 N/m to 2200 N/m.

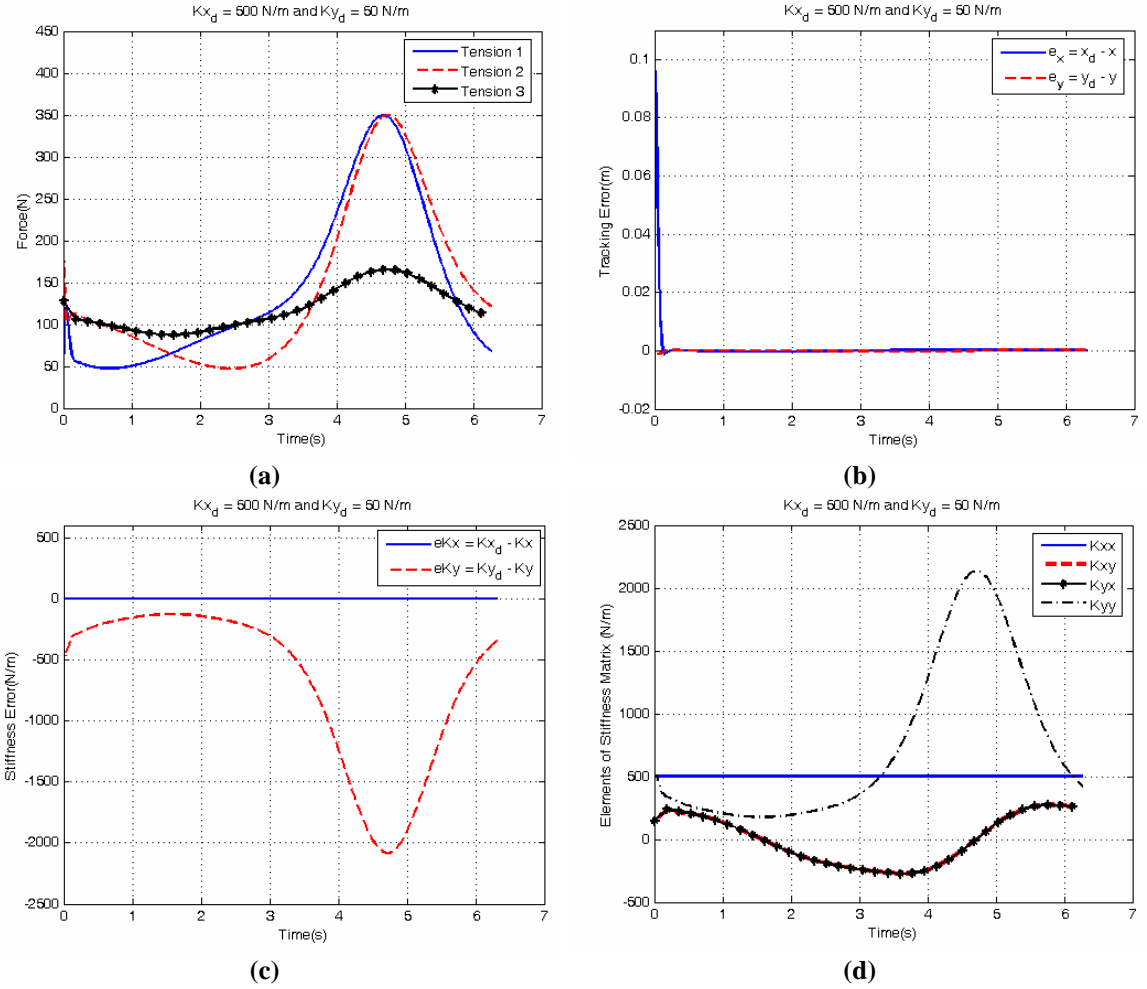


Figure 7-17 Controlling the stiffness in X directions with Case A, $K_d = 500 \text{ N/m}$

7.2.2.1.2 Control of Stiffness in X and Y Directions

Case Study 1: $[K_{dx} \ K_{dy}] = [100 \ 50] \text{ N/m}$

In this case, the desired stiffness $K_d = \text{diag}[K_{dx} \ K_{dy}] = [100 \ 50] \text{ N/m}$, we assume that the stiffness in X and Y directions (K_x and K_y) are primarily important. Hence, our goal is to reduce $dK_x = (K_{dx} - K_x)$ and $dK_y = (K_{dy} - K_y)$ with equal priority. Accordingly, we set the weighting matrix in Eq.(7.6) as $W = \text{diag}[\sqrt{0.5} \ 0 \ \sqrt{0.5}]$, which means $W_{K_x} = \sqrt{0.5}$, $W_{K_y} = \sqrt{0.5}$. In Figure 7-18 (b),

we can see the end-effector tracks the desired trajectory very well, while the corresponding tension profile among cables that driving the end-effector shown in Figure 7-18 (a) are always positive. Moreover, in Figure 7-18 (c-d), we can see the stiffness in x -direction are near the desired stiffness 100 N/m. Meanwhile, the stiffness in y -direction is also near the desired stiffness 50 N/m, moreover, its error to the desired stiffness is less than that of in x -direction.

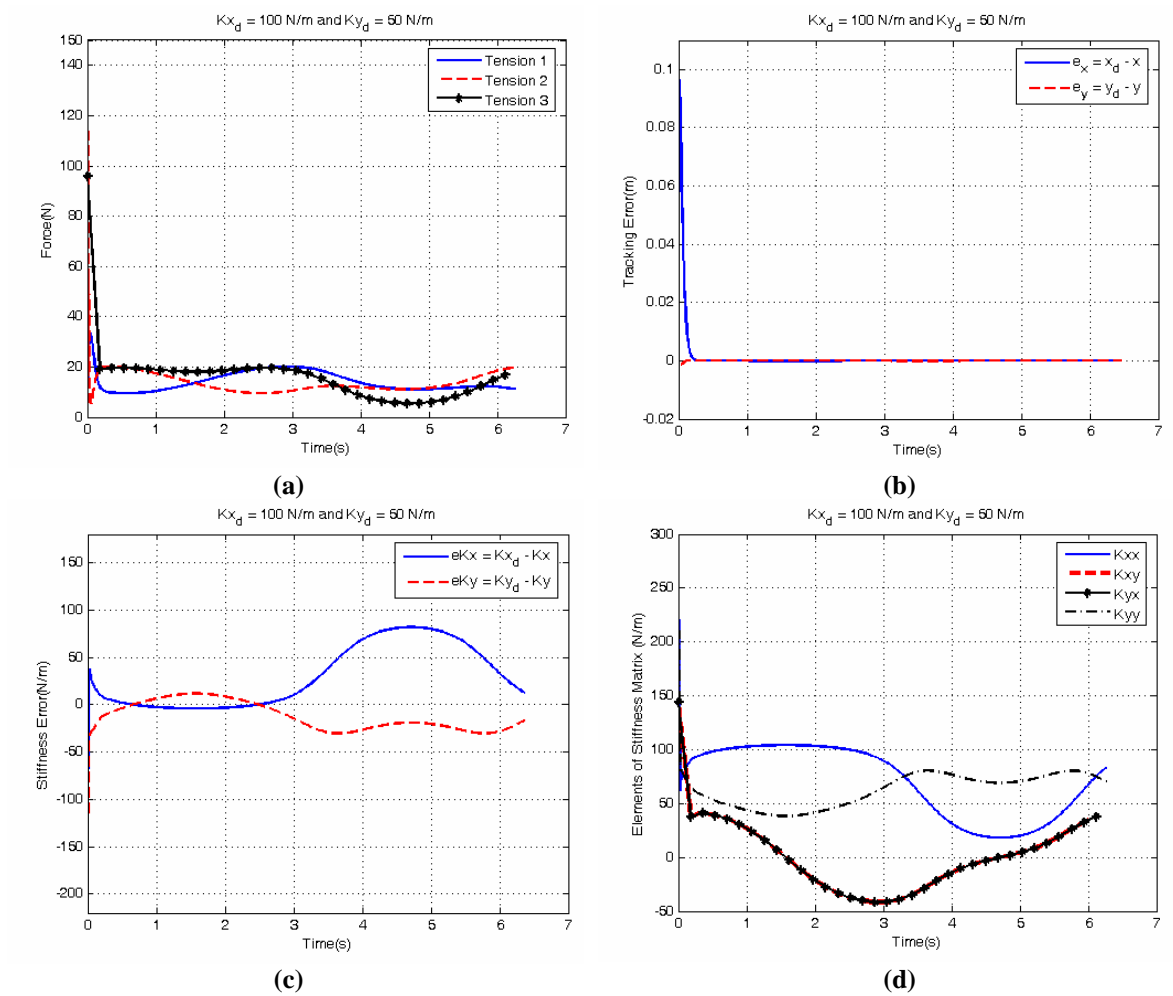


Figure 7-18 Controlling the stiffness in X and Y directions with Case A, $[K_{dx} \ K_{dy}] = [100 \ 50]$ N / m

7.2.2.2 Lower Bound Stiffness Control

According to Section 5.2.3.3 , for Case A we have,

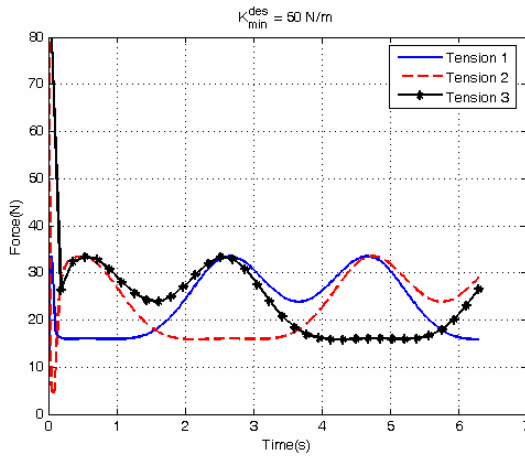
$$\sigma_{\min}(K_g - J^T K_l J) = \sigma_{\min}^{des} \quad (74)$$

where

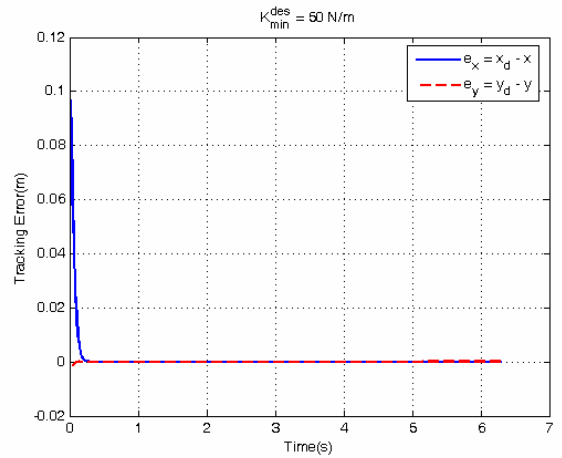
$$K_g = \left[\frac{\partial S}{\partial x} F \quad \frac{\partial S}{\partial y} F \right], F = [F_1 \ F_2 \ F_3]^T \geq 0 \quad (75)$$

Case Study 1: $K_{\min}^{des} = 50 \text{ N/m}$

In this case, the desired lower bound for the main diagonal elements of the stiffness matrix is $\sigma_{\min}^{des} = 50 \text{ N/m}$. In Figure 7-19 (b), we can see the end-effector tracks the desired trajectory very well, while the corresponding tension profile among cables that driving the end-effector shown in Figure 7-19 (a) are always positive. Moreover, in Figure 7-19 (c-d), we can see the lower bound stiffness of all directions are at the desired value 50 N/m. Moreover, in Figure 7-19 (e) we can see the maximum and minimum eigenvalue (or stiffness) generated by LBSC along the trajectory, the minimum stiffness of the system is always at 50 N/m.



(a)



(b)

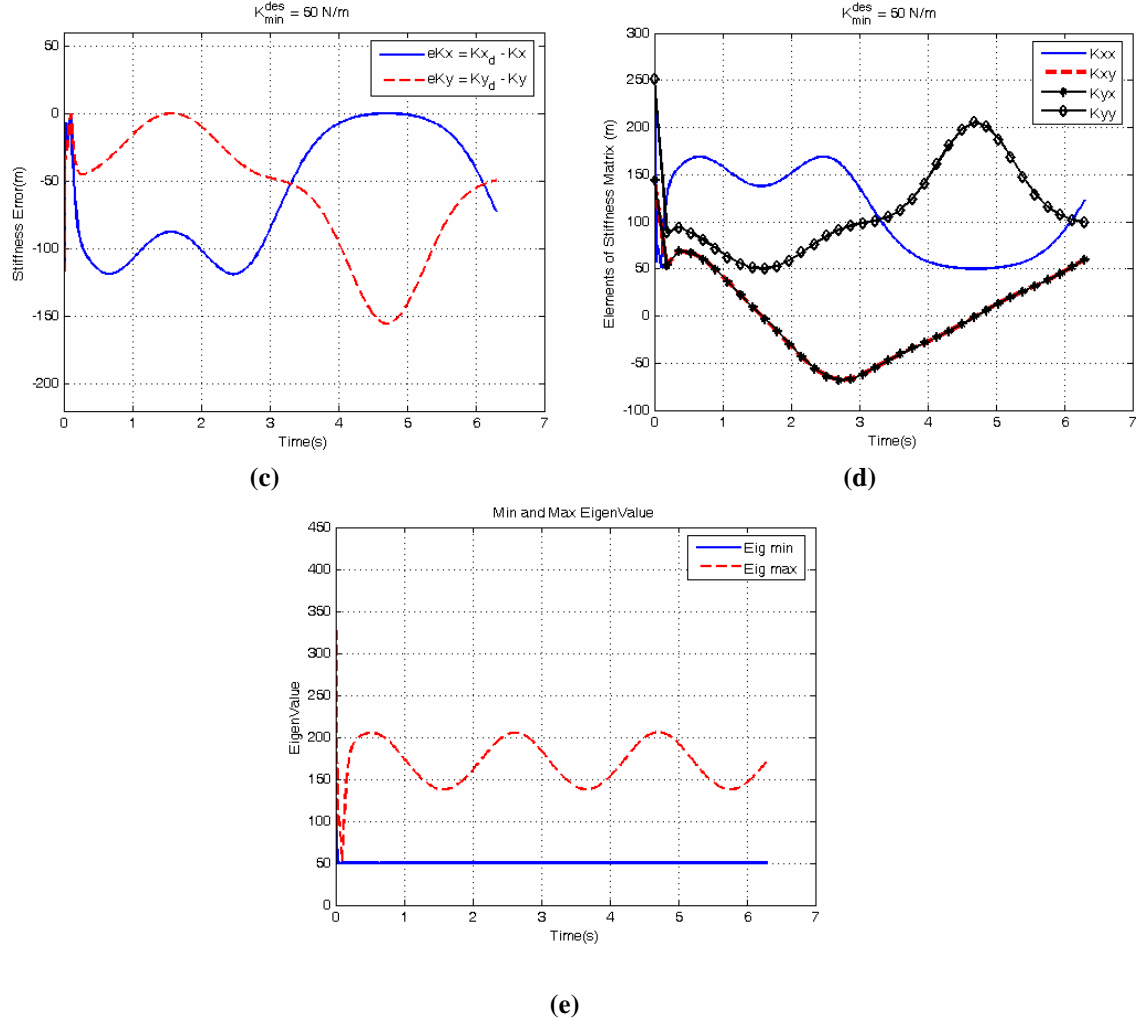


Figure 7-19 Lower bound stiffness control with Case A, $K_{\min}^{des} = 50 \text{ N/m}$

Case Study 2: $K_{\min}^{des} = 100 \text{ N/m}$

In this case, the desired lower bound for the main diagonal elements of the stiffness matrix is $\sigma_{\min}^{des} = 100 \text{ N/m}$. In Figure 7-20 (b), we can see the end-effector tracks the desired trajectory very well, while the corresponding tension profile among cables that driving the end-effector shown in Figure 7-20 (a) are always positive. Moreover, in Figure 7-20 (c-d), we can see the lower bound stiffness of all directions are at the desired value 50 N/m. Moreover, in Figure 7-20 (e) we can see the maximum and minimum

eigenvalue (or stiffness) generated by LBSC along the trajectory, the minimum stiffness of the system is always at 100 N/m.

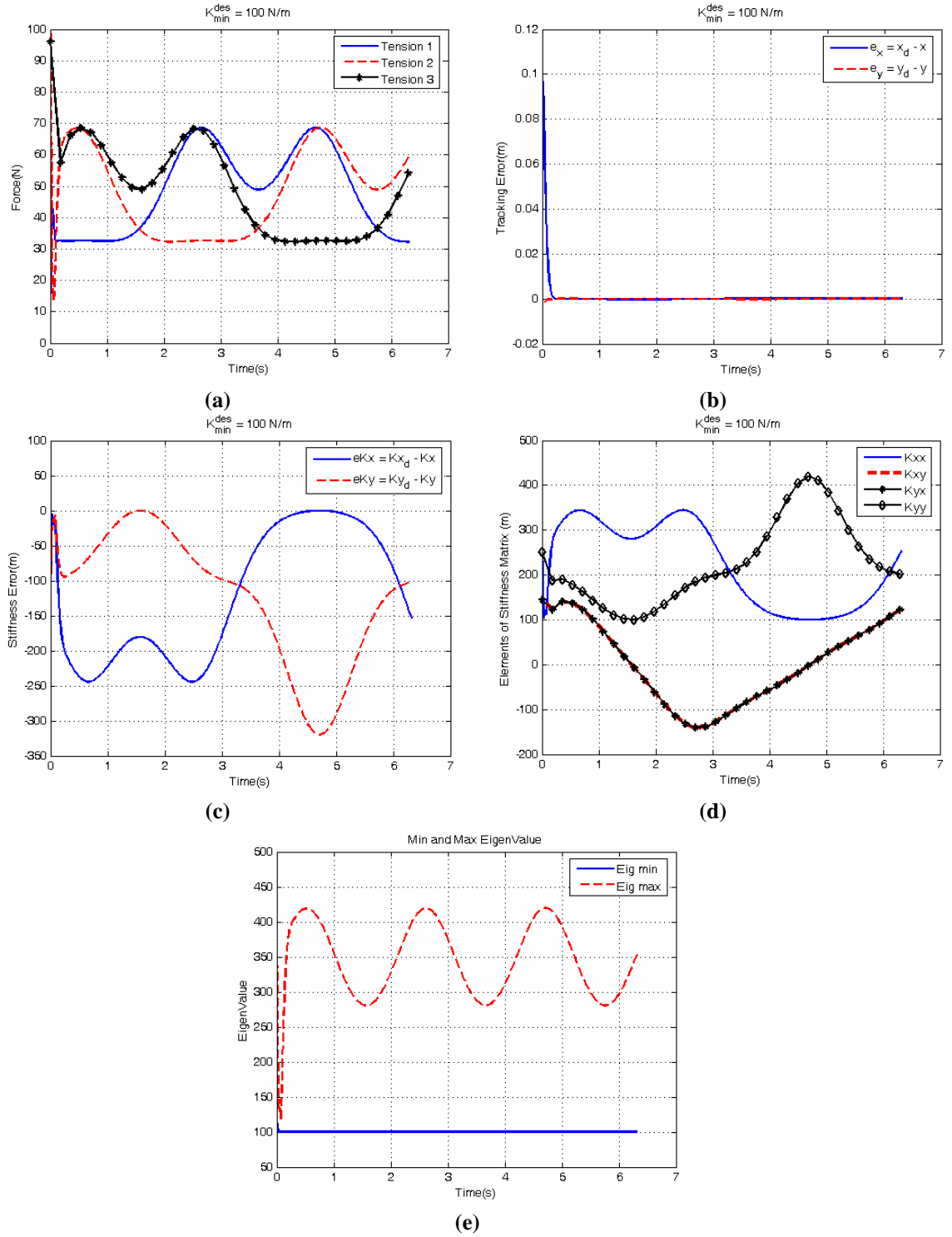


Figure 7-20 Lower bound stiffness control with Case A, $K_{min}^{des} = 100 \text{ N/m}$

7.3 Disturbance Rejection -- Straight Line Tracking

In this section, simulation results show the performance of LBSC developed in Section 5.2.3.3 under two different disturbances as follows

Disturbance Case 1: $F_x = 0 \text{ N}$, $F_y = 5 \sin(4\pi t) \text{ N}$ is applied to the end-effector at time period: $0.5 \text{ s} < t < 1.5 \text{ s}$.

Disturbance Case 2: $F = (5, -5) \text{ N}$ is applied to the end-effector at time period: $0.5 \text{ s} < t < 1.5 \text{ s}$.

We will use case B model as our test bed though out this section. Moreover, case studies are performed both with and without LBSC under each disturbance to illustrate the effectiveness of our approach.

7.3.1 Straight Line Tracking under Disturbance Case 1

In this simulation scenario, the end-effector of case B is initially at $(0.55, 0.5) \text{ m}$ and the desired end-effector trajectory (as shown in Figure 7-3) is a straight line $x = 0.55 \text{ m}$, $y = (0.5 + 0.1t) \text{ m}$, such that the desired velocity is 0.1 m/s .

7.3.1.1 Case 1 without LBSC

In this case, the end-effector is controlled under trajectory tracking control with minimal cable force distribution as shown in Chapter (4). In Figure 7-21 (a), we can see the actual trajectory of end-effector deviate from the desired trajectory under the sinusoid disturbance, the maximum position error is about $6 \times 10^{-3} \text{ m}$ as shown in Figure 7-21 (c). The corresponding tension profiles of cables shown in Figure 7-21 (b) are always positive, and their magnitude change corresponding to the disturbance. Similar results are

shown in Figure 7-21 (d-e) for the profiles of the task space stiffness. This can be explained as the effect of control force generated by the position feedback gain in the trajectory tracking controller in implementation.

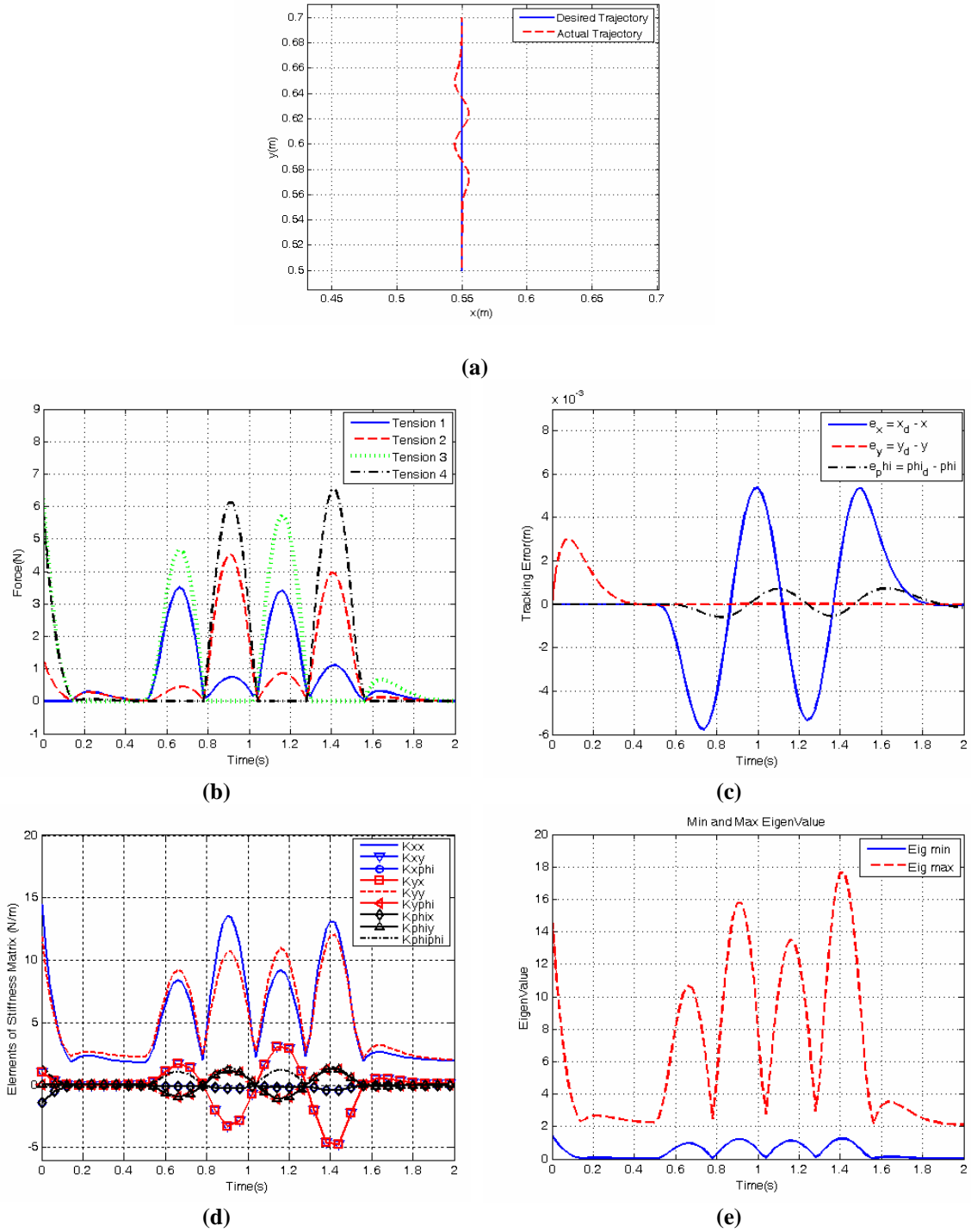
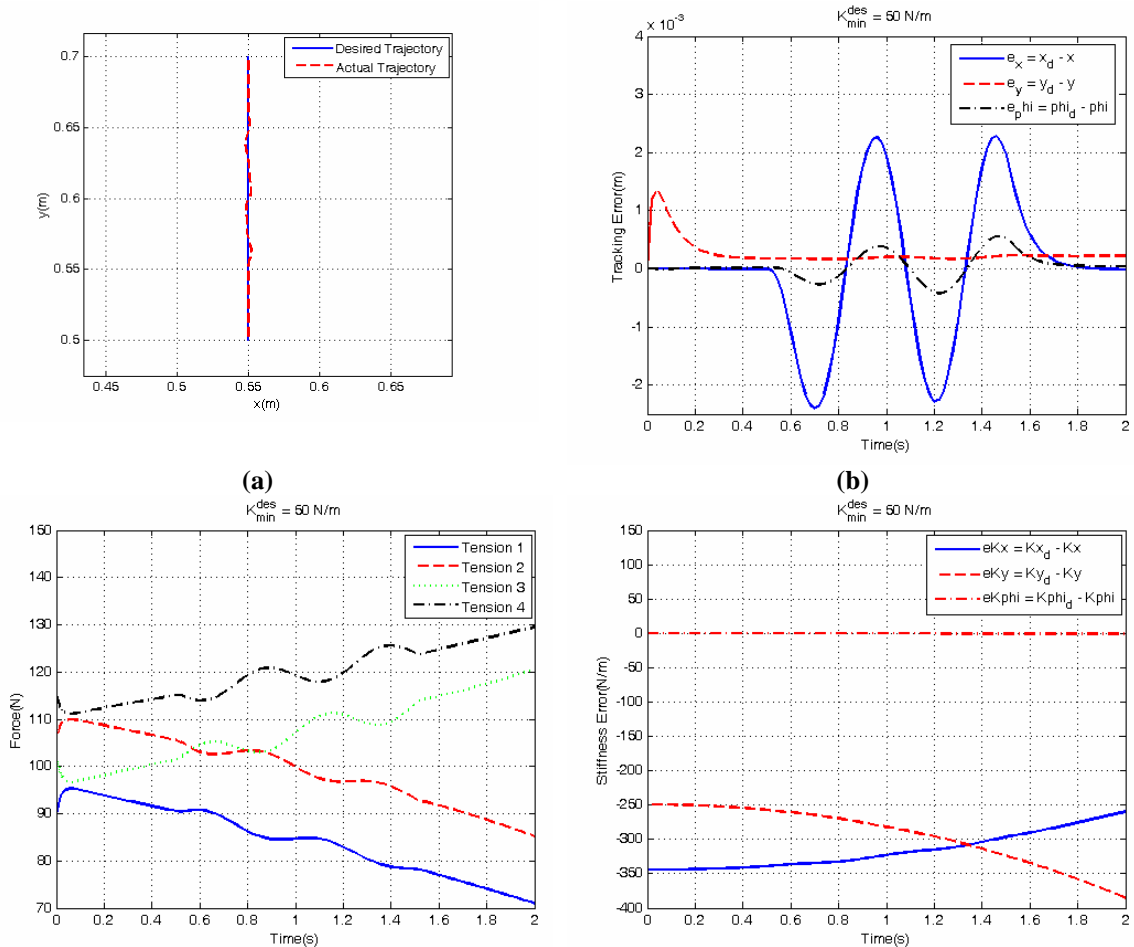


Figure 7-21 Straight Line Tracking under disturbance 1 without LBSC with Case B

7.3.1.2 Case 1 with LBSC $K_{\min}^{des} = 50 \text{ N/m}$

In this case, the end-effector is controlled under trajectory tracking control augmented LBSC with lower bound stiffness at 50 N/m . In Figure 7-22 (a), we can see the end-effector tracks the desired trajectory much better than the case without LBSC, the maximum position error is about $2.3 \times 10^{-3} \text{ m}$ as shown in Figure 7-22 (b). The corresponding tension profiles of cables shown in Figure 7-22 (c) are always positive and controlled at larger magnitude than in Figure 7-21 (b) in order to achieve the desired task space stiffness of the end-effector. In Figure 7-22 (d-f), we can see the lower bound stiffness of all directions is at the desired value 50 N/m . As the result of that, necessary resorting force is generated to compensate disturbance in certain level.



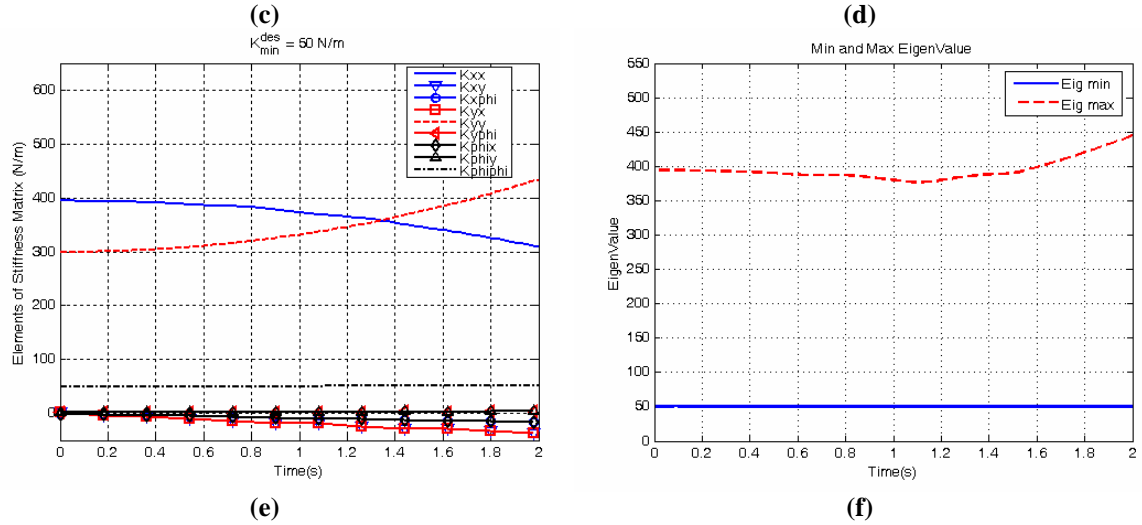
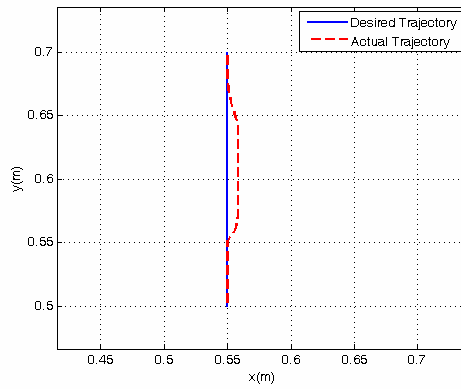


Figure 7-22 Straight Line Tracking under disturbance 1 with LBSC with Case B

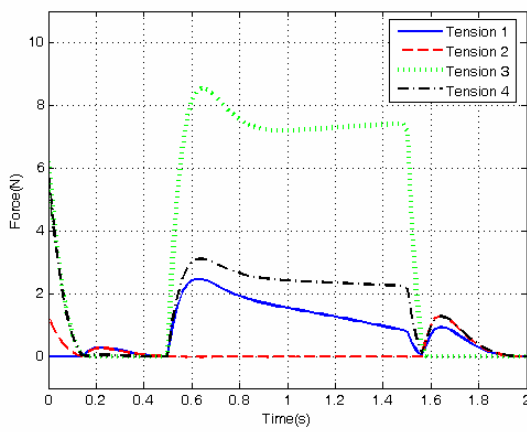
7.3.2 Straight Line Tracking under Disturbance Case 2

7.3.2.1 Case 2 without LBSC

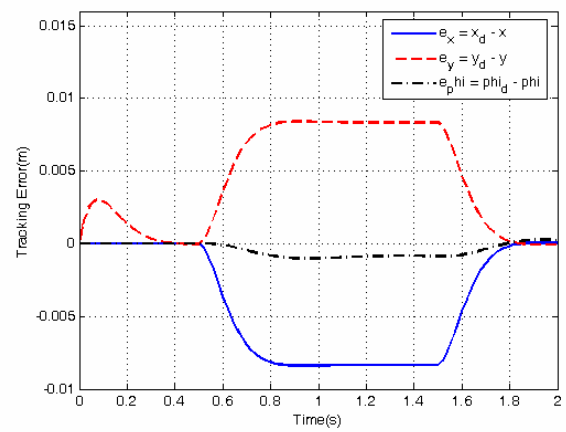
In this case, the end-effector is controlled under trajectory tracking control with minimal cable force distribution as shown in Chapter (4). In Figure 7-23 (a), we can see the actual trajectory of end-effector deviate from the desired trajectory under the sinusoid disturbance, the maximum position error is about $8 \times 10^{-3} \text{ m}$ as shown in Figure 7-23 (c). The corresponding tension profiles of cables shown in Figure 7-23 (b) are always positive, and their magnitude change corresponding to the disturbance. Similar results are shown in Figure 7-23 (d-e) for the profiles of the task space stiffness. This can be explained as the effect of control force generated by the position feedback gain in the trajectory tracking controller in implementation.



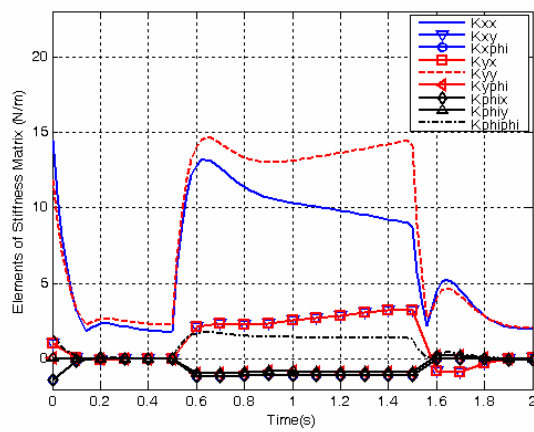
(a)



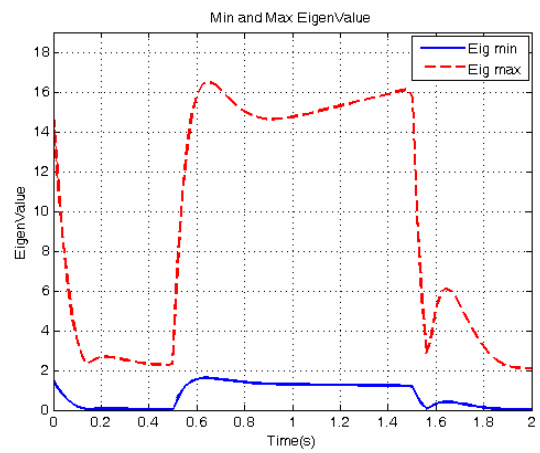
(b)



(c)



(d)

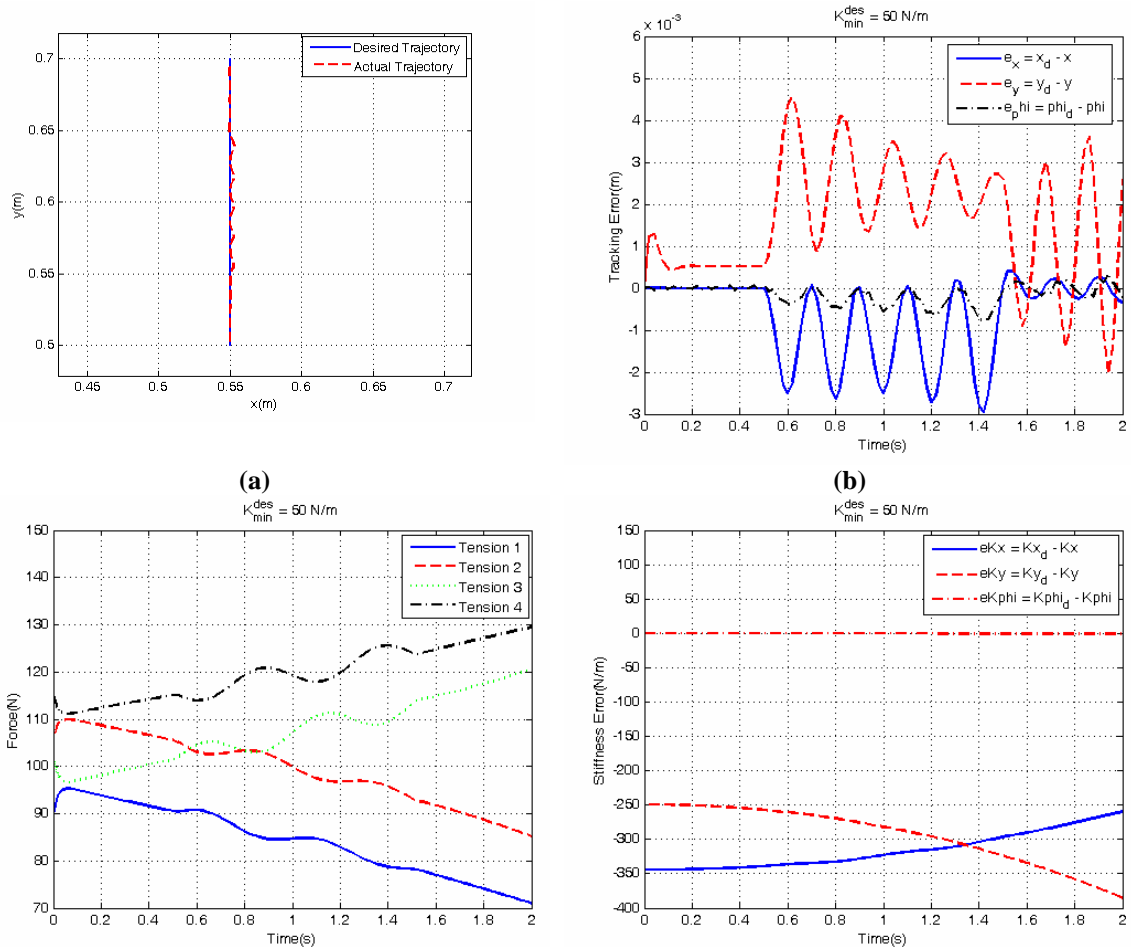


(e)

Figure 7-23 Straight Line Tracking under disturbance 2 without LBSC with Case B

7.3.2.2 Case 2 with LBSC $K_{\min}^{des} = 50 \text{ N/m}$

In this case, the end-effector is controlled under trajectory tracking control augmented LBSC with lower bound stiffness at 50 N/m . In Figure 7-24 (a), we can see the end-effector tracks the desired trajectory much better than the case without LBSC, the maximum position error is about $4.5 \times 10^{-3} \text{ m}$ as shown in Figure 7-24 (b). The corresponding tension profiles of cables shown in Figure 7-24 (c) are always positive and controlled at larger magnitude than in Figure 7-23 (b) in order to achieve the desired task space stiffness of the end-effector. In Figure 7-24 (d-f), we can see the lower bound stiffness of all directions is at the desired value 50 N/m . As the result of that, necessary resorting force is generated to compensate disturbance in certain level.



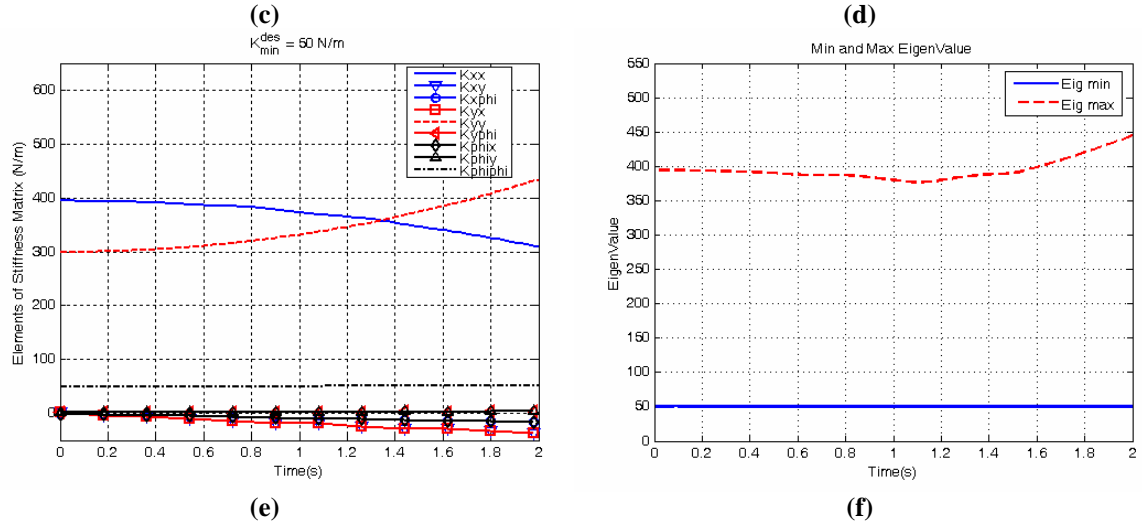


Figure 7-24 Straight Line Tracking under disturbance 2 with LBSC with Case B

7.4 Discussion

The results verify that the control schemes developed in Chapter 4 and Chapter 5 are capable of achieving combinations of our goals: 1. Trajectory tracking 2. Optimal cable force distribution 3. Active (task space) stiffness control. Specifically, trajectory tracking with optimal cable force distribution in the form of minimal energy/force consumption or active task space stiffness control. Critical conclusions of the simulation results can be summarized as follows

1. Trajectory tracking nonlinear controller based on feedback linearization technique provides good system performance to cable robots in different complication level.
2. Actuation redundancy provides feasible solution to address the control input constraint issue (in our case, positive tension force exerting by cables) in the control of cable robot system. Moreover, it provides flexibility and usability in the context of optimal cable force distribution and task space stiffness specification and adjustment.

3. CCT based task space stiffness mapping method [70] provides insight and complete to the understanding of relationship between redundant actuation forces and task space stiffness, which is redundant actuation forces will not generate effective work in task space, but it can generate and change task space stiffness of the system. Simulation results shown in Section 7.2 verify this assumption – larger task space stiffness can be achieved by higher level of redundant actuation forces in magnitude. Moreover, stiffness in rotational direction is harder to realize: as shown in Figure 7-12 and Figure 7-14, much larger stiffness in transitional direction is generated to obtain desired stiffness in rotational direction, as the results of that, much larger cable input force is required, which would introduce exceptional high level of energy resulting in unstableness of the system.
4. Disturbance-rejection issue in steady state can be effectively handled by means of active task space stiffness control, through the effect of restoring force in term of position error.

8 Conclusions and Future Work

8.1 Summary

In this work, the design and implementation of several cable robot systems along with some control schemes are proposed to address trajectory tracking and disturbance-rejection issue. Trajectory tracking is achieved by a feedback linearization controller in dynamics level of cable robot. Moreover, new control approaches based on actuation redundancy are proposed to achieve: 1. optimal force distribution or 2. desired end effector Cartesian/task space stiffness (or can be called active stiffness control). In the optimal force distribution, the goal is to achieve minimal energy consumption needed to achieve desired performance or tasks. In other words, minimal control forces combination exerted among cables. Based on the criteria, optimization schemes are formulated in the context of null space control introduced by actuation redundancy. In active stiffness control issue, Relationship between joint space stiffness, configuration, cable actuation and work/task space stiffness is studied and formulated based CCT stiffness mapping. Studies of effectiveness of stiffness control on disturbance force compensation are performed. The technical significance of the control output compensation for feedback controller by such stiffness control scheme which directly generates corresponding restoring forces immediately responding to unexpected disturbances is pointed out.

8.2 Future Work

Hardware-in-the-loop (HIL) Testing: A Cable Robot Based Aerial Vehicle Simulator

Over the past decade, in field of field robotics research such as autonomous air vehicles, most of the engineering problems have been overcome, including for example vibration isolation for sensing pods and the design of a low-cost inertial sensing unit. However, when it comes to experimenting with physical prototype of such system, researches are still facing research productivity issues, which are mainly from the time and cost involved in the development and reliability of the test bed. For example, failures from testing with physical prototypes of such system are usually unpredictable and catastrophic, so most of them lead to inevitable repair or rebuild expenses.

Being able to provide an excellent range of motion and provide good position control and risk-free test environment, a cable robot based air vehicle simulator is found to be the excellent hardware-in-the-loop test bed before final experimentation on a free-flying vehicle in field of field robotics research.

Thus, our future work is to continue on: 1) hardware development of a cable robot based air vehicle simulator, 2) realization and verification of control purpose and algorithms proposed in this work. Improvements and new approaches might be necessary while taking into account the factors like computer computational efficiency, cable physical properties, motor-spool-pulley mechanism, etc.

Bibliography

- [1] D. Stewart, "A platform with six degrees of freedom," in *Proceedings of the Institution of Mechanical Engineers*, 1965, pp. 371-386
- [2] S. Kawamura and K. Ito, "A new type of master robot for teleoperation using a radial wire drive system," in *Proceedings of the IEEE/RSJ International Conference on Intelligent Robots and Systems, IROS '93*, Yokohama, Japan, 1993, pp. 55-60.
- [3] I. Ebert-Uphoff and P. A. Voglewede, "On the connections between cable-driven robots, parallel robots and grasping," in *Proceedings of IEEE International Conference on Robotics and Automation*. vol. 5 New Orleans, LA, 2004, pp. 4521- 4526.
- [4] "http://abroad.dongguk.edu/asp/tambang/relay/upfiles/IMG_1565.jpg."
- [5] "http://www.nist.gov/public_affairs/images/06MEL001_USAFrobo1_LR.jpg."
- [6] "<http://www.cablecam.com/WHATWEDO.HTML>."
- [7] R. Bostelman, J. Albus, N. Dagalakis, A. Jacoff, and J. L. Gross, "Applications of the NIST ROBOCRANE," in *Proceedings of the 5th International Symposium on Robotics and Manufacturing*, Maui, Hi, 1994, pp. 403-410.
- [8] C. Bonivento, A. Eusebi, C. Melchiorri, M. Montanari, and G. Vassura, "WireMan: a portable wire manipulator for touch-rendering of bas-relief virtual surfaces," in *Proceedings of 8th International Conference on Advanced Robotics*, Montreal, CA, 1997, pp. 13-18.
- [9] S. Kawamura, W. Choe, S. Tanaka, and S. Pandian, "Development of an ultrahigh speed robot FALCON using wire drive system," in *Proceedings of the 1993 IEEE/ICRA International Conference on Robotics and Automation*, Nagoya, Japan, 1995, pp. 215-220.
- [10] "<http://www.seicor.com/>."
- [11] J. J. Gorman, K. W. Jablokow, and D. J. Cannon, "The cable array robot: Theory and experiment," in *Proceedings of the 2001 IEEE International Conference on Robotics and Automation*, Seoul, Korea, 2001, pp. 2804-2810.
- [12] "<http://www.ent.ohiou.edu/~bosscher/research.html>."
- [13] C. J. Thompson and J. Campbell, P. D., "Tendon suspended platform robot," in *U.S. Patent No. 5,585,707*, 1996.

- [14] D. Chakarov, "Study of the antagonistic stiffness of parallel manipulators with actuation redundancy," *Mechanism and Machine Theory*, vol. 39, pp. 583-601, 2004.
- [15] J. F. O'Brien and J. T. Wen, "Redundant actuation for improving kinematic manipulability," in *Robotics and Automation, 1999. Proceedings. 1999 IEEE International Conference on*, 1999, pp. 1520-1525 vol.2.
- [16] M. A. Nahon and J. Angeles, "Force optimization in redundantly-actuated closed kinematic chains," in *Robotics and Automation, 1989. Proceedings., 1989 IEEE International Conference on*, 1989, pp. 951-956 vol.2.
- [17] B. J. Yi, R. A. Freeman, and D. Tesar, "Open-loop stiffness control of overconstrained mechanisms/robotic linkage systems," in *Robotics and Automation, 1989. Proceedings., 1989 IEEE International Conference on*, 1989, pp. 1340-1345 vol.3.
- [18] C. Gosselin, "Stiffness mapping for parallel manipulators," *Robotics and Automation, IEEE Transactions on*, vol. 6, pp. 377-382, 1990.
- [19] Anon,
["http://ami.usc.edu/projects/ami/projects/bion/musculoskeletal/human_arm_model.html."](http://ami.usc.edu/projects/ami/projects/bion/musculoskeletal/human_arm_model.html)
- [20] H. Gray, *Anatomy of the human body*, 1985.
- [21] N. Hogan, "Mechanical Impedance Control in Assistive Devices and Manipulators," in *proceedings of the IEEE Joint Automatic Controls Conference*, 1980, pp. 361-371.
- [22] D. Whitney, "Historical perspective and state of the art in robot force control," in *Robotics and Automation. Proceedings. 1985 IEEE International Conference on*, 1985, pp. 262-268.
- [23] N. G. Dagalakis, J. S. Albus, B. L. Wang, J. Unger, and J. D. Lee, "Stiffness Study of a Parallel Link Robot Crane for Shipbuilding Applications," *ASME Journal of Offshore Mechanics and Arctic Engineering*, vol. 111, pp. 183-193, 1989.
- [24] R. Verhoeven, M. Hiller, and S. Tadokoro, "Workspace, stiffness, singularities and classification of tendon-driven stewart platforms," in *Proceedings of the ARK '98 6th International Symposium on Advances in Robot Kinematics*, Strobl, Austria, 1998, pp. 105-114.
- [25] D. Chakarov, "Approaches of Stiffness Control of Parallel Manipulators with Actuation Redundancy," in *Pros of the International Scientific Conference PRACTRO'03*, Varna, 2003, pp. 199-206.

- [26] A. Ming and T. Higuchi, "Study on multiple degree-of-freedom positioning mechanism using wires (part 1) - concept, design and control," *International Journal of the Japanese Society for Precision Engineering*, vol. 28, pp. 131-138, June 1994.
- [27] A. Ming and T. Higuchi, "Study on multiple degree-of-freedom positioning mechanism using wires (part 2) - development of a planar completely restrained positioning mechanism," *International Journal of the Japanese Society for Precision Engineering*, vol. 28, pp. 235-242, September 1994.
- [28] P. A. Voglewede and I. Ebert-Uphoff, "Application of the Antipodal Grasp Theorem to Cable-Driven Robots," *IEEE Transactions on Robotics*, vol. 21, pp. 713- 718, August 2005.
- [29] M. Gouttefarde and C. M. Gosselin, "Analysis of the wrench-closure workspace of planar parallel cable-driven mechanisms," *Robotics, IEEE Transactions on [see also Robotics and Automation, IEEE Transactions on]*, vol. 22, pp. 434-445, 2006.
- [30] R. L. Williams II, " Cable-suspended haptic interface," *International journal of Virtual Reality*, vol. 3, pp. 13-21, 1998.
- [31] R. L. Williams II and P. Gallina, "Planar Cable-Direct-Driven Robots: Design for Wrench Exertion," *Journal of Intelligent and Robotic Systems*, vol. 35, pp. 203-219, 2002.
- [32] J. S. Albus, R. Bostelman, and N. Dagalakis, "The NIST RoboCrane," *Journal of National Institute of Standards and Technology*, vol. 97, May-June 1992.
- [33] A. B. Alp and S. K. Agrawal, "Cable suspended robots: Design, planning and control," in *Proceedings of the 2002 IEEE International Conference on Robotics and Automation*, Washington, D.C., 2002, pp. 4275-4280.
- [34] A. Fattah and S. K. Agrawal, "Workspace and design analysis of cable-suspended planar parallel robots," in *Proceedings of the ASME 2002 Design Engineering Technical Conferences and Computer and Information in Engineering Conference (DETC '02)*, Montreal, Canada, 2002, pp. 1-9.
- [35] R. G. Roberts, T. Graham, and T. Lippitt, "On the Inverse Kinematics, Statics, and Fault Tolerance of Cable-Suspended Robots," *Journal of Robotic Systems*, vol. 15, pp. 581-597, 1998.
- [36] H. Osumi, Y. Utsugi, and M. Koshikawa, "Development of a manipulator suspended by parallel wire structure " in *Proceedings of IEEE/RSJ International Conference on Intelligent Robots and Systems*, 2000, pp. 498-503.

- [37] P. Bosscher, "Disturbance Robustness Measures and Wrench-Feasible Workspace Generation Techniques for Cable-Driven Robots." vol. Ph.D. Atlanta, GA: Georgia Institute of Technology, 2004.
- [38] R. Verhoeven, "Analysis of the workspace of tendon-based stewart platforms." vol. Ph.D. : University of Duisburg-Essen, 2004.
- [39] S.-R. Oh and S. K. Agrawal, "The feasible workspace analysis of a set point control for a cable-suspended robot with input constraints and disturbances," *IEEE Transactions on Control Systems Technology*, vol. 14, pp. 735-742 July 2006.
- [40] R. Verhoeven and M. Hiller, "Estimating the controllable workspace of tendon-based stewart platforms," in *Proceedings of the ARK 2000: 7th International Symposium on Advances in Robot Kinematics*, Piran, 2000, pp. 277-284.
- [41] M. Gouttefarde and C. M. Gosselin, "On the properties and the determination of the wrench-closure workspace of planar parallel cable-driven mechanisms," in *Proceedings of the ASME 2004 Design Engineering Technical Conferences and Computers and Information in Engineering Conference (DETC 04)*, Salt Lake City, UT, 2004, pp. 1-10.
- [42] K. Maeda, S. Tadokoro, T. Takamori, M. Hiller, and R. Verhoeven, "On design of a redundant wire-driven parallel robot WARP manipulator," in *Proceedings of the 1999 IEEE International Conference on Robotics and Automation*, Detroit, MI, 1999, pp. 895-900.
- [43] A. T. Riechel and I. Ebert-Uphoff, "Force-feasible workspace analysis for underconstrained, point-mass cable robots," in *IEEE International Conference on Robotics and Automation*, 2004.
- [44] P. Bosscher and I. Ebert-Uphoff, "Wrench-Based Analysis of Cable-Driven Robots," in *IEEE International Conference on Robotics and Automation*. vol. 1 New Orleans, LA, 2004, pp. 4950-4955.
- [45] P. Bosscher, A. Riechel, and I. Ebert-Uphoff, "Wrench-Feasible Workspace Generation for Cable-Driven Robots," *IEEE Transactions on Robotics*, vol. 22, pp. 890-902, October 2006.
- [46] E. Stump and V. Kumar, "Workspace Delineation of Cable-Actuated Parallel Manipulators," in *ASME International Design Engineering Technical Conferences, Mechanics and Robotics Conference*, Salt Lake City, 2004.
- [47] E. Stump and V. Kumar, "Workspaces of Cable-Actuated Parallel Manipulators," *ASME Journal of Mechanical Design*, vol. 128, January 2006.
- [48] G. Barette and C. M. Gosselin, "Kinematic analysis and design of planar parallel mechanisms actuated with cables," in *Proceedings of the ASME 2000 Design*

Engineering Technical Conferences and Computers and Information in Engineering Conference (DETC'00), Baltimore, Maryland, 2000, pp. 391-399.

- [49] Y. Guilin, Y. Song Huat, and P. Cong Bang, "Kinematics and singularity analysis of a planar cable-driven parallel manipulator," in *Intelligent Robots and Systems, 2004. (IROS 2004). Proceedings. 2004 IEEE/RSJ International Conference on*, 2004, pp. 3835-3840 vol.4.
- [50] O. Ma and J. Angeles, "Architecture singularities of platform manipulators," in *Robotics and Automation, 1991. Proceedings., 1991 IEEE International Conference on*, 1991, pp. 1542-1547 vol.2.
- [51] L.-F. Yang, M. M. Mikulas Jr., and J.-C. Chiou, "Stability and 3-D spatial dynamic analysis of a three-cable crane,," in *Proceedings of the 1992 AIAA/ASME/ASCE/AHS/ASC Structures, Structural Dynamics, and Materials Conference*, Dallas, TX, 1992, pp. 2069-2076.
- [52] P. Bosscher and I. Ebert-Uphoff, "A Stability Measure for Underconstrained Cable-Driven Robots," in *IEEE International Conference on Robotics and Automation*. vol. 1 New Orleans, LA, 2004, pp. 4943-4949.
- [53] P. Bosscher and I. Ebert-Uphoff, "Disturbance robustness measures for underconstrained cable-driven robots," in *Proceedings 2006 IEEE International Conference on Robotics and Automation, ICRA 2006.*, Orlando, Florida, 2006, pp. 4205- 4212.
- [54] A. B. Alp and S. K. Agrawal, "Cable suspended robots: Feedback controllers with positive inputs," in *Proceedings of the 2002 American Control Conference*, Anchorage, AK, 2002, pp. 815-820.
- [55] S.-R. Oh and S. K. Agrawal, "Cable-Suspended Planar Parallel Robots with Redundant Cables: Controllers with Positive Cable Tensions," in *Proceedings of IEEE International Conference on Robotics and Automation*, Taipei, Taiwan, 2003, pp. pp. 3023-3028.
- [56] S.-R. Oh, K. Mankala, S. K. Agrawal, and J. S. Albus, "A dual-stage planar cable robot: Dynamic modeling and design of a robust controller with positive inputs," *ASME Journal of Mechanical Design*, vol. 127, pp. 612-620, August 2005.
- [57] N. Yanai, M. Yamamoto, and A. Mohri, "Feedback control for wire-suspended mechanism with exact linearization," in *Proceedings of IEEE/RSJ International Conference on Intelligent Robots and System*, Lausanne, Switzerland, 2002, pp. 2213-2218.
- [58] N. Yanai, M. Yamamoto, and A. Mohri, "Anti-sway control for wire-suspended mechanism based on dynamics compensation," in *Proceedings of the 2002 IEEE International Conference on Robotics and Automation*, Washington, D.C., 2002, pp. 4287-4292.

- [59] M. Yamamoto, N. Yanai, and A. Mohri, "Trajectory control of incompletely restrained parallel-wire-suspended mechanism based on inverse dynamics," *IEEE Transactions on Robotics*, vol. 20, pp. 840-850, October 2004.
- [60] L.-W. Tsai, *Robot Analysis: The Mechanics of Serial and Parallel Manipulators* John Wiley & Sons, Inc., 1999.
- [61] K. J. Waldron and K. H. Hunt, "Series-Parallel Dualities in Actively Coordinated Mechanisms," *The International Journal of Robotics Research*, vol. 10, pp. 473-480, October 1, 1991 1991.
- [62] V. Kumar, K. J. Waldron, G. Chirikjian, and H. Lipkin, "Applications of Screw System Theory and Lie Theory to Spatial Kinematics: A Tutorial," in *ASME Design Engineering Technical Conferences*, 2000.
- [63] J.K. Davidson and K. H. Hunt, *Robots and Screw Theory: Applications of Kinematics and Statics to Robotics*. New York, NY: Oxford University Press, 2004.
- [64] Slotine, Jean-Jacques E, and W. Li, *Applied Nonlinear Control*: Prentice Hall, 1991.
- [65] Francesco Bullo and A. D. Lewis, *Geometric Control of Mechanical Systems: Modeling, Analysis, and Design for Simple Mechanical Control Systems*: Springer, 2004.
- [66] V. Kumar and K. J. Waldron, "Force distribution in closed kinematic chains," in *Robotics and Automation, 1988. Proceedings., 1988 IEEE International Conference on*, 1988, pp. 114-119 vol.1.
- [67] A. Muller, "Internal Preload Control of Redundantly Actuated Parallel Manipulators & Its Application to Backlash Avoiding Control," *IEEE Transactions on Robotics and Automation*, vol. 21, pp. 668-677, 2005.
- [68] Y. Xiaoping and N. Sarkar, "Unified formulation of robotic systems with holonomic and nonholonomic constraints," *Robotics and Automation, IEEE Transactions on*, vol. 14, pp. 640-650, 1998.
- [69] Mark W. Spong and M. Vidyasagar, *Robot Dynamics and Control*: Wiley, 1989.
- [70] L. Yanmei, C. Shih-Feng, and K. Imin, "Stiffness control and transformation for robotic systems with coordinate and non-coordinate bases," in *Robotics and Automation, 2002. Proceedings. ICRA '02. IEEE International Conference on*, 2002, pp. 550-555 vol.1.
- [71] J. K. Salisbury, "Active stiffness control of a manipulator in cartesian coordinates," in *Decision and Control including the Symposium on Adaptive Processes, 1980 19th IEEE Conference on*, 1980, pp. 95-100.

- [72] M. Zefran and V. Kumar, "Affine connections for the Cartesian stiffness matrix," in *Robotics and Automation, 1997. Proceedings., 1997 IEEE International Conference on*, 1997, pp. 1376-1381 vol.2.
- [73] M. M. Svinin, S. Hosoe, and M. Uchiyama, "On the stiffness and stability of Gough-Stewart platforms," in *Robotics and Automation, 2001. Proceedings 2001 ICRA. IEEE International Conference on*, 2001, pp. 3268-3273 vol.4.
- [74] S. Behzadipour and A. Khajepour, "Stiffness of Cable-based Parallel Manipulators With Application to Stability Analysis," *Journal of Mechanical Design*, vol. 128, pp. 303-310, 2006.
- [75] S. Kock and W. Schumacher, "A parallel x-y manipulator with actuation redundancy for high-speed and active-stiffness applications," in *Robotics and Automation, 1998. Proceedings. 1998 IEEE International Conference on*, 1998, pp. 2295-2300 vol.3.
- [76] R. M. Bhatt, Tang, C. P., Lee, L.-F. and Krovi, V., "Web-Based Self-Paced Virtual Prototyping Tutorials," in *ASME 2003 Design Engineering Technical Conferences and Computers and Information in Engineering Conference*, Chicago, Illinois USA, 2003.